Technischen Universität München

Institute for Advanced Study

Design and Synthesis of Highly Active and Selective α5β1 Integrin Ligands Containing the New *Iso*DGR Binding Sequence

Elke Otto

Vollständiger Abdruck der von der Fakultät für Chemie der Technischen Universität München zur Erlangung des akademischen Grades eines

Doktors der Naturwissenschaften

genehmigten Dissertation.

Vorsitzender: Univ.-Prof. Dr. Stephan A. Sieber

Prüfer der Dissertation:

1. Univ.-Prof. Dr. Dr. h.c. Horst Kessler
2. Univ.-Prof. Dr. Aphrodite Kapurniotu

Die Dissertation wurde am 20.04.2011 bei der Technischen Universität München eingereicht und durch die Fakultät für Chemie am 07.06.2011 angenommen.

für meine Familie

Die vorliegende Arbeit wurde in der Zeit von Mai 2007 bis April 2011 am Institut für Organische Chemie und Biochemie der Technischen Universität München unter Anleitung von Herrn Prof. Dr. Horst Kessler angefertigt.

Danksagung

- Dr. **Burkhardt Laufer** für die stete Hilfe im Labor und für witzigen gemeinsamen Dienstreisen, für seine Freundschaft und für die vielen wunderbaren Abende und lustigen Skiausflüge,
- Dipl. Chem. **Steffanie Neubauer** für die Freundschaft, für die sehr witzige Zeit in Amerika und die vielen Gespräche auch über die Chemie hinaus.
- Dr. **Carlos Mas-Moruno** für das Vertrauen in mich, die Unterstützung bei der Arbeit, die Freundschaft und die vielen Gespräche auch über die Chemie hinaus.
- Dr. **Bele Boeddinghaus** Dr. **Sabine Scholz**, Dr. **Fatima Bilic-Dugonjic**, Dipl. Chem. **Anja Zierhut** und Dipl. Chem. **Gerhard Richter** für die vielen aufbauenden Gespräche und das sie stets ein offenes Ohr für mich hatten.

Großer Dank gebührt meinen **Freunden**, die immer für mich da waren und mich stets auf andere Gedanken bringen konnten, wenn die Chemie mal wieder nicht das machte was sie sollte.

Meiner **Familie** bin ich unendlich dankbar, dass sie mich stets während meines Studium und der Promotion unterstützt hat, und besonders, dass sie mich in den letzten Woche der Doktorarbeit aufgefangen haben.

Mein besonderer Dank gilt meinem Mann, Dr. **Martin Otto**, für seine Unterstützung, sein Verständnis und seinen Rückhalt während den Höhen und Tiefen meiner Doktorarbeit. Danke für die zahllosen wunderschönen Momente, die mir das Leben so bereichern.

Index

‒ Abbreviations

Å	Ångstrom, 10^{-10} m
Ac	Acetyl-
ACN	Acetonitrile
ADDP	Azodicarboxylic dipiperidide
ADME	Absorption, Distribution, Metabolism, Elimination
ADMIDAS	Adjacent Metal Induced Adhesion Site
Bn	Benzyl-
Boc	*tert*-Butyloxycarbonyl-
Bu	Butyl
^{t}Bu	*tert*-Butyl
CAM	Cell Adhesion Molecule
d	Doublet or Days
δ	Chemical Dhift
1D, 2D, 3D	One / two / Three-dimensional
DCM	Dichloromethane
dd	Dublett of Dubletts
dest.	Destilled
DIAD	Diisopropylazodicarboxylate
DIEA	Diisopropylethylamine
DMAP	4-Dimethylaminopyridine
DMF	*N,N*-Dimethylformamide
DMSO	Dimethylsulfoxide
DPPA	Diphenylphosphoric Acid Azide
ECM	Extracellular Matrix
E.COSY	Exclusive Correlation Spectroscopy
ESI-MS	Electrospray Ionization-Mass Spectrometry
Et	Ethyl-
FAK	Focal Adhesion Kinase
ERK	Extracellular Regulated Kinases
Fmoc	9-Fluorenylmethoxycarbonyl
FN	Fibronectin
h	Hour
HATU	*O*-(7-Azabenzotriazol-1-yl)-*N,N,N',N'*,-tetramethyluronium-hexafluorophosphat
HMBC	Heteronuclear Multiple Bond Correlation
HMQC	Heteronuclear Multiple Quantum Coherence
HOAc	Acetic Acid
HOAt	1-Hydroxy-7-azabenzotriazol
HOBt	1-Hydroxybenzotriazol

Hphe	Homo-phenylalanine
HPLC	High Performance Liquid Chromatography
HSQC	Heteronuclear Single Quantum Coherence
Hz	Hertz
ILK	Integrin-Linked Kinase
IC	Inhibitory Capacity
*iso*D	*Iso*-Aspertate
J	Scalar Coupling Constant
LC-MS	Liquid Chromatography Mass Spectrometry
LIMBS	Ligand-induced Metal Ion Dependent Binding Site
m	Multiplett
M	Molar
Me	Methyl-
MeOH	Methanol
MHz	Megahertz
MIDAS	Metal Ion-dependent Adhesion Site
min	Minutes
mL	Milliliter
mmol	Millimol
MS	Mass Spectroscopy
MW	Molecular Weight
^{n}J	Scalar Coupling Constant over n-Bonds
N	Normal
NMP	*N*-Methylpyrrolidone
NMR	Nuclear Magnetic Resonance
NOESY	Nclear Overhauser Enhancement Spectroscopy
PBS	Phosphate Buffered Saline
PBST	Phosphate Suffer Saline Tween-20
Phg	Phenylglycine
ppm	Parts Per Million
q	Quartett
R_f	Retention Factor
ROESY	Rotating Frame Nuclear Overhause Effect Spectroscopy
R_t	Retention Time
RT	Room Temperatur
s	Singulett
SDL	Specificity-determining Loop
SPPS	Solid Phase Peptide Synthesis
t	Triplett
TBTU	*O*-(1H-Benzotriazol-1-yl)-*N,N,N',N*-tetramethyluronium-tetrafluoroborat
TCP	Tritylchlorid-Polystyrene-resin

TEA	Triethylamine
TFA	Trifluoroacetic Acid
TFE	Trifluoroethanol
THF	Tetrahydrofurane
TIPS	Triisopropylsilane
TMS	Trimethylsilyl-
TOCSY	Total Correlation Spectroscopy
UV	Ultraviolett
Vn	Vitronectin
vWF	*von Willebrand* Factor

I. Introduction

An ongoing battle of mankind is the design of appropriate drugs in the fight against diseases. Especially cancer is still a major public health problem, even though the overall cancer incidence rate has decreased in recent years.[1, 2] through better cancer prevention, early detection, and treatment.[1] However, for some forms of cancers, e.g. brain tumors, the incidence rate is still increasing and the survival rate is low. Conventional treatments, such as surgical excisions, chemotherapy, and radiotherapy, have large disadvantages due to the damage of healthy tissue.[3] Therefore, new approaches focusing on targeted drug therapies, with the intent to effect molecular and cellular changes specific to cancer cells. Cancer-specific targets could be cell division, cell movement, cell responses, or cell death, to name a few. In this context, integrins as transmembrane receptors, especially αvβ3, αvβ5, and α5β1, were found to play an essential role in tumor angiogenesis.[4, 5] Hence, research in integrine inhibitions for potential cancer treatment is still a hot research topic.

A prominent recognition sequence of integrins is Arg-Gly-Asp (RGD), which is able to promote integrin-mediated cell adhesion to extracellular matrix proteins like fibrinogen, vitronectin, or fibronectin (FN).[6] Based on this sequence the *N*-methylated cyclic peptide *cyclo*(-RGDf*N*-MeVal-) was developed in our group in cooperation with MERCK KGaA, Darmstadt, and is now in clinical phase III under the name Cilengitide.[7, 8] Additionally, a new binding sequence for integrins has recently been discovered[9] consisting of the three amino acid sequence *iso*Asp-Gly-Arg (*iso*DGR). In contrast to RGD, the *in vivo* formation of *iso*-aspartate by a rearrangement of aspartate or arginin potentially leads to a loss of protein function.[10] However, it was shown that in FN the diamidation of the Asn-Gly-Arg (NGR) motif into *iso*DGR results in a gain of protein function by creating a new binding site.[9] Consequently, this sequence came into the focus of cancer research.

As a first step on the long road to a potential use in cancer treatment, integrin ligands must be identified as they are both: highly selective for a specific integrin **as well as** highly active. This thesis deals with the design and synthesis of potential integrin ligands based on head-to-tail-cyclized peptides containing the new binding sequence *iso*DGR.

Section II will gives a short introduction in the principle of medical chemistry and solid phase peptide synthesis. Furthermore, a short summary of the structure, the function and the role of integrins in antiangiogenic cancer therapy will be given.

Section III deals with the rational design of new cyclic peptides as potential αvβ3 and α5β1 integrin ligands. Here, several head-to-tail-cyclized peptide libraries have been constructed based on different approaches. Moreover, this section presents insight and basic theories about the reasons for the observed difference in selectivity and activity of the created libraries.

The first goal of this thesis was to mimic *cyclo*(-RGDfV-), which is highly active for αvβ3 integrins. Then, a second approach will feature the return to NGR loop, where *iso*DGR was identified as a binding motif. Furthermore, a retro-inverso approach will be discussed.

In addition, the influence of an aromatic residue on the activity will be displayed by NMR structures docked to αvβ3 and α5β1 receptors. A short excursion on linear peptides will be made for clarity of differentiation. Then the influence of different amino acids as well as their combination, and their optimization will be investigated. Moreover, cyclic hexapeptides as possible ligands will be investigated.

Finally, a short insight into the importance of αvβ6 and the rational design of cyclic peptides as potential ligands will be described.

II. Theoretical Background

II.1. Basics of Medical Chemistry

II.1.1. Pharmacological Relevance of Peptides and Peptidomimetics

Biologically active peptides play a crucial role in physiological processes. Their *non-covalent* interactions with proteins affect cellular functions, cell-cell communication and immune response.[11-13] During the last decade, many active peptides such as *somatostatin*, *substance P*, *cholecystokinin*, *endorphin*, *enkephalin, angiotensin II,* or *endothelin* have been discovered and characterized.[14-16] Their function is enabled by binding as neurotransmitters, neuronal modulators, or hormones to membrane-bound receptors.[17] In contrast, inappropriate interactions can lead to pathological conditions. Therefore, peptides became important targets for drug discovery.[18, 19] Even though the number of native or modified peptides developed for disease treatment is increasing continuously, their use is still strictly limited. First, they have poor metabolic stability against proteolytic degradation. Second, they have low bioavailability due to their high molecular mass and a lack of active transporters. Third, the degradation by liver and kidneys is either poor or too fast. And finally based on interactions with multiple receptors they cause adverse effects.

To overcome these disadvantages, different strategies have been developed. One strategy is the restriction of the conformational space of the amino acid sequence, which is a significant approach to influence the binding affinity (for more details see Section II.1.3).[20] Another strategy is the incorporation of *N*-methylated amino acids into the sequence, which proved to be a determining structural modification to modulate the pharmacokinetic profile and biological activity of peptides.[21]

A successful application of this concept was demonstrated by the peptidic integrin ligand *cyclo*(-RGDf*N*-MeVal-), which is developed in our group in cooperation with MERCK KGaA, Darmstadt, named Cilengitide[7, 8] and is now in phase III of clinical investigation.

Apart from enhanced peptides, peptidomimetics describe a totally different approach. Peptidomimetics have a secondary structure analogue to peptides and are thus able to mimic peptidic function.[22] As an advantage over peptides, peptidomimetics show improved physiological properties.

II.1.2. Optimization of Lead Structures

A lead structure is the first step of developing a new drug. As long as the structure of the target is not available, the development concentrates on more or less screening based methods. After identifying a hit, the next step is optimization of this lead structure, and determination of the pharmacophoric groups, which are responsible for the interaction. This approach is called "ligand-oriented drug design".[23] However, if the target's 3D-structure can be determined using X-ray or NMR spectroscopy, "structure-based drug design" is favored. With this method, the process of drug development is more rationalized, depending on an iterative procedure of design, chemical synthesis, and subsequent biological testing of specific compounds. So far, the most successful theoretical approach to bypass the discrepancy between known protein sequences and 3D-structure is homology modeling. If the sequence of a known protein conforms more than 40% to an unknown protein, it is possible to construct an approximate 3D-model out of the reference 3D-structure. Such a homology modeled structure is suitable for rational drug design.[24]

To find an appropriate lead structure, a highly varied synthesis of compound libraries is still needed, as an *ab initio* design of a bioactive agent has not yet been achieved, despite all benefits of structure-based design. Furthermore, due to the complexity of biological processes, a high receptor affinity is not enough for drug development, as the *in vivo* affinity might highly differ compared to the activity measured *in vitro* activity. An active compound has to interact with both aqueous (cytoplasm) and lipophilic (membranes) environments in order to reach its target. Consequently, only substances with medium lipophilicity are water soluble *and* able to cross membrane barriers. Commonly, the lipophilicity is expressed by the logP value, where P is the *partition coefficient* between octan-1-ol and water (Equation II-1).[25]

$$P = \frac{[c]_{oc\tan ol}}{[c]_{water} * (1 - \alpha)}$$

Equation II-1: Calculation of the partition coefficient P. ☐ is the degree of dissociation in water.

One of the main goals in drug research is the development of highly selective and active drug candidates that are also orally available. To correlate structure and bioavailability about 2200 orally available drugs where analyzed by *Lipinsky et al.*, revealing a number of common properties, the so called "*Pfizer's rule of five*":[26, 27]

1) logP < 5
2) Molecular weight < 500 g/mol
3) Number of hydrogen-bond donors < 5
4) Number of hydrogen-bond acceptors < 10
5) One rule may be violated

However, these rules are not useful for all compounds, as for example *cyclosporin* violates each of the five rules. Hence, those aspects should be considered as guidelines rather than rules. The "*Veber rules*" as another approach postulating that oral bioavailability for molecules with less than 10 rotatable bonds and a polar surface of less than 140 $Å^2$ (which corresponds to < 12 H-bond donors / acceptors) is favored.[28]

Even with the help of these rules, prediction about the compound's metabolic stability is hardly possible. Normally, if penetrating molecules are unknown to the body, they are fought by antibody formation. However, if they are too small to be recognized by the immune system, non-specific enzymes (e.g., cytochrome P460) convert them into more polar metabolites. These metabolites are secreted from the body via kidneys, bile, or feces. The factors, which account for the pharmacological profile of a compound, are summarized as ADMET-parameters. They describe the **a**bsorption, **d**istribution, **m**etabolism, **e**limination, and **t**oxicity.[23] In the process of drug development, all those parameters have to be taken into account and should be constantly optimized.

II.1.3. Structural Properties of Cyclic Peptides

Great effort has been made to improve peptides to overcome their disadvantages as drugs. Physiologically active peptides like hormones or neuro peptides normally have a relatively small active region consisting of four to five amino acids.[20] Structural changes in this region have an extreme impact on the biological activity of the peptides, as according to the key-lock-principle of Emil Fischer[29] it is important that a ligand is able to form a complex with its receptor.[20, 29-32] Hence, a main task is to fix the bioactive conformation in order to gain increased binding affinities (*matched case,*

Figure II-1). In contrast, if the pharmacophoric groups are not capable of adopting the biologically active conformation, the affinity towards the target receptor is lost *(mismatched case*, Figure II-1). On the other hand, during complexation, receptors as well as hormones are able to undergo conformational changes. This extended concept is known as „induced fit".[33, 34]

Cyclization of short peptide sequences is a common method to enable fixation or stabilization of distinct conformations by adaptation of turn-like structures. Additionally, enhanced metabolic stability is achieved, as these cyclic peptides mostly fails to fit into the binding pockets of enzymes used for metabolism.[32, 35-37]

flexible molecule in solution

receptor

not active   active

constrained molecules in solution

complex

inactive   super-active

mismatched   matched
case   case
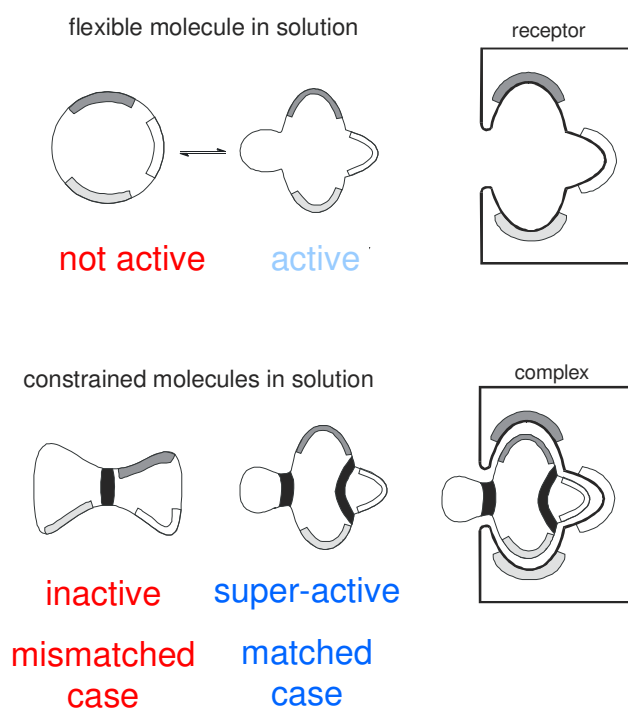
Figure II-1: Comparison of a flexible and a fixed molecule in solution.[38]

Cyclization of peptides is typically achieved through amide bonds or disulfide bridges using the cysteine side chain functionality. Depending on the position of the bridging atoms in the primary structure of the peptide, one speaks of head-to-tail-, backbone-, side-chain-, or side-chain-backbone-cyclization (see Figure II-2).[30, 39-41]

Head-to-tail cyclized penta- and hexapeptides are the cyclic peptides most frequently investigated[20, 42, 43], as they provide enough conformational restrictions without forcing *cis*-peptide bonds. Their main features are β- and γ-turn structures.
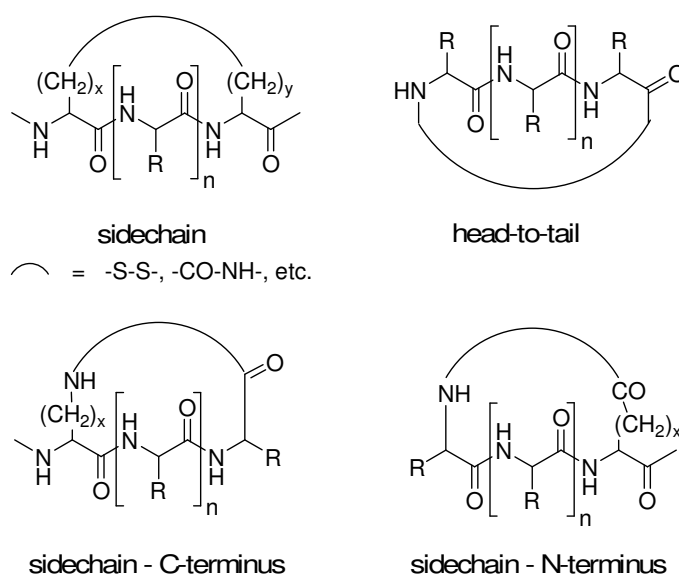
Figure II-2: Different kinds of cyclizations via amide bonds or disulfide bridges.[44]

A β-turn is formed by four amino acids having a hydrogen bond between the NH-group of the fourth amino acid (*i+3*) and the carbonyl group of the first amino acid *(i)* facilitating an antiparallel hairpin structure of the peptides (see Figure II-3).[20] Smaller cyclic peptides have a γ-turn structure based on a hydrogen bond between the NH-group of the third (*i+2*) and the carbonyl group of the first amino acid *(i)*.[20] For the different types of β-turns, the structure is defined by the dihedral angles Φ and Ψ of (*i+1*) and (*i+2*), while for definition of a γ-turn the Φ and Ψ of (*i+1*) are sufficient.[45] Several different basic motives are known, just differing in their Φ and Ψ angles.

Table II-1: Φ- and Ψ-angles of ideal β-and γ-turn structures.[46]

Turn structure	Φ (*i+1*) [°]	Ψ (*i+1*) [°]	Φ (*i+2*) [°]	Ψ (*i+2*) [°]
βI	-60	-30	-90	0
βI´	60	30	90	0
βII	-60	120	80	0
βII´	60	-120	-80	0
βVIa	-60	120	-90	0
βVIb	-120	120	-60	150
γ	70 - 85	-60 - (-70)		
γᵢ	-70 - (-85)	60 - 70		

Figure II-3: Stereoplot of β- and γ-turns as typical structure characteristics of cyclic peptides.[46]

On closer examination of the β-turn backbone structure, βI compared to βI' or βII to βII', respectively, are mirror-symmetric to each other. All other β-turn variations show a characteristic hydrogen bond between amino acids (*i*) and (*i+3*), which can be found between the amino acids (*i*) and (*i+2*) in the case of γ-turns. The βVI-turn has an exceptional position as it forms a *cis* amide bond between (*i+1*) and (*i+2*) but no hydrogen bond like the other turn structures. Additionally, it is known that in βII'-turns the (*i+1*) position is normally occupied by a D-amino acid residue.[46, 47]

II.1.4. Solid Phase Peptide Synthesis

Solid phase peptide synthesis (SPPS) was developed by Robert Bruce Merrifield (Solid phase synthesis of peptides, Nobel prize 1984)[48, 49] and it is a powerful tool to synthesize large libraries of compounds in a short time. T. Curtius and E. Fischer

provided the basis for SPPS by synthesizing simple derivates.[50] Moreover, the development of the benzyloxycarbonyl protecting-group by M. Bergmann was a major breakthrough.[51] The principle of SPPS consists of the covalent linkage of growing peptide strains to an unsolvable polymer carrier. Hence, a stepwise assembling of the peptide from the *C-* to the *N-* terminus through sequential coupling and cleaving cycles is possible (see Figure II-4).[52-54] The crucial advantage is the fact that simple wash and filter processes of the polymer bound peptide can remove excess of reagents and byproducts. Hence, the synthesis became simple and automatable.

For the synthesis of more than two peptides the utilization of orthogonal temporary amino- and permanent side chain-protecting groups is required.[55] The used method is the *tert.*-Butyloxycarbonyl (Boc)-strategy[48, 49] along with the later developed and more prominent 9-Fluorenylmethoxycarbonyl (Fmoc)/*tert.*-butyl-strategy.[52, 54, 56] In the case of the Fmoc-strategy, the protection of amino functionalities[53] with the Fmoc-protecting group offers the possibility to deprotect under mild basic and non hydrolysable conditions.
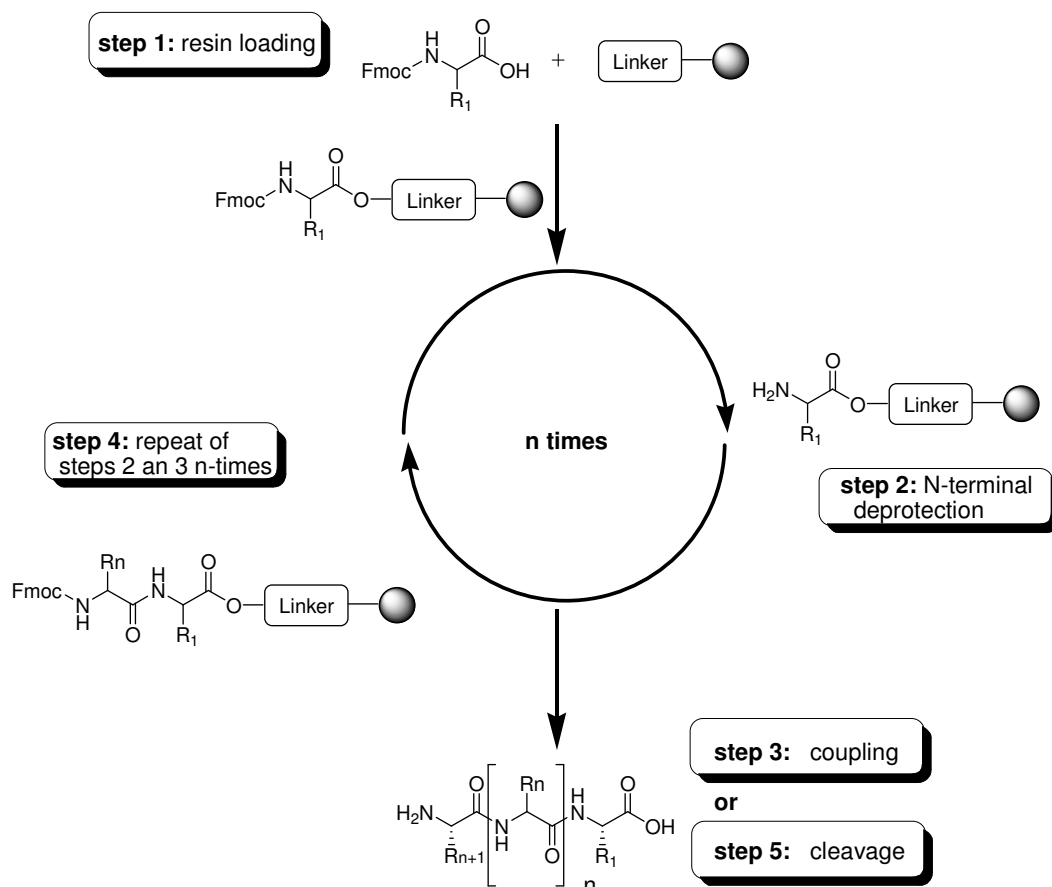
Figure II-4: Schematic representation of solid support peptide synthesis.[57]

Functionalized polymers, known as resins, are required for SPPS. They need to be mechanically stable and inert against solvents and reagents. Most resins, which are used today, are variants of the original chlormethylated polystyrene resin (PS) utilized by Merrifield. The coupling of the first amino acid to the resin is accomplished by addition of DIPEA in DCM under elimination of hydrogenchlorid.

The deprotection of the temporary Fmoc protecting group is carried out with 20% piperidine in *N*-methyl-pyrrolidinone (NMP) (v/v).

The originally used carbodiimide-derivatives for activation formed dicyclohexylurea, which have a low solubility. In addition, the amino acids are especially prone for racemization. Hence, they are usually replaced by other coupling reagents such as HATU or TBTU. In order to decrease racemization, additives (*e.g.,* HOBt or HOAt), as well as sterically hindered and weak bases (*e.g.,* DIPEA or 2,4,6-collidine) are used in the coupling reactions. In the first step of activation, TBTU immediately builds an acyluroniumderivat after reaction with the amino acid. The added HOBt quickly removes the intermediate by forming an OBt-active ester after an nucleophilic attack. Hence, a possible cyclization and epimerization of the acyluroniumderivat is avoided.[58]

Cleaving of the resin with preservation of the side-chain protecting groups is usually achieved by the treatment with weak acids such as hexafluorisopropanol (HFIP) or acetic acid in DCM. Full deprotection of peptides and cleaving is achieved with trifluoracetic acid (TFA). In order to prevent the irreversible alkylation of nucleophilic amino acid side chains, the so formed carbo cations are intercepted by suitable scavengers (water, anisole, thioanisole, ethandithiole, phenol, or TIPS).

II.2.   Integrins as Targets in Medicinal Chemistry

Cells must recognize their surrounding environment and rapidly adapt to changes, in order to accomplish their functions in tissues and organisms.[59] In order to communicate with other cells in a very precise manner and over short distances, the *extracellular matrix* (ECM) provides a physical scaffold for cell positioning and an instructive interface. Cell surface receptors of the integrin family are essential mediators and integrators of ECM-dependent communication. This function has not significantly changed during evolution from metazoas to mammals, which

demonstrates its essential role in multicell organisms.[60] Adhesion receptors of this family are involved in cell adhesion to the ECM as well as platelet aggregation, homing of leucocytes, and immune response. That is the reason why 1980s scientists working in different fields of biomedical research initially identified them.

The identification of FN as an ECM protein led the to identification of the arginine-glycine-aspartic acid (RGD) sequence as a crucial recognition motif,[61] and enabled the identification and purification of the FN / vitronectin receptors by affinity chromatography.[62, 63] RGD was initially - but too early - named "universal recognition motif", due to its appearance in many ECM proteins such as FN, Vitronectin, Fibrinogen, Laminin, Osteopontin, etc. However so far, many different recognition sequences from several natural integrin ligands have been discovered.[6, 64] As a result of molecular cloning and sequencing, these receptors were combined together with other adhesion receptors such as the platelet fibrinogen receptor, the *very late antigens* (VLAs), and *leucocyte-function associated antigen* (LFA) as one family of adhesion receptors.[65] *Tamkun* and *Hynes* introduced the term "integrin" to indicate their role of an integral membrane complex involved in the transmembrane association between the extracellular matrix and the cytoskeleton.[66] Integrins are important for a varity of biological processes, but beyond that, they are involved in many pathological processes such as inflammation, vascular homeostasis, thrombosis, restenosis, bone resorption, cardiovascular disorders, cancer invasion, metastasis, and tumor angiogenesis.[67-70]

II.2.1. Integrin Structure

Integrins are αβ-heterodimeric, type I transmembrane proteins with a large extracellular and a short cytoplasmic domain linked by a short, transmembrane region.[71] In mammals, 18 different α and 8 β subunits are identified, which can assemble non-covalently to 24 heterodimers (Figure II-5).

First analyses of integrin structures were conducted by electron microscopy. In the case of α5β1, a 28 nm long molecule consisting of a 8 x 12 nm globular head region and two 2 x 20 nm rod-like tails was revealed.[72] Structure examinations were continued employing various methods such as mutagenesis or monoclonal antibody

epitope mapping [71] until the first crystal structure of the αvβ3 headgroup[73] was achieved. The crystal structure of the headgroup in association with Cilengitide followed shortly after this breakthrough.[74]
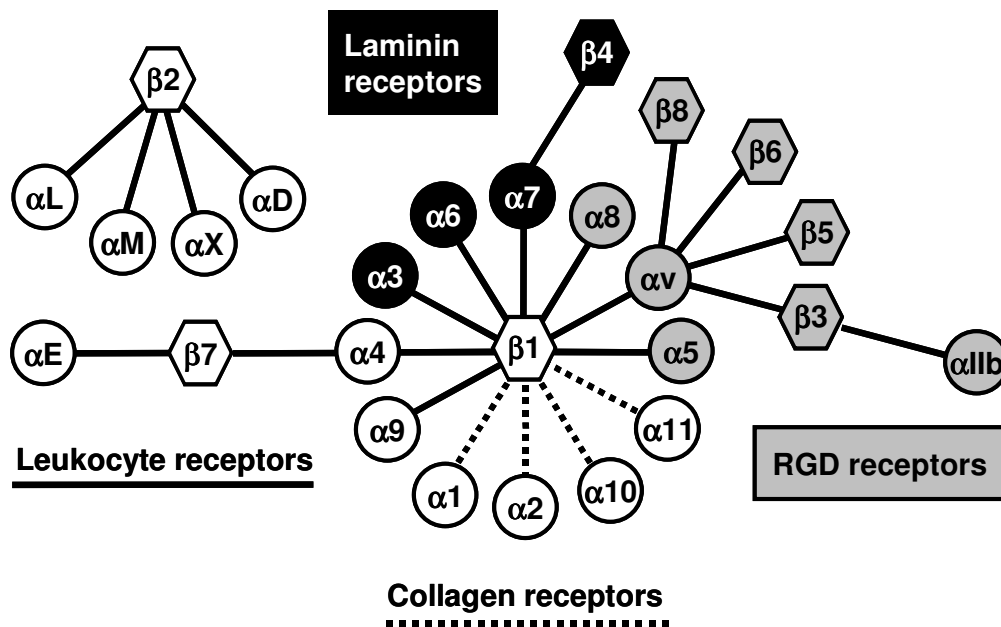
Figure II-5: The integrin family: Combinations of α and β subunits, which have been identified on cells up to now.[75]

The X-ray structure revealed that both integrin subunits have a recognizable domain structure (Figure II-6), and they assemble an ovoid-like shape consisting of a 9 x 6 x 4.5 nm head and two almost parallel tails.

Except for RGD-dependent integrins, a ~200-residue module homologous with the cation-binding A-domain of *von Willebrand factor* is found. This so called αA-domain or αI-domain (*inserted domain*) is inserted into a seven-blade β-propeller with 438 residues in αv. An A-domain-like polypeptide segment is also presented in the β-subunit (βI) with 243 residues in β3. This domain loops out from a unique immunoglobulin (Ig)-like "hybrid" domain with 133 residues in β3. The tail of the αv-subunit is composed of three β-sandwich domains, an Ig-like "thigh" domain and two very similar domains that form the "calf" module. The β3-tail consists of a PSI module which is found in several protein families (plexins, semaphorins, and integrins),[76] four cysteine-rich, epidermal-growth-factor (EGF)-like domains, and a β-tail domain (βTD). The first obtained crystal structure showed a tail for both subunits, which is folded back at a ~135° angle. Hence, it results in a V-shape with a

kink between the thigh-domain and the calf module of αv. Recently, it was assumed that integrins appear to be extended even in their resting state.[77]
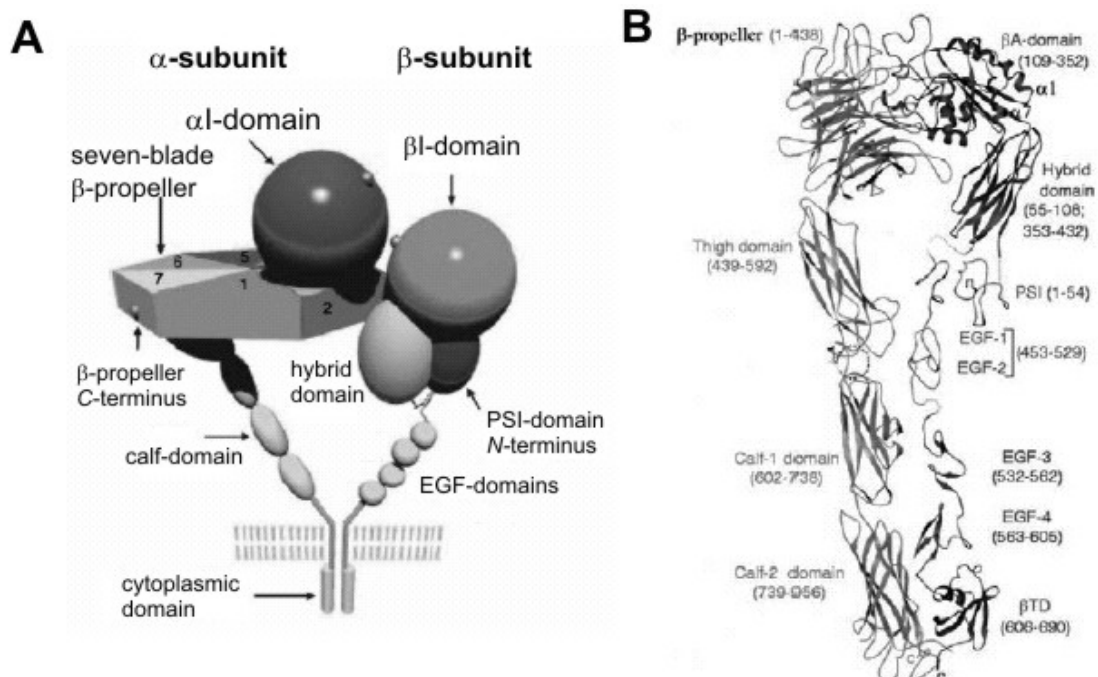
Figure II-6: Comparison of the schematic domain structure (**A**) with the ribbon drawing of the X-ray structure of αvβ3,[73] shown as a straightened model (**B**). The αI-domain is not present in αvβ3.

The binding site for the RGD ligand is located at the interface of the β-propeller domain of the αv subunit and the βI-domain of the β3-subunit.

The β-propeller is shaped from the amino terminal of αv out of a seven fold ~60 residue long sequence. It consists of seven radially arranged "blades", each formed from a four-stranded antiparallel sheet. Each of the seven blades reveals a unique consensus sequence with three aromatic residues per blade, all pointing towards the center of the propeller, thus forming a "cage"-like, hydrophobic cavity. This induced space is occupied by the Arg^{261} of the β-subunit, stabilizing the αβ-heterodimer by cation-π-interaction. The other binding side of RGD, the βI-domain, is inserted into the B-C-loop of the β3-hybrid domain and adapts a so-called *Rossmann fold* structure, which is also found in G-proteins as nucleotide binding motif.[78] The domain consists of a central six-stranded β-sheet surrounded by eight helices. Moreover, it contains of three binding sites for divalent cations, e.g., Ca^{2+}, Mg^{2+}, Mn^{2+}, etc. The ion favored for the binding depends on the used buffer.

A *metal ion dependent adhesion site* (MIDAS) motif is set in a cleft at the top of the central β-strand. In contrast to the unbound, inactive αvβ3, this adhesion site is only

occupied by a metal ion in the protein-ligand complex. The MIDAS is flanked by the ADMIDAS, an *adjacent MIDAS*, which is taken by a metal ion in both bound and unbound state. Furthermore, the LIMBS (*ligand induced metal binding site*), another metal ion binding site, was revealed through conformational changes induced by the binding event. Metal ion binding to the LIMBS might stabilize the ligand-bound conformation of the integrin.[74]

The nature of the divalent ions and their effects still cause much discussion. It seems that Mg^{2+} and particularly Mn^{2+} have a strong agonistic effect on the activity of integrin α5β1 and αvβ3, while Ca^{2+} reveals antagonistic effects[79, 80]. However, Ca^{2+} was not found to be inhibitory in αIIbβ3.

II.2.2. Mechanisms of Integrin Activation and Signal Transduction

There are several theories about the mode of activation and about conformational changes of the heterodimer during ligand-binding. There were plenty controversies about whether a transition to an extended conformation precedes or follows activation. However, integrins seem to have an extended structure even in their resting state (see Figure II-7).[77, 80-82] The previous idea of a bent conformation might be due to the fact that integrins can revert to fully or partially bent forms under certain conditions. Adhesion to substrates in electron microscopy or in crystals trigger this formation.[77]

Recently, the structure of the integrin αIIbβ3 transmembrane complex was determined in a phospholipid bilayer environment of small bicelles using solution NMR spectroscopy.[83] This proved the hypothesis that the α and β subunits dissociate and associate during transmembrane signalling (see Figure II-8).[83, 84] In the signalling processes integrins are essential to link the extracellular and the intracellular domains. Therefore, several groups have published different theories and calculations about the role of the transmembrane domain in signalling.[84-86]
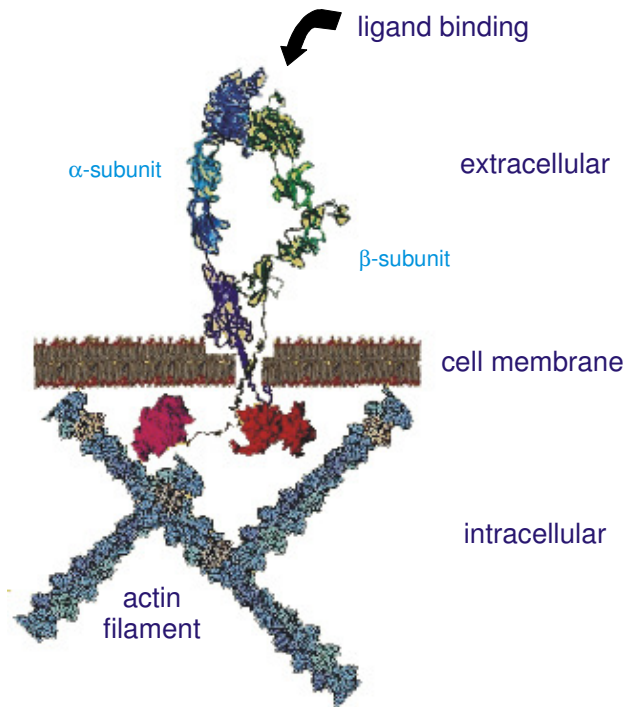
Figure II-7: An integrin receptor in the fully extended conformation.[77]
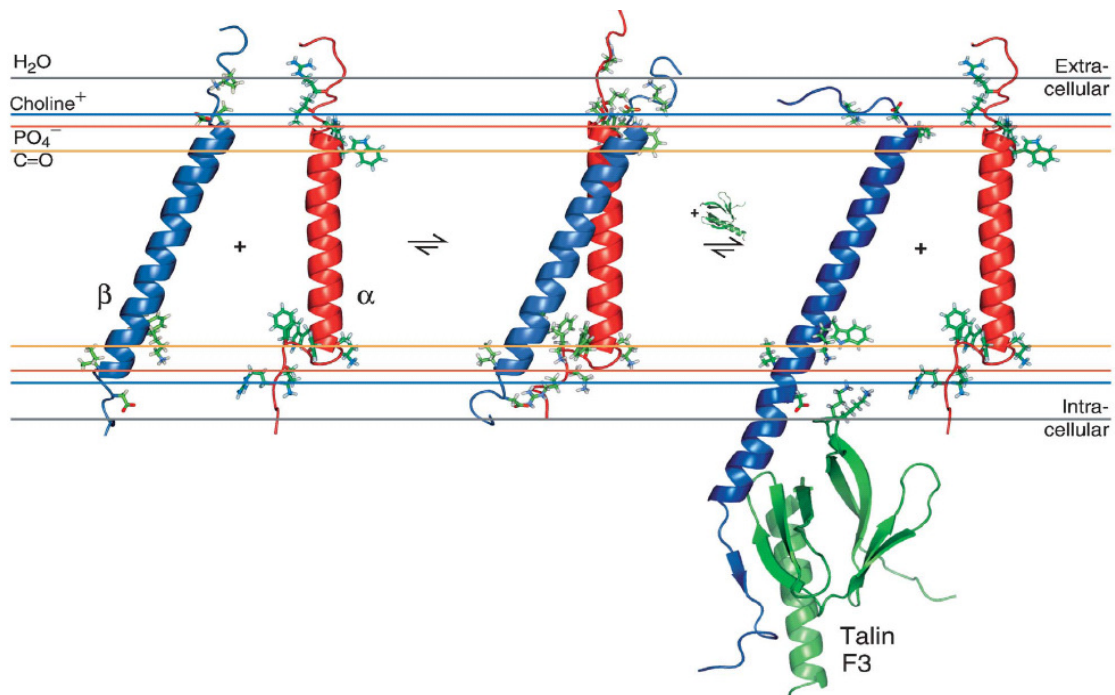
Figure II-8: Predicated orientations of the αIIb and β3 transmembrane segments in their monomeric and associated states[83] in consistent with the formar achieved computer modelling structure.[87]. The α subunit is shown in red and the β subunit in blue.

Integrins are able to address a high number of different proteins, which are involved in construction and anchorage of the cytoskeleton (actin stressfibers), and in various signaling pathways, even though their intracellular domains are relatively small (see

Figure II-9). Furthermore, clustering of active integrins in focal adhesion points induce binding to the proteins talin, paxillin, and vinculin (see Figure II-9). That is the reason why integrins get connected to the actin cytoskeleton. Integrin clusters can also bind and activate various tyrosine kinases such as the *focal adhesion kinase* (FAK), the *integrin-linked kinase* (ILK), or Fyn. The non-receptor tyrosine kinase FAK is the most prominent one, because it can be activated by almost all integrins. Due to the ligation of integrins with the ECM, FAK is able to undergo autophosphorylation at Tyr^{397}. Thus, it can bind other kinases such as Src, which also phosphorylate FAK at other tyrosine residues. This signaling complex accommodates a high number of proteins. Among them, some behave like kinases or scaffolds, and some have not yet been fully understood.

Phosphorylation is followed by several signaling pathways. First the binding of the Grb2-Sos-complex activates the Ras-cascade, which then leads to the activation of the *extracellular regulated kinases* (ERKs). ERKs are known to activate transcription factors, which regulate progression through the G_1 phase of the cell cycle and contribute to cell growth. Additionally, FAK activates the serine / threonine kinase PKB through phosphatidylinositol-3-kinase. PKB phosphorylates itself and thus inactivates proapoptotic molecules such as Bad, Bax, and caspase-9.

If the attachment to the matrix is lost, the cells undergo apoptosis, a phenomenon also referred as "anoikis" (homelessness). Hence, this process is crucial for the integrity of tissue, as it prevents cells without contact to their surrounding to establish themselves at inappropriate locations.

The nuclear factor κB (NF-κB) is a key transcription factor for the regulation of the immune and inflammatory response. Moreover, it promotes cell survival by inducing the expression of anti-apoptotic molecules.[88] The exact mechanism of how the nuclear factor is activated by integrins is still under investigation. Furthermore, it is assumed that unligated integrins can actively recruit pro-apoptotic molecules such as caspase-8, a phenomenon, which is known as integrin-mediated death (IMD).[89]

As another function, integrins can activate the Rho GTPases (Rho, Rac, and Cdc42), which act as molecular switches that provoke changes in the organization of the actin cytoskeleton. Rac, for example, is involved in the formation of lamellipodia, and new focal adhesion points, as well as their disassembly. These are all crucial factors for cell migration.
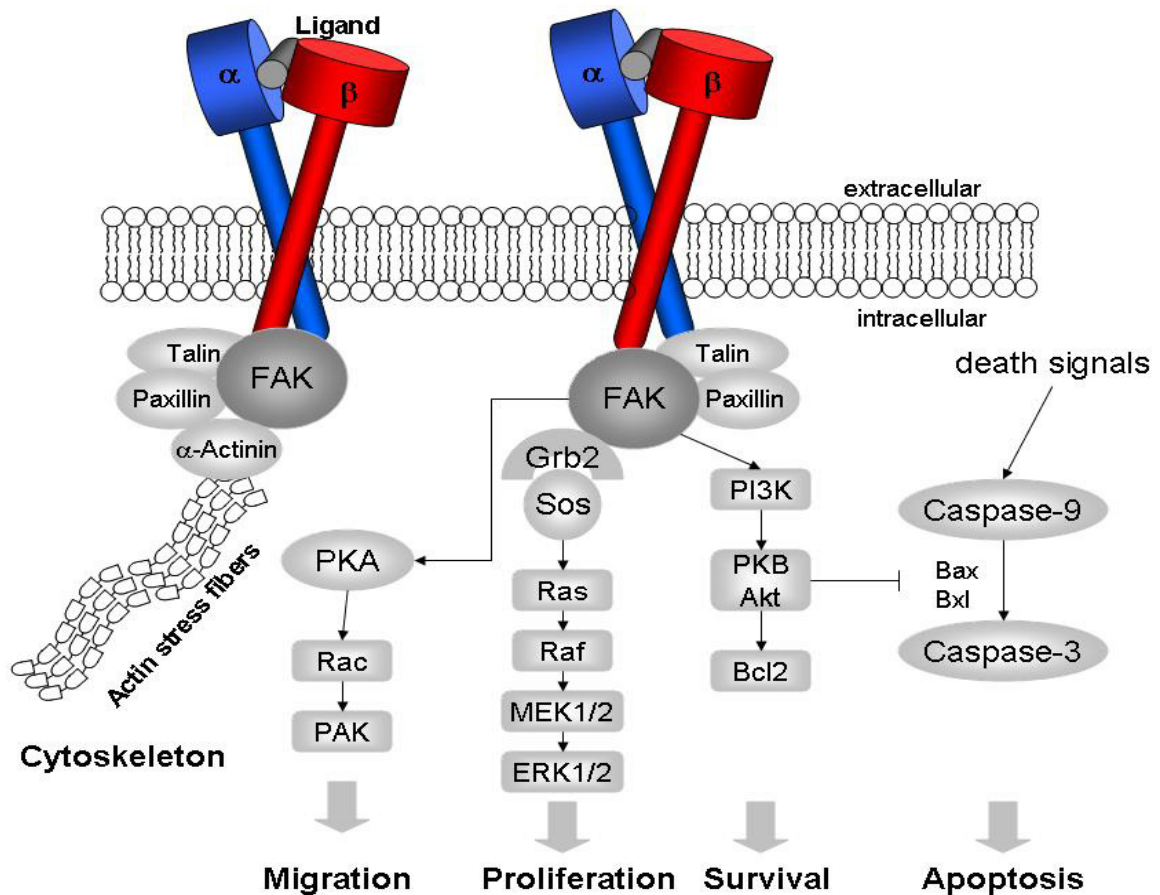
Figure II-9: Integrin-dependent signaling pathways (excerpt).[90]

All mechanisms of signal transduction mentioned above contribute to the *outside-in* signaling, which allows the cells to react on changes in the binding to the ECM. The mechanisms of the corresponding *inside-out* signaling are still not clear. However, there is strong evidence that the state of integrin activation is at least partly regulated by GTPases such as Ras and Rap-1.[91, 92]

Recent results demonstrate that interactions between different integrins present on the cell surface can strongly influence the adhesive functions of individual receptors. This effect, referred to as integrin "cross-talk", has been demonstrated in a number of systems.[93]

II.2.3. Ligand Binding to Integrins

Integrins without an I-domain, such as α5β1, αvβ3, αvβ5, and αIIbβ3 have their ligand binding site located between the β-propeller of the α-subunit and the βI-domain

of the β-subunit. Figure II-10 shows the binding modes of the RGD-peptide Cilengitide in integrin αvβ3 and the binding mode of Tirofiban in αIIbβ3 based on crystallographic data.[74, 80]
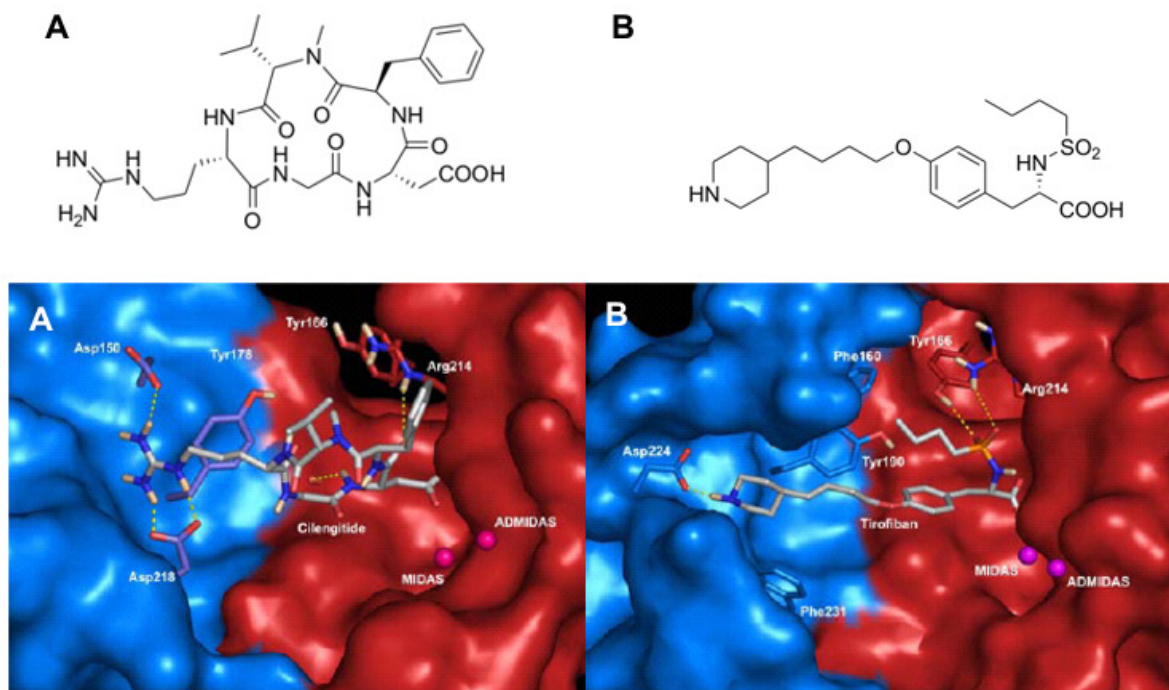
Figure II-10: Comparison of ligand binding in αvβ3 and αIIbβ3 integrin. Binding modes of Cilengitide in αvβ3 (**A**) and Tirofiban in αIIbβ3 (**B**) as derived from crystal structures.[94]

The guanidinium group of Cilengitide, *cyclo*(-RGDf*N*-MeVal-), is fixed inside a narrow groove formed by the D3-A3- and D4-A4-loops of the β-propeller in the αv subunit, through a bidentate salt bridge to (αv)Asp[218] at the bottom of the groove and via an additional salt bridge with (αv)Asp[150] at the rear. In the side-chain carboxylate group of Asp the ligand mainly forms the contacts between the Asp of the ligand and the βI-domain, which protrudes into a cleft between the βI loops A'-α1 and C'-α3. This carboxylate function coordinates the metal ion at the MIDAS in βI and is also involved in a hydrogen bond with the backbone amide proton of (β3)Asn[215]. In addition, hydrogen bonds are formed with the backbone carbonyl of (β3)Arg[216] and the side-chain of (β3)Arg[214]. The D-Phe residue of Cilengitide contributes to the binding by a weak π–π interaction with (β3)Tyr[122]. Gly does not interact with the receptor, but enables the formation of a γ-turn in the cyclic peptide. Due to extensive SAR studies, the optimal distance between the Arg-C^ζ and the Asp-C^β of Cilengitide has been determined to be ~14 Å.[95]

The binding mode of Tirofiban to αIIbβ3 is very similar to Cilengitide. The carboxylic function of the tyrosine scaffold coordinates the metal ion at the MIDAS, while the basic piperidine moiety is engaged in a salt bridge with the (αIIb)Asp[224]. In contrast to the αv subunit, the responsible aspartic acid residue is more immersed in the receptor, which leads to a longer groove in the β-propeller. Hence, αIIbβ3-ligands have to be longer, about 16 Å, to reach both anchoring points.

Another difference between the integrins is the higher hydrophobic environment of αIIbβ3 due to the replacement of (αv)Asp[218] by (αIIb)Phe[231], together with (αIIb)Phe[160], and (αIIb)Tyr[190]. This hydrophobic cleft is occupied by the *n*-butyl-side chain of the sulfonamide, that itself is positioned by two hydrogen bonds with the (β3)Tyr[166]-hydroxyl function and the guanidine group of (β3)Arg[214].

II.2.4. Integrin Ligands

Over the past decades, integrins have been a promising target for medical chemistry due to their biological relevance in many pathological and physiological processes.
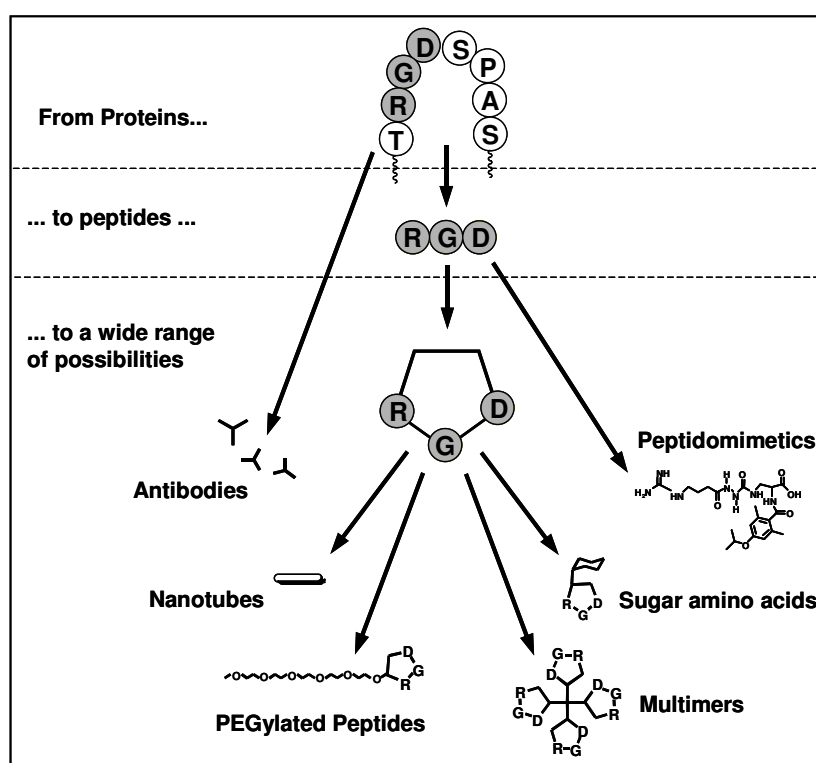
Figure II-11: Development of integrin ligands starting from proteins and resulting in small molecule ligands.[75]

After the identification of the RGD sequence as a crucial integrin binding sequence, a lot of new ligands have been synthesized. The monoclonal antibodies target a certain epitope on the receptor, while peptides and small-molecule ligands mimic the natural ligands, like for example FN.[96]

II.2.4.1. Natural Integrin Ligands

Extracellular matrix proteins like *FN, vitronectin,* and *fibrinogen* are the most abundant class of integrin ligands.

FN is widely expressed by multiple cell types and is critically important in vertebrate development.[97] FN is a large glycoprotein, which exists as a dimer of two nearly identical ~250 kDa subunits linked covalently near their *C*-termini by a pair of disulfide bridges. Each monomer consists of three types of repeating units: FN-I, FN-II, and FN-III (see Figure II-12).
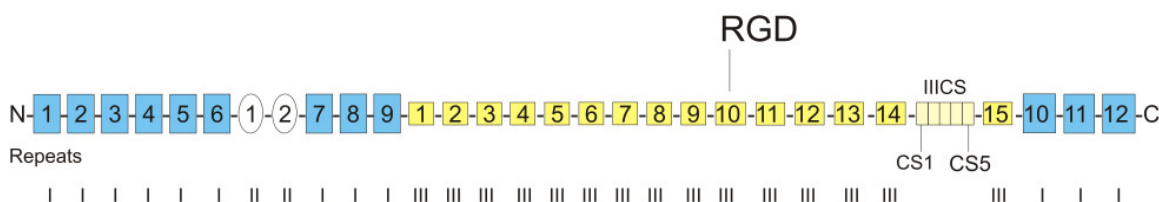
Figure II-12: Schematic representation of FN fragments. The three types of repeating homologous of which each subunit consists, are termed FN-I (blue rectangles), FN-II (ovals),and FN-III (yellow squares) repeats.

FN is an abundant soluble constituent of plasma and other body fluids. The assembly of soluble FN on cell surfaces results in insoluble, associated FN, which becomes a part of the ECM. The process, known as *FN fibrillogenesis*, depends on the self-association of FN molecules directed by multiple binding sites along the molecule.[98, 99] Especially the α5β1 integrin has been found to be critical for this process, because it can be inhibited by anti-α5β1 antibodies as well as other antagonists. The binding site of FN to the RGD sequence, which is present in the FN-III$_{10}$ repeat, has been determined via mutagenesis studies. This recognition sequence is mainly responsible for FN binding and assembly, but not the only binding sequence. For instance, a "synergy site" PHSRN has been identified in FN-III$_9$, which promotes specific binding of α5β1, apparently via interaction with the α5 subunit.

Additional α5β1 binding sites could be identified in the *N*-terminal region of FN, which seem to be distinct from those generated in response to ligation with the RGD sequence.[97]

II.2.4.2. Synthetic Integrin Ligands

The observation that integrins, in particular αvβ3 and α5β1, are characteristics of metastatic cancer and seriously involved in the process of tumor angiogenesis, made them attractive targets for cancer therapy. Especially the subtype α5β1 came into focus of research due to its genuine role in angionesis which was found by a reevaluation of the integrin receptors.[100] Before that, a lot of effort was spent on the design of integrin ligands containing the integrins αIIbβ3 and αvβ3. Inhibition of the platelet receptor αIIbβ3 seemed to be a promising method to inhibit fibrinogen-dependent platelet aggregation for the treatment of thrombosis. So far, the main target of antiangiogenic cancer therapy was αvβ3.
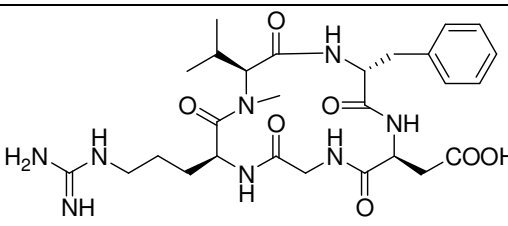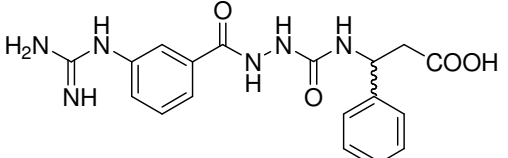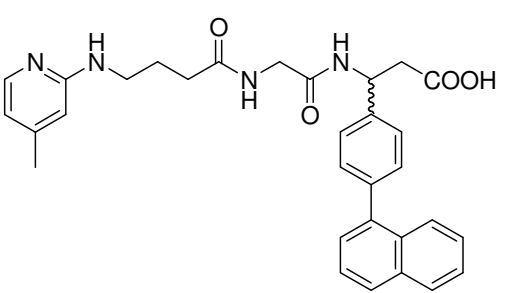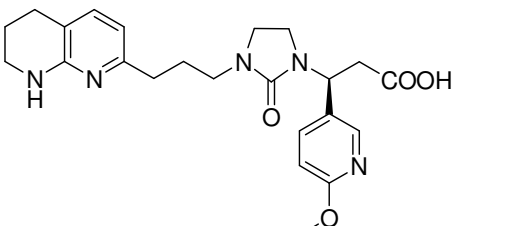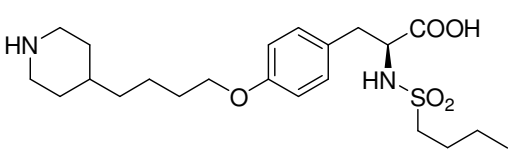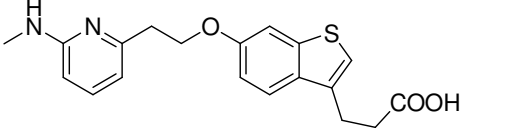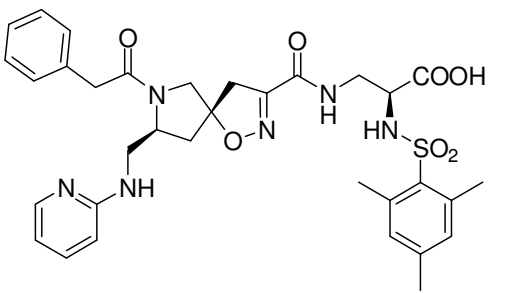
The main issue for the development of ligands is high activity and the gain of selectivity, because of the prospect of strong adverse effects by non-selective ligands. The progress in structure determination of the different receptors generally accelerated the process of ligand design.

The comparison of the different ligands (see Table II-2) outlines the general similarities: a basic moiety imitates the guanidyl group of the Arg side chain in RGD. A carboxyl group, which represents the aspartic acid, is attached to a more or less rigid scaffold arranging the ligands in the appropriate three-dimensional manner. In most cases, an aromatic residue in the vicinity of the carboxylate improves the binding properties by additional interactions with the receptor.

The αIIbβ3 inhibitor Tirofiban (Aggrastat®)[101] is an authorized drug for the treatment of *angina pectoris* and *myocardial infarct*. Abciximab (ReoPro®) targeting αIIbβ3 is another authorized drug, which is a fragment of a chimeric, monoclonal antibody against αIIbβ3. It shows higher receptor affinity than Tirofiban, but lacks selectivity.[102] The αvβ3 antagonist Cilengitide is currently in clinical phase III trials in patients with *glioblastoma multiforme*, *metastatic prostate cancer,* and *lymphoma*.[103] SJ749 was the first selective ligand reported for α5β1, enabling the set-up of the homology model calculated by *Marinelli et al.*[104, 105]

Table II-2: Structures and activities of selected integrin ligands.

Entry	Structure	IC_{50} [nM]	Reference
1 Cilengitide		0.5 ($\alpha v \beta 3$) 70 ($\alpha v \beta 5$) 860 ($\alpha IIb \beta 3$)	[7]
2		2.6 ($\alpha v \beta 3$) 280 ($\alpha v \beta 5$) 8300 ($\alpha IIb \beta 3$)	[106]
3		8 ($\alpha v \beta 3$) 5170 ($\alpha v \beta 5$) 4230 ($\alpha IIb \beta 3$)	[107]
5		0.1 ($\alpha v \beta 3$) 10 ($\alpha v \beta 5$) 35000 ($\alpha IIb \beta 3$)	[108]
6 Tirofiban		36 ($\alpha IIb \beta 3$)	[101]
7		30 ($\alpha v \beta 3$) 140 ($\alpha v \beta 5$) 7800 ($\alpha 5 \beta 1$) >20000 ($\alpha IIb \beta 3$)	[109]
8 SJ749		49 ($\alpha v \beta 3$) >100000 ($\alpha IIb \beta 3$) 0.2 ($\alpha 5 \beta 1$)	[104]

II.2.5. The α5β1 Homology Model

α5β1 has been excluded in the past as a target for structure-based drug design due to the lack of reliable structural data. However, based on the high homology between the different integrin subtypes, the structure of α5β1 was recently determined using homology modeling.[105, 110] Homology modeling is possible, if the homology of proteins is 40% or higher.[24]

This condition is satisfied by the integrins αvβ3 and α5β1 with 53% homology for αv/α5 and 55% for β3/β1. A particularly low homology in the sequence was found in the *specificity determining loop* (SDL). This short (CZDMKTTC) loop is stabilized by a disulfide bridge and is located in the β3-subunit of αvβ3. The SDL is considered to be important for the αvβ3 specificity towards natural ligands.[111] In the case of small-molecule ligands, the SDL is supposed to be rather unimportant for selectivity due to its distance to the binding site.[112] The metal ion binding sites MIDAS, ADMIDAS, and LIMBS were found to be highly conserved, which is consistent with the importance of metal ion coordination for ligand binding. Interestingly, the $(β3)Arg^{261}$, which stabilizes the heterodimer by π-cation interaction with the aromatic residues of the αv-β propeller is mutated to a Lys. Since several possible homology models could be determined, they were optimized by adjusting the binding site of the receptor model to a highly active ligand to find a reliable model for docking experiments. The finding that the integrin α5β1 is the only unambiguously proangiogenic integrin, caused its biological relevance and therefore has been drawn into the focus of research. Many known αvβ3 antagonists are most likely to be biselective on both integrins based on the structural similarities of both receptors. Apart from some published cyclic peptides with mostly micromolar activity, the most active α5β1 ligands are a series of spirocyclic isoxazolines with an IC_{50} of 0.2 nM towards α5β1 and a 200 fold selectivity against αvβ3 synthesized by Smallheer *et al.*[104] Docking of the most potent ligand SJ749 into the optimized homology model and superposition with the corresponding αvβ3 head group derived from the X-ray structure reveals a number of differences (see Figure II-13).

SJ749 binds in a manner similar to other RGD peptides / mimetics (Figure II-14).[105] The carboxylic function coordinates the metal ion located in the MIDAS, while the basic aminopyridinyl moiety is inserted into a narrow groove between the D3-A3 and the D4-A4 loop of the (α5)-propeller. Thus, a hydrogen bond to the highly conserved

(α5)Asp^{227} (Asp^{218} in αv) is formed. Notably, a second (αv)Asp^{150}, which is able to participate in binding, is mutated to (α5)Ala^{159}. The groove of the α5 subunit is terminated by a (α5)Gln^{221} (Thr^{212} in αv) resulting in a slightly extended binding pocket. For this reason, the more hydrophobic pocket should favor a more lipophilic and basic moiety in α5. Furthermore, the extended binding pocket could be an important issue to induce selectivity *against* αvβ3 by employing bulkier basic groups.

The most obvious difference between the two β-subunits is the C'-a3 loop. In this loop, β1(Gly^{217}) is exchanged by (β3)Arg^{214}, which forms a hydrogen bond with the sulfonamide of SJ749 (Figure II-14). In addition, the residues (β3)Arg^{216} and (β3)Tyr^{166} are replaced by (β1)Leu^{219} and (β1)Ser^{171} respectively, which are less sterical demanding and open a new cleft in β1, which is relatively hydrophobic. Therefore, a promising approach towards α5β1-selective ligands could be to directly address this hydrophobic cavity by a bulky aromatic group. This would result in a clash with (β3)Arg^{214}, and thus disabling the binding in αvβ3.
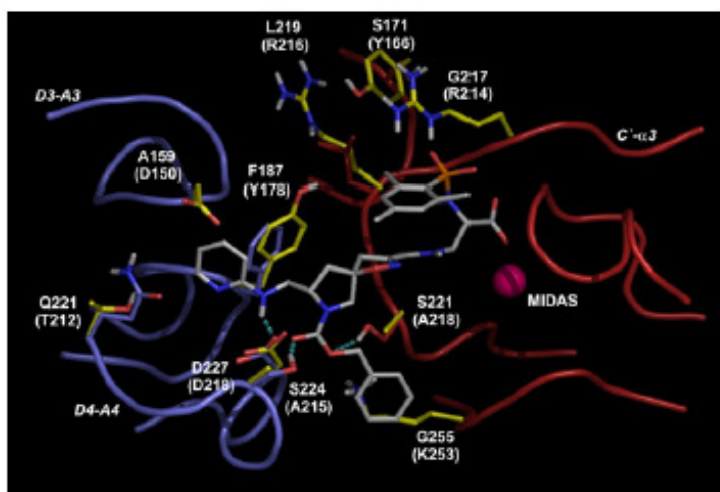
Figure II-13: Comparison of the binding pockets of α5β1 and αvβ3 integrins. Mutations in the sequence are marked gray. Ribbon drawing of α5β1 (α5 in blue, β1 in red), with its analog amino acids of αvβ3 are shown in yellow.[105]

The benzyl carbamate of the ligand SJ749 is an additional feature, as it forms an additional interaction with the (α5)Ser^{224} and the (β1)Ser^{221} which are both replaced by Ala in αvβ3 (Ala^{215} and Ala^{218}, respectively). This substitution pattern increases affinity towards α5β1 without interfering the binding towards αvβ3.

Based on this homology model the design of highly active and selective α5β1 ligands was achieved in our group.[113]
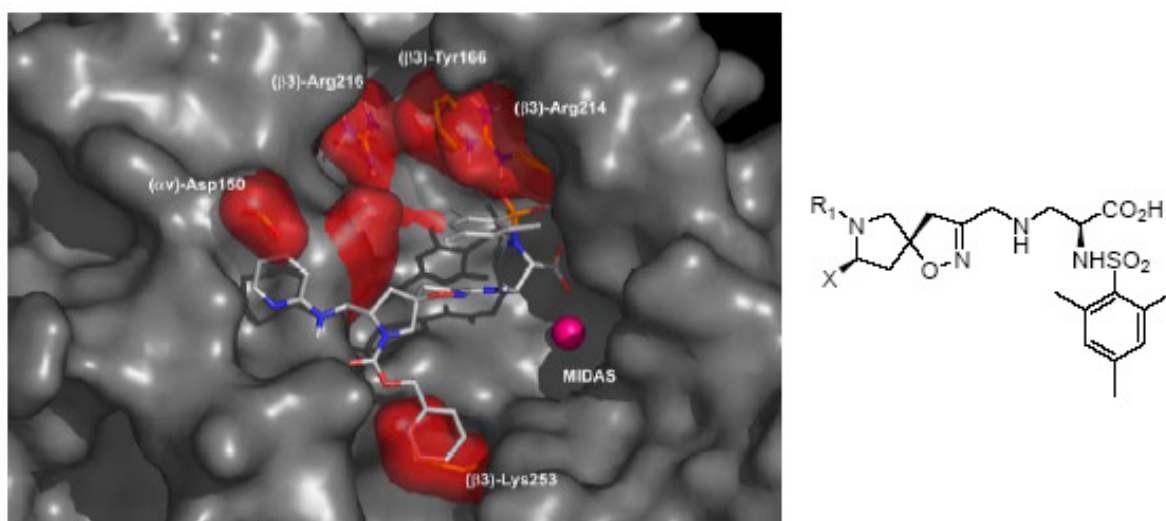
Figure II-14: Docking of the spiroisoxazolin (SJ749) into the homology model of α5β1. The superposition of the Connolly-surfaces of α5β1 (gray) and αvβ3 (transparent red) is shown.[105]

II.2.6. Antiangiogenic Cancer Therapy

Many *knock-out* studies have been performed in various models, to elucidate the functions of integrins *in vivo*. (see Table II-3)

The phenotypes of the gene deletions highlight the importance of integrins for embryogenesis. Embryonic lethality is mostly the result of an impaired formation of the vasculature. Naturally, these findings constitute a basis for antiangiogenic therapy. Angiogenesis is the formation and differentiation of new blood vessels from pre-existing ones via recruitment of endothelial progenitor cells. It plays a key role during embryonic development, as well as in wound healing, and in the female reproductive system.[90] The vascular network, in adults, is quiescent. Therefore, angiogenesis is triggered only locally and transiently. The fine balance between local inhibitory control and pro-angiogenetic signals is deregulated under certain abnormal conditions. This down-regulation leads to pathological neovascularization, as detected in a variety of diseases like diabetic retinopathy, restenosis, adipositas, rheumatoid arthritis, psoriasis, and tumor growth.[114] To activate the angiogenetic process, endothelial cells have to dissociate from neighboring cells and degrade the underlying basement membrane, before they are able to invade the underlying tissue.

Table II-3: Phenotypes of mice with constitutive gene deletion.[59, 64]

Gene deleted	Heterodimers affected	Major ECM Ligand	Knockout phenotype
α5β1	α1β1, α2β1, α10β1, α5β1, α9β1, α7β1, α6β1, α3β1, α8β1, αvβ1, α5β1, α4β1	FN, Vn, Ln, Co	Lethal at E5.5 Failure of organizing the embryonic inner mass.
β3	αIIbβ3, αvβ3	Fb, Vn, FN, Ln, OPN, vWF, Fibrin	Viable, bleeding disorders (Glanzmann's thrombasthenia). Osteoclast functional defects in bones. Extensive Angiogenesis
αv	αvβ1, αvβ3, αvβ5, αvβ6, αvβ8	Vn, FN, Ln, Fb, vWF, OPN, Fibrin	8% die at E10.5-12.5. 92% die soon after birth due to brain hemorrhages (malformation of cerebral vasculature)
α5	α5β1	FN	Lethal at E10. Vasculogensis but no maturation / angiogenesis
αIIb	αIIbβ3	Fb	Viable, bleeding disorders (Glanzmann's thrombasthenia).

The interaction of endothelial cells with the ECM is mediated, during invasion and migration, through integrins.[115] In the final stages of the angiogenic process, integrins are also involved. Finally, the construction of capillary loops and the

determination of the polarity of the endothelial cells, finally allows lumen formation of new vessels.

The formation of a tumor-associated vasculature (tumor angiogenesis) has been observed already over 100 years ago. Due to the pioneering work of *Judah Folkman* in the 1970s, the biological relevance of tumor angiogenesis to tumor biology was broadly recognized and investigated within the cancer research community.[116] Since then, tumor angiogenesis has emerged as a critical stromal reaction essential for tumor progression. In the absence of tumor angiogenesis, the tumor enters a state of dormancy characterized by a balance between cell proliferation and apoptosis. Its mass stabilizes at a volume of a few cubic millimeters (~10^5-10^6 cells). This so-called "angiogenetic switch" is often triggered through release of growth factors from hypoxic cells, because neovascularization is essential for an adequate nutrition of the tumor (Figure II-15). Angiogenesis allows the unhampered growth of the solid tumor and also favors the escape of tumor cells into the blood circulation, which constitutes the initial step of metastatic spreading.[117]
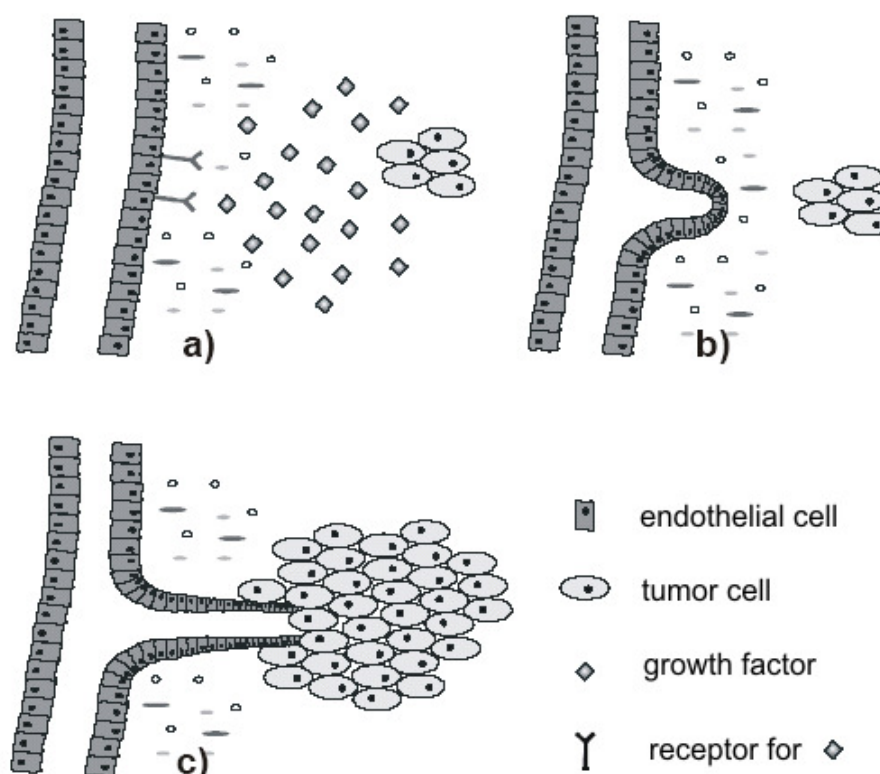
Figure II-15: Schematic view on tumor angiogenesis. a) hypoxic tumor cells release growth factors and stimulate proliferation of endothelial cells. b) Cells increase expression of integrins and activate proteolytic enzymes leading to directed invasion towards the tumor. c) Nutrition of the tumor is maintained, tumor is able to grow and metastasize.[94]

Conventional cancer therapies targeting tumor cells with cytostatic drugs are limited by strong side-effects. All cells that exhibit a generally high proliferation rate are affected. Therapies against angiogenetic blood vessels take advantage of the distinct biochemical differences between neovascular vessels and the pre-existing vascular network. A promising approach for cancer therapy extensively studied in the last decades was the selectivity towards tumor cells. The prospect to disable angiogenesis by blocking ligation of integrins to their native ECM ligands let to the discovery of numerous integrin antagonists. Up to now, these consist of monoclonal antibodies, peptide antagonists, and small molecules with varying affinities to the respective integrin subtype.[118]

One of the first antiangiogenic drugs is the recently approved Ranibizumab (Luzentis®), a humanized fragment of an antibody against VEGF-A. It is authorized for treatment of *age-related macula degeneration*, a disease where extensive angiogenesis destroys the retina, normally resulting in *ablepsia* (blindness).

II.2.7. Role of Integrins αvβ3 and α5β1

The integrins αvβ3, αvβ5, and α5β1 are attractive targets for anti-angiogenetic cancer therapy because of their primary expression on activated endothelial cells.[4] The αvβ3 integrin was found to be involved in tumor angiogenesis. Blocking of αvβ3 with a monoclonal antibody[119] and the peptide cyclo(RGDfV)[120, 121] was shown to suppress cornea vascularization, hypoxia-induced retinal neovascularization, and tumor angiogenesis in mouse models.[122] Moreover, ligation of αvβ3 to the ECM was found to activate proliferation and anti-apoptotic pathways such as EFK-activation,[123] NF-κB activation,[124] increase in the Bcl-2/Bax ratio,[125] and blocking of activator-caspase 8.[126] The integrin αvβ3 was also found to be activated by *vascular endothelial growth factor* (VEGF), hence enhancing ligand binding, cell adhesion, and migration.[127] These findings illustrate the role of αvβ3 as a pro-angiogenic integrin.

The phenotype of β3 or β5 knockout mice (viable, fertile, Table II-3) displays a rather dispensable role in contrast to α5 (lethal at E5).[128]

Additionally, the β3-negative mice displayed an enhanced postnatal angiogenesis in response to hypoxia and VEGF.[129, 130] The results are supported by the observation

that αv-deficient mice undergo extensive developmental vasculogenesis and angiogenesis.[124] The discrepancy between normal and extensive angiogenesis in αvβ3 deficient mice on the one hand, and the suppression of angiogenesis by pharmacological αvβ3 inhibitors in wild-type mice on the other hand, give rise to the question whether αvβ3 regulates angiogenesis in a positive or negative way.[89, 100, 128] The role of these peptides or small molecules has to be re-evaluated in respect to their function as antagonists or agonists. However, this problem is complicated due to the impact of integrin activation on different integrin types (integrin "cross-talk").[93]

The binding of αvβ3 to selective antibodies or a peptide inhibitor inhibits cell migration not only on vitronectin, but also on FN in the presence of α5β1.[131] Similar results were obtained with a mutated β3 subunit, thus indicating a modulation of the α5β1 activity by αvβ3. The role of an integrin ligand as agonist or antagonist may also be a question of concentration. Small picomolar doses of a cyclic RGD peptide were found to increase the binding affinity of αvβ3 towards vitronectin, FN, and fibrinogen, while higher doses of up to 10 µM resulted in a dramatic loss of affinity.[79] Nevertheless, there is a high number of αvβ3 ligands in different stages of clinical trials.

The results indicate a certain ambivalent effect of αvβ3, which highlights the importance of the integrin α5β1 in anti-angiogenetic therapy. The integrin α5β1 was also found to induce angiogenesis *in vitro*, while anti α5 antibodies suppressed VEGF-induced tumor angiogenesis in both chick embryos and murine models.[5, 132, 133] Engagement of α5β1 to FN promotes proliferation via the NF-κB-pathway and PKA / caspase 8 suppression. Blocking of α5β1 by antibodies resulted in a caspase 8 induced apoptosis due to sustained PKA activation. Hence, α5β1 came into focus as drug-targets for anti-angiogenetic tumor therapy due to the unambiguously pro-angiogenic function of α5β1. The setup of a homology model of α5β1 based on the crystal structure of αvβ3 and the first slightly selective α5β1 integrin ligand SJ749,[74, 104, 105] was a major step towards the synthesis of highly selective compounds for α5β1. Thus, first ligands showing a promising selectivity against αvβ3 and good activity for α5β1 have recently been published.[134, 135]

II.2.8. *Iso*DGR as a New Binding Motif for Integrins

Even though the two key FN receptors αvβ3 and α5β1 share the same ligand-recognition motif, their function is not the same. Binding of integrins to FN induce different cellular signals and behaviors, which is important for many physiological and pathophysiological conditions such as wound healing, angiogenesis, and cancer metastasis.[136] To investigate the role of FN-RGD in the 10th type III repeat FN module for the integrin binding (see Figure II-16), knock-out mice with inactive RGE sequence, instead of the natural RGD sequence, were generated.[137] Thus, this mutated motif is unable to interact with integrins anymore.[137] Interestingly, despite this binding defect, the RGE containing mutant can still assemble into FN fibrils.[137] However, these fibrils have a slightly different phenotype than the wild-type FN. The assembly of the fibrils occurred via αvβ3 integrin interaction, even though the RGD binding sequence was inactivated, which revealed that FN contains a previously unknown binding site for αvβ3 integrin. Recent findings show that deamidation of the NGR sequences in 5th type I repeat FN module (see Figure II-16) into *iso*DGR serves as novel integrin binding site.[137] Therefore, this new binding epitop was suggested to be the reason for the unexpected FN assembly via αvβ3 interactions.
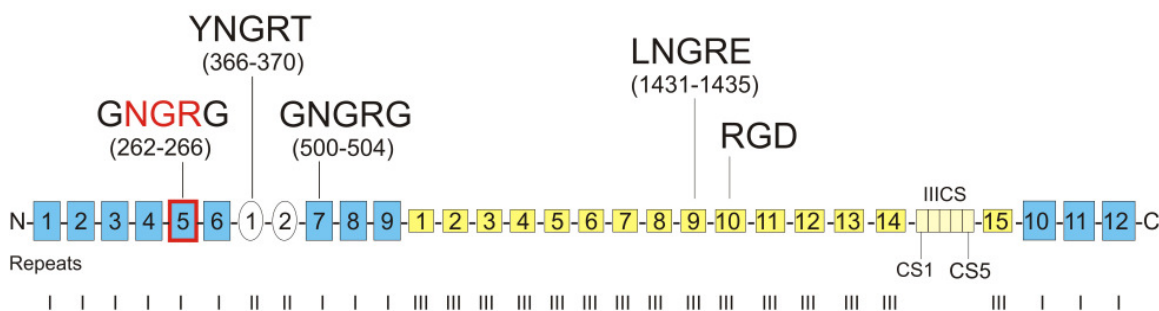
Figure II-16: Schematic representation of FN fragments. The position of the possible new binding site, is highlighted with a red rectangle.

Rearrangement of asparagine into *iso*-aspartate is a side reaction in peptide synthesis already known for a long time (Figure II-17).[138] It generally results in structures that lose biological activity. *Iso*Asp is an aspartate bound via its side chain, and as a result it is a non-standard β-amino acid. The rate of deamidation depends on the neighboring amino acid sequences, the temperature, the buffer composition, and the ionic strength.[139, 140] Furthermore, it also occurs *in vivo,* which is potentially leading to a loss of protein function.[10, 141] Especially, the presence of a Gly residue

following Asp or Asn generally accelerates the reaction due to its small size and flexibility.[140] Hence, deamidation has been proposed to act as a biochemical clock that limits protein lifetimes.[142] Notable, the protein-L-*iso*Asp-O-methyltransferase is able to repair this non-enzymatic *isoAsp* formation enzymatically,[141, 143]
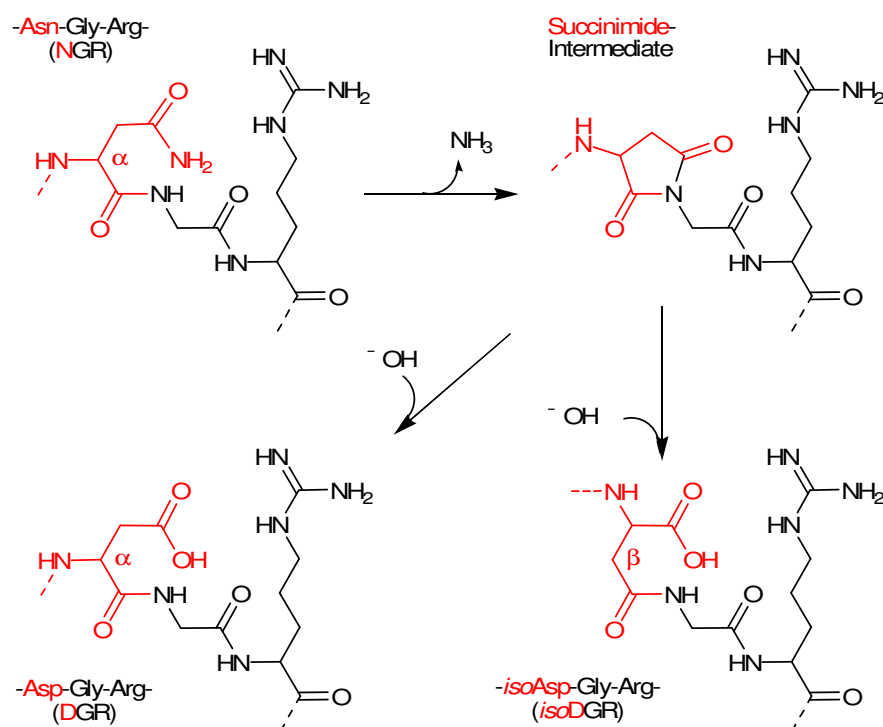
Figure II-17: *Deamidation of NGR occurs via hydrolysis of a succinimide intermediate which leads to the formation of isoDGR or DGR, depending on neighboring amino acid sequences, temperature, and ionic strength.*[139, 140]

Curnis et al.[9] revealed that deamidation of the NGR motif in FN-I$_5$ into *iso*DGR results in a gain of protein function by creating a new adhesion binding site for integrins, mainly for αvβ3.[9, 137] However, the assumption that the formation of *iso*DGR in FN-I$_5$ is the reason for FN assembly has been questioned. This is due to the fact that mutation of recombinant FN at the NGR motif is still able to form fibrils.[144]

Peptides containing an NGR motif have been discovered by phage display libraries[145-147] and have been exploited for ligand directed delivery of various drugs and particles to tumor vessels to increase their antitumor activity.[148] Moreover, NGR together with DGR has been proposed as an alternative binding motif for integrins, although, controversial data have been reported.[148-150] Structure analysis of NGR,

DGR, and *iso*DGR containing cystein cyclized penta petides followed by docking experiments revealed that only *iso*DGR fits into the RGD binding pocket, while DGR and NGR do not fit.[151] Thus, a possible explanation for the controversial data might be the spontaneous transformation from inactive NGR or DGR into active *iso*DGR.[152] So, formation of *iso*Asp might be used as a switching element to enable integrin recognition.

Cystein cyclized *iso*DGR penta petides are able to bind to αvβ3 with higher affinity than other integrins[153] and have therefore been suggested as a new tumor vasculature-targeting motif.[154] Replacement of Cys with Gly leads to a linear peptide and to a significant loss of activity for integrins and a change of specificity.[153] Hence, interaction of *iso*DGR with the integrin, like RGD, depends on its molecular scaffold.[153]

III. Results and Discussion

III.1. Design of αvβ3 and α5β1 Selective Integrin Ligands Based on the New Binding Sequence *Iso*DGR

To prove that the deamidation side-reaction in FN generates *de novo* binding epitopes for αvβ3, a study of constrained *iso*DGR peptides for their integrin subtype affinities was performed. For this purpose, different libraries of head-to-tail cyclized peptides containing the *iso*DGR amino acid motif were created.

Inspired by previous findings that the conformation of the RGD sequence controls selectivity between αvβ3 and the platelet integrin αIIbβ3,[155] the peptides were tested also for selective binding to the closely related integrin α5β1.

All peptides presented in this work were synthesized using standard Fmoc solid phase conditions. Note however, that it is important to start the loading of the resin with Arg, as the β-amino acid *iso*-Asp turned out to have a strong influence on the peptide conformation. Thus, cyclization can only be achieved if *iso*Asp is located in the middle of the sequence.

The biological testings (ELISA assays) were primarily performed by *Dr. Dörte Vossmeyer, Dr. Grit Zahn,* and *Roland Stragies* at the Jerini AG (Berlin) but then resumed by Dr. *Carlos Mas-Moruno* and Dipl. Chem. *Alexander Bochen* of our group. Here, the ability of the compounds to inhibit the binding of soluble α5β1 / αvβ3 to their immobilized natural ligands FN and vitronectin was tested.

Structures were determined by Dr. *Andreas Frank* in our group. Dr. *Luciana Marinelli* and *Dr. Sandro Cosconati* from the group of *Prof. Ettore Novellino* at the Università di Napoli "Federico II, Napoli" (Italy), accomplished docking studies for αvβ3 and α5β1 integrins.

Cellular testings were performed by Dr. *Herbert Schiller* in the group of *Prof. Reinhard Fässler* at the Max-Planck-Institute für Biochemie, Martinsried. He determined the ability of the compounds to inhibit the cell adhesion of pre-incubated mouse fibroblasts expressing either αvβ3 or α5β1 against FN.

The results presented in chapter **III.1.1**, **III.1.2**, **III.1.3**, and **III.1.5** have already been published in *Angew. Chem. Int. Ed.* **2010**, *49*, 9278-9281.

III.1.1. First *Iso*DGR Libraries Based on *Cyclo*(-RGDfV-)

A promising starting sequence for the first head-to-tail cyclic library containing the *iso*DGR amino acid motif seemed to be the cyclic peptide *cyclo*(-RGD-fV-),[120, 156] as it is a highly active αvβ3 integrin binding ligand. The resulting peptide contains the new binding motive is *cyclo*(-Vf-*iso*DGR-). Furthermore, a D-amino acid scan of this compound was performed to reveal the most bioactive conformation.[157] The resulting peptides were tested for their ability to bind to the αvβ3 and α5β1 integrins. Unfortunately, the peptides of this first library showed, in general, moderate to poor affinities for αvβ3 and no activity for the α5β1 integrin (see Table III-1). A reason for the inactivity might be the modification of the structure caused by the additional methylene group, which probably leads to an absent interaction of the aromatic moiety of the ligand with the integrin receptor.

Table III-1: *Receptor assays of compounds **1-5** based on the highly active peptide cyclo(-RGDfV).*

Code	Sequence	IC_{50} (α5β1) [nM]		IC_{50} (αvβ3) [nM]	
1	*cyclo*(-**f**-*iso*DGR-V-)	846	(± 199)	146	(± 10)
2	*cyclo*(-F-***iso*d**GR-V-)	31892	(± 10371)	1362	(± 10)
3	*cyclo*(-F-*iso*D**G**R-V-)	2004	(± 128)	403	(± 154)
4	*cyclo*-(-F-*iso*DG**r**-V-)	>40000		8240	(± 1330)
5	*cyclo*(-F-*iso*DGR-**v**-)	1860	(± 59)	88	(± 3)

Table III-2: *Receptor assays of compounds **6-14** based on the highly active peptide cyclo(-RGDfV-).*

Code	Sequence	IC_{50} (α5β1) [nM]		IC_{50} (αvβ3) [nM]	
6	*cyclo*(-**f**-*iso*DGR-VA-)	9927	(± 4547)	16096	(± 1418)
7	*cyclo*(-F-***iso*d**GR-VA-)	8906	(± 1774)	2143	(± 595)
8	*cyclo*(-F-*iso*D**G**R-VA-)	5588	(± 220)	2278	(± 1023)
9	*cyclo*(-F-*iso*DG**r**-VA-)	1145	(± 259)	1478	(± 15)
10	*cyclo*(-F-*iso*DGR-**v**A-)	>40000		>20000	
11	*cyclo*(-F-*iso*DGR-V**a**-)	565	(± 149)	649	(± 241)
12	*cyclo*(-F-*iso*DGR-**p**V-)	12185	(± 3691)	502	(± 3)
13	*cyclo*(-F-*iso*DGR-V**p**-)	1179	(± 197)	227	(± 30)
14	*cyclo*(-**p**-*iso*DGR-VF-)	>20000		2350	(± 1210)

Cyclic hexapeptides as well as cyclic pentapeptides are commonly used cyclic backbone structures in medicinal chemistry. Hence, cyclic hexapeptides containing one Ala or one Pro and based on the retro sequence were synthesized. For these compounds no affinity for αvβ3 and α5β1 integrins was detected (see Table III-2).

III.1.2. FN Loop as a New Pattern for *Iso*DGR Peptides

As the first libraries showed poor integrin binding affinity, the starting point was changed back to the active *iso*DGR in FN-I$_5$ (see Figure II-16).[158] Therefore, the new sequence intended to mimic the GNGRG loop found in FN-I$_5$, which is able to deamidate into *iso*DGR and is thus able to interact with integrins. To perform a D-amino acid scan, the *iso*DGR sequence was flanked by two Gly. Again these peptides showed no activities for αvβ3 and α5β1 (see Table III-3).

Table III-3: *Receptor assays of compounds **15-17** mimicking the GNGRG loop in FN.*

Code	Sequence	IC_{50} (α5β1) [nM]	IC_{50} (αvβ3) [nM]
15	*cyclo*(-G-*iso*DGR-G-)	>2000	256 (± 24)
16	*cyclo*(-G-**iso**d**GR-G-)	7638 (± 24)	>1000
17	*cyclo*(-G-*iso*DG**r**-G-)	8035 (± 24)	>1000

III.1.3. Investigation of the Importance of the Aromatic Moiety

Finally, the combination of the first approaches by using one aromatic amino acid next to the *iso*Asp led to a ligand with an interesting biological profile, i.e., high affinity for α5β1 with good selectivity. It is well known from the *cyclo*(-RGDfV-) peptide that the aromatic moiety of Phe is essential for αvβ3 integrin binding while Val can be replaced by other amino acids, e.g., Lys, without affecting receptor affinity.[121] Therefore, cyclic *iso*DGR pentapeptides containing Phe as the aromatic residue were synthesized and a D-amino acid scan was performed (Table III-4, peptides **18-21**).

The pharmacophoric range of these peptides might differ from the structures observed for *cyclo*(-RGDfV-), because of the extra methylene group of *iso*Asp in the

backbone. This might result in a different distance between the integrin binding pocket and the aromatic group. To get insight into this potential difference, the spatial position of the pharmacophoric phenyl group was modified. A D-amino acid scan of the resulting peptides using homo-phenylalanine (Hphe) (Table III-4, peptides **22-25**) and phenylglycine (Phg) (Table III-4, peptides **26-29**) was performed.

Table III-4: *Receptor assays of compounds **P18-29** with one aromatic amino acids next to isoAsp.*

Code	Sequence	IC_{50} (α5β1) [nM]		IC_{50} (αvβ3) [nM]	
18	*cyclo*(-F-*iso*DGR-G-)	>2000		633	(± 524)
19	*cyclo*(-**f**-*iso*DGR-G-)	838	(± 160)	377	(± 272)
20	*cyclo*(-F-***iso*d**GR-G-)	>1700		>1000	
21	*cyclo*(-F-*iso*DG**r**-G-)	1279	(± 36)	>1000	
22	*cyclo*(-Hphe-*iso*DGR-G-)	>2000		>1000	
23	*cyclo*(-**hphe**-*iso*DGR-G-)	83	(± 21)	410	(± 107)
24	*cyclo*(-Hphe-***iso*d**GR-G-)	>20000		>1000	
25	*cyclo*(-Hphe-*iso*DG**r**-G-)	818	(± 71)	>1000	
26	*cyclo*(-Phg-*iso*DGR-G-)	57	(± 8)	753	(± 150)
27	*cyclo*(-**phg**-*iso*DGR-G-)	19	(± 4)	>1000	
28	*cyclo*(-Phg-***iso*d**GR-G-)	7031	(± 4929)	>1000	
29	*cyclo*(-Phg-*iso*DG**r**-G-)	711	(± 101)	>1000	
	Cilengitide	15	(± 3)	0.54	(± 0.15)

In consistence with the results of *Curnis et al.,*[9] peptides containing a D-*iso*Asp showed no activity at all. Surprisingly, for some compounds activity towards α5β1 was detected which is in contrast to the preference of αvβ3 activity observed by these authors.[9] Especially the peptides **23**, **26**, and **27** with D-Hphe, L-Phg, and D-Phg, respectively, as aromatic residue showed good to high affinities for α5β1 with moderate to good selectivity against αvβ3. This result confirms that interaction of the aromatic group with the integrin binding pocket is important for the binding. Moreover, it also shows that the different spatial position of the pharmacophoric phenyl group was probably the reason for the previously observed inactivity. It should be highlighted that the activity of peptide **27** for the α5β1 integrin is comparable to the anti-cancer drug Cilengitide[7] but is inactive for αvβ3 (see Tab. III-4). Hence, **27** with its high activity and selectivity for α5β1 seems to be a promising integrin ligand.

Therefore the structure of this peptide was determined, docked to the receptors, and tested in cellular assays (see IV.1.5.).

III.1.4. The Retro-Inverso Approach

*Iso*DGR can be considered as a kind of retro sequence of RGD, therefore the retro-inverso concept was performed. Inversion of chirality (inverso) combined with the invertation of the sequence (retro) is postulated to lead to a side chain orientation similar to the parent peptide (see Figure III-1).[159] The advantage of retro-inverso peptides is their high metabolic stability, as D-amino acids containing peptides are usually more stable against enzymatic cleavage. To verify this approach, the inverso (Table III-5, peptides **30-42**), retro (Table III-6, peptides **43-57**), and retro-inverso (Table III-7, peptides **58-70**) compounds of the previous library were synthesized.
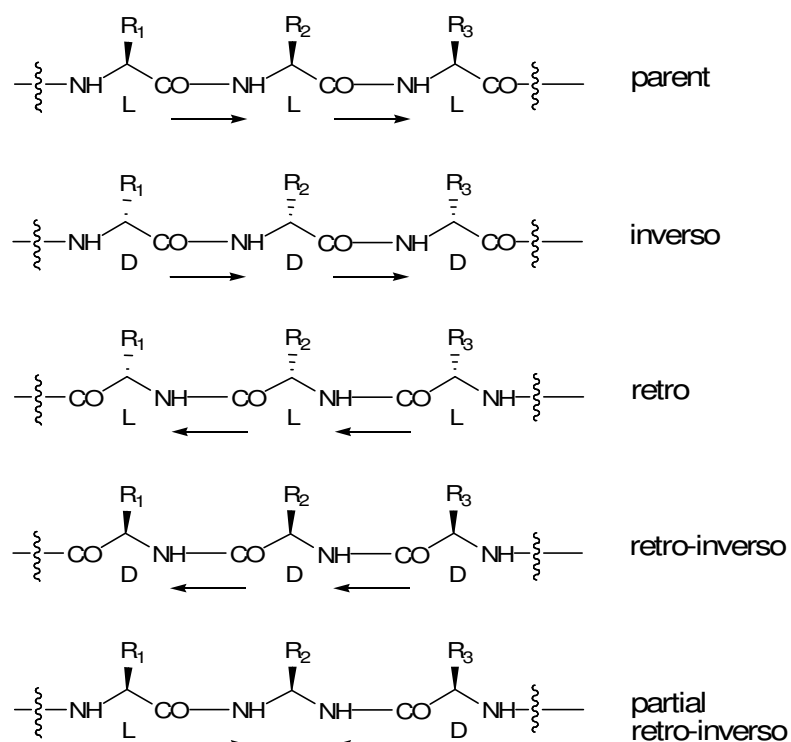
Figure III-1: Retro-Inverso concept. The arrows indicate the direction of the amide bond. The side chains orientation of the parent, the retro-inverso peptide and the partial retro-inverso are similar.

The inverso peptides showed moderate or no binding ability for αvβ3 and α5β1 integrins (see Table III-5). In the case of the retro **43-57** and the retro-inverso

peptides **58-70** (see Tables III-6 and III-7), at first the most promising compounds, based on the α5β1 active parent sequence cyclo(-phg-*iso*DGR-G-), have been tested. This was due to the fact that our initial co-operation partner, Jerini, AG (Berlin), responsible for the activity testings, stopped doing these assay after acquisition by the British Shire Ldt. Hence, the testing system was established in our group, which required a significant effort and considerable delay in testing, with the result that not all peptides mentioned in this thesis could be fully tested. However, as the tested retro and retro-inverso peptides showed no activity, no further tests were performed due to the lake of manpower.

Table III-5: *Receptor assays of inverso compounds **30-42** of cyclo(-X-isoDGR-G-).*

Code	Sequence	IC_{50} (α5β1) [nM]	IC_{50} (αvβ3) [nM]
30	*cyclo*(-G-***isod*Gr**-G-)	>10000	604
31	*cyclo*(-**f**-***isod*GR**-G-)	>1000	372
32	*cyclo*(-**f**-*iso*DG**r**-G-)	>1000	>1000
33	*cyclo*(-F-***isod*Gr**-G-)	>1000	>1000
34	*cyclo*(-**f**-***isod*Gr**-G-)	>1000	905
35	*cyclo*(-**hphe**-***isod*GR**-G-)	>1000	250
36	*cyclo*(-**hphe**-*iso*DG**r**-G-)	>1000	220
37	*cyclo*(-Hphe-***isod*Gr**-G-)	>1000	>1000
38	*cyclo*(-**hphe**-***isod*Gr**-G-)	>1000	>1000
39	*cyclo*(-**phg**-***isod*GR**-G-)	>1000	186
40	*cyclo*(-**phg**-*iso*DG**r**-G-)	>1000	>1000
41	*cyclo*(-Phg-***isod*Gr**-G-)	565	>1000
42	*cyclo*(-**phg**-***isod*Gr**-G-)	>1000	540

The results obtained are comparable to the retro approach of cyclo(-RGDfV-) investigated in 1996 by *Wermuth et al.* where only a few compounds showed activity towards αvβ3.[160] Even though partially modified retro-inverso cyclic tetrapeptides were reported as dual αvβ3 / α5β1 integrin inhibitors recently,[161] the biological activity of retro-inverso peptides is often modified compared to their parent compounds. There are two effects that may explain these observations: first, the spatial structure may not be retained, since the retro-inverso concept disregards conformational features. For example, if the donor acceptor property is modified, this

could lead to different hydrogen-bonding patterns of the inverted peptide formed in the backbone or from the backbone to its side chains. Second, due to the inverted orientation in the retro-inverso peptide, the interaction of the pharmacophoric groups with the receptor may not be possible anymore.

Table III-6: *Receptor assays of retro compounds **43-57** of cyclo(-X-isoDGR-G-).*

Code	Sequence	IC_{50} (α5β1) [nM]	IC_{50} (αvβ3) [nM]
54	*cyclo*(-G-RG*iso*D-Phg-)	>10000	>10000
57	*cyclo*(-G-RG*iso*D-**phg**-)	>10000	>10000

Table III-7: *Receptor assays of retro-inverso compounds **58-70** of cyclo(-X-isoDGR-G-).*

Code	Sequence	IC_{50} (α5β1) [nM]	IC_{50} (αvβ3) [nM]
67	*cyclo*(-G-**r**G***iso*d**-Phg-)	>10000	>10000
70	*cyclo*(-G-**r**G***iso*d**-**phg**-)	>10000	>10000

However, in the case of peptides containing the RG*iso*D, another structural influence must be considered. *Iso*Asp is considered a β-amino acid, because the Asp is connected via its side chain to the next amino acid. Hence, the backbone contains an additional methylene group. In cyclic *iso*DGR peptides this methylene group is located between the guanidinium and carboxylic group, while in cyclic RG*iso*D peptides it is not found between the pharmacophoric groups (see Figure III-2).

This structural difference might be the reason for inactivity as the number of atoms between the guanidinium and carboxylic group required for an integrin interaction was postulated to be 11 carbon atoms.[162] In the case of cyclic RG*iso*D peptides just 10 carbon atoms are present (see Figure III-2). Besides, in structure investigations the backbone conformations including the C_β atoms in active peptides are nearly analogous.[163] Hence, changes in the fixed backbone conformation affect the binding affinity.[121] Moreover, distance comparisons between C_β atoms of Arg and Asp indicate that 6.7 Å is most favorable for αvβ3 or α5β1 interaction.[164] For cyclic RG*iso*D peptides with the missing methylene group this distance probably cannot be achieved, which thus leads to inactivity. To verify this assumption, the structures of the peptides could be determined, and docked to both αvβ3 and α5β integrin binding pockets. In this way, it might be checked whether the distance of the pharmacophoric

groups is too short, or there is another reason for the inactivity of the compounds. However, this task remains for future research.
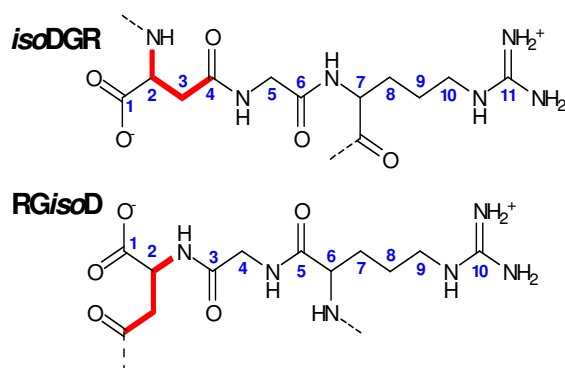
Figure III-2: Different distance between guanidinium and the carboxylic group. In the case of *iso*DGR the methylene group (3) of *iso*Asp in the backbone is involved in the distance needed for the binding whereas in the case of RG*iso*D the group is not in between the two pharmacophoric groups.

III.1.5. Influence of Distinct Position of the Aromatic Moiety

The position for the aromatic moiety in the approaches described above was chosen analogously to the position in the highly active peptide *c*(-RGDfV-). Hence, to test the influence of the position of the aromatic moiety, a library containing Phe (Table III-8, peptides **71**-**72**), Hphe (Table III-8, peptides **73**-**74**), and Phg (Table III-8, peptides **75**-**76**) next to the Arg was synthesized. After having demonstrated that activity was only gained when *iso*DGR is composed of L-amino acids no more D-amino acid scans were performed.

The compounds showed moderate affinity for αvβ3 and no activity for α5β1. Interestingly, the relative position of the *iso*DGR flanking residues (aromatic amino acid and Gly) determines the affinity of the pentapeptides to either αvβ3 or α5β1. This effect is mainly observed when the aromatic residue was introduced as a D-Phg, confirming the importance of the interaction of the aromatic group with the integrin binding pocket.

Moreover, these results prove that head-to-tail cyclized pentapeptides containing the *iso*DGR sequence are useful templates for targeting different integrin receptor subtypes. Even though the two key FN receptors αvβ3 and α5β1 share the same

ligand recognition motif, their function is not redundant. Upon FN binding they induce different cellular signals and behavior, which is important for many physiologic and pathophysiologic conditions such as wound healing, angiogenesis, and cancer metastasis.[136]

Table III-8: *Receptor assays of compounds **71-76** with one aromatic amino acids next to Arg compared to their analogues **18, 19, 22, 23, 26, 27**, and Cilengitide.*

Code	Sequence	IC_{50} (α5β1) [nM]		IC_{50} (αvβ3) [nM]	
71	*cyclo*(-**G**-*iso*DGR-**F**-)	816	(± 345)	168	(± 63)
72	*cyclo*(-**G**-*iso*DGR-**f**-)	>2000		521	(± 39)
18	*cyclo*(-**F**-*iso*DGR-**G**-)	>2000		633	(± 524)
19	*cyclo*(-**f**-*iso*DGR-**G**-)	838	(± 160)	377	(± 272)
73	*cyclo*(-**G**-*iso*DGR-**Hphe**-)	>1000		203	(± 49)
74	*cyclo*(-**G**-*iso*DGR-**hphe**-)	558	(± 105)	102	(± 45)
22	*cyclo*(-**Hphe**-*iso*DGR-**G**-)	>2000		>1000	
23	*cyclo*(-**hphe**-*iso*DGR-**G**-)	83	(± 21)	410	(± 107)
75	*cyclo*(-**G**-*iso*DGR-**Phg**-)	>2000		467	(± 162)
76	*cyclo*(-**G**-*iso*DGR-**phg**-)	406	(± 191)	89	(± 19)
26	*cyclo*(-**Phg**-*iso*DGR-**G**-)	57	(± 8)	753	(± 150)
27	*cyclo*(-**phg**-*iso*DGR-**G**-)	19	(± 4)	>1000	
	Cilengitide	15	(± 3)	0.54	(± 0.15)

To further understand the selectivity profile of the most interesting peptides **27** and **76**, due to their opposite integrin affinities, their structures were determined by solution-state NMR spectroscopy and molecular dynamics (MD) calculations,[165, 166] and docked to the αvβ3 and the α5β1 receptors, respectively. In the case of αvβ3 an X-ray structure of the cilengitide-αvβ3 complex[74] was used for docking, whereas for α5β1 only an homology model[135] was available.

According to docking results, **27** binds to the α5β1 receptor with the *iso*Asp carboxylate group coordinating the metal ion at the MIDAS, and the Arg guanidinium moiety establishing a bidentate salt bridge with (α5)-Asp²²⁷ and a H-bond with the backbone CO of (α5)-Ala²²² (see Figure III-4). An additional H-bond was detected between the Gly NH of the peptide and the (β1)-Ser²²¹ side chain. Interestingly, the D-

Phg is in the proximity of (β1)-Tyr[127] (rings centroids distance 5.6 Å) and a π-π interaction is likely to occur.
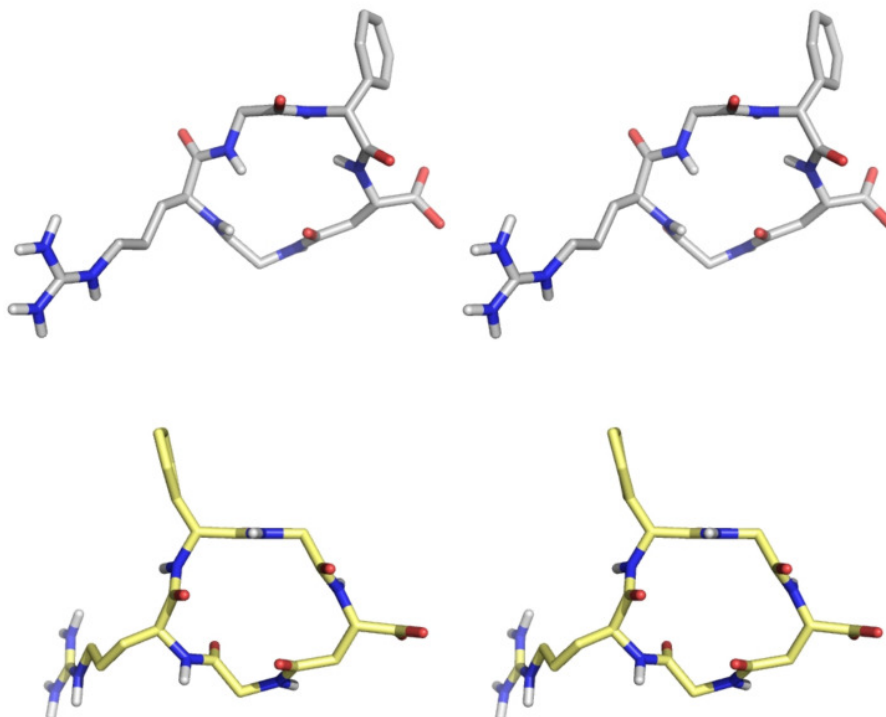
Figure III-3: Stereostructures of the cyclic pentapeptides **27** (top) and **76** (bottom) containing the *iso*DGR motif which binds to different integrin receptor subtypes. The peptide **27** *c*(-phg-*iso*D-G-R-G-) shows nanomolar affinity towards α5β1 whereas **76** *c*(-G-*iso*D-G-R-phg-) binds better to αvβ3 integrin.

Notably, the D-Phg points towards the wide pocket below the SDL, which consists of amino acids (β1)-Leu[219], (β1)-Ser[171], and (β1)-Gly[217]. The predicted binding mode could explain the observed high activity of **27** towards the α5β1 receptor. The above-described favorable binding mode of **27** cannot be found in the αvβ3 receptor due to the fact that the pocket below the SDL is remarkably narrower in αvβ3 compared to α5β1 due to the substitution of (β1)-Leu[219], (β1)-Ser[171], and (β1)-Gly[217] by (β3)-Arg[216], (β3)-Tyr[166], and (β3)-Arg[214] respectively. Indeed, targeting the α5β1-selective region was successful.[135] Moreover, docking calculations of **27** into the αvβ3 receptor suggest a certain difficulty for the Arg guanidinium group to insert into the narrow groove at the top of the propeller domain, where salt bridges to Asp[218] and/or Asp[150] should occur. Probably, this is due to the specific conformation of the peptidic cycle together with the forced position of the phenyl ring which cannot occupy the wide pocket below the SDL. This is characteristic for the α5β1 receptor.

This evidence together with the unfavorable position of the Phg phenyl ring seems to be the reason for the low affinity to the αvβ3 receptor.
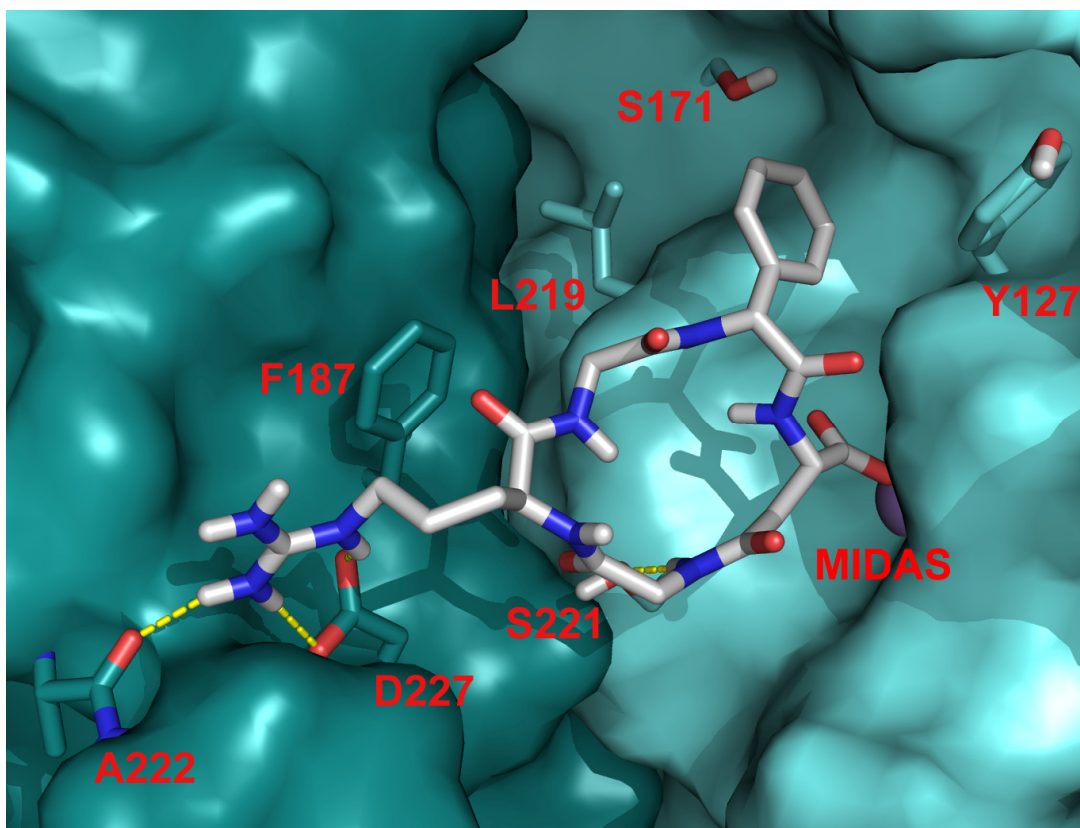
Figure III-4: Docked structure of **27** (white) in the α5β1 integrin binding pocket. The α5 and β1 subunits are represented by the deep and light cyan surface, respectively. In both subunits, amino acid side chains relevant for the ligand binding are highlighted as sticks. The metal ion in the MIDAS region is represented by a purple sphere.

Conversely, besides the interaction with the metal ion and with (αv)-Asp[218] (see Figure III-5), the lowest energy conformation of **76**, which bound to αvβ3, places the D-Phg between the (αv)-Tyr[178] and (β3)-Tyr[166] aromatic side chains. In particular, the hydroxyl groups of both Tyr residues point towards the edge of the D-Phg ring, establishing favorable interactions while an H-bond is formed between the D-Phg NH and the (αv)-Tyr[178] OH. An alternative binding conformation close in energy to the lowest energy structure places the D-Phg in the same pocket but forming a cation-π interaction with the (β3)-Arg[214] side chain (see Figure III-6).
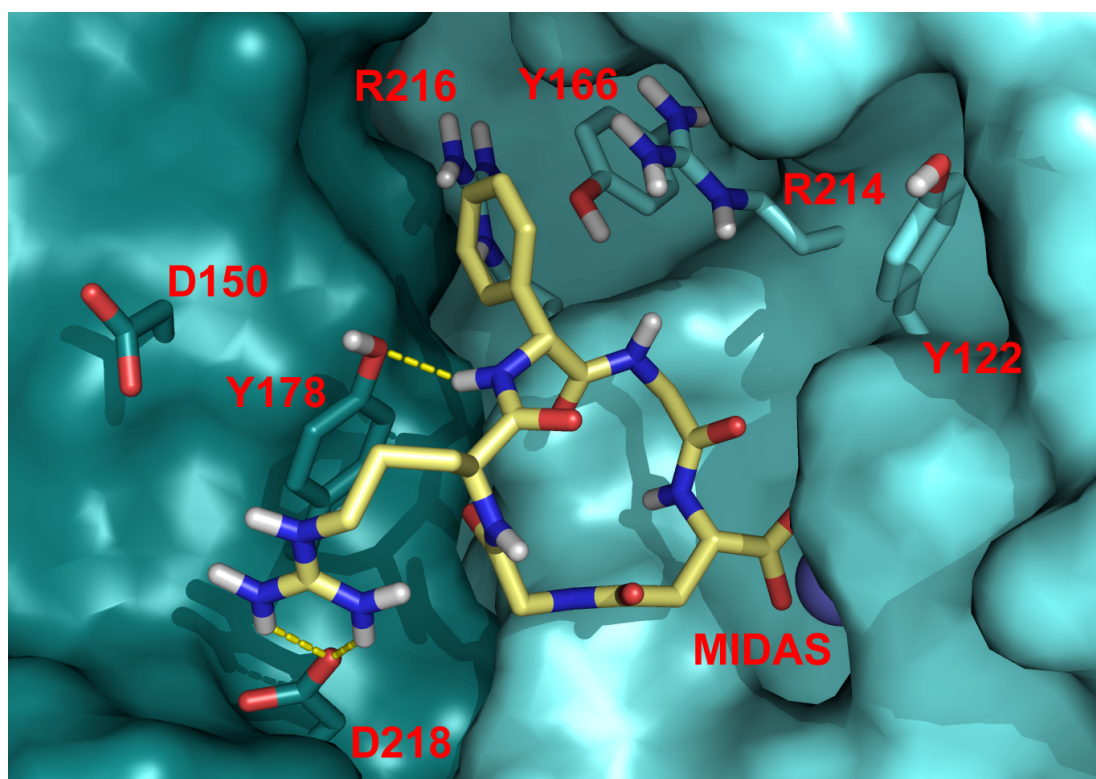
Figure III-5: Docked structure of **76** (pale yellow) in the αvβ3 integrin binding pocket. The αv and β3 subunits are represented by the blue and cyan surface, respectively.

Docking studies of **76** in the α5β1 receptor resulted in an ambiguous position of the Phg aromatic ring within the RGD binding pocket. Indeed, two main positons were found, which have in common the interactions with metal in the MIDAS and with the Asp^{227} side chain, and which primarily differ in the orientation of the Phg aromatic ring (see Figure III-7).

Interestingly, the two binding modes show similar free energy of binding and this is in perfect line with the observation that in both orientations the Phg aromatic ring of **76** does not engage in any strong interaction with the receptor residues as found when docking of **76** was performed in αvβ3. Thus, it seems that the favorable interactions between the Phg aromatic ring of **76** and the (αv)-Tyr^{178}, (β3)-Tyr^{166}, and (β3)-Arg^{214} residues, which are characteristic for αvβ3, are the reason for a higher binding to the αvβ3 receptor.
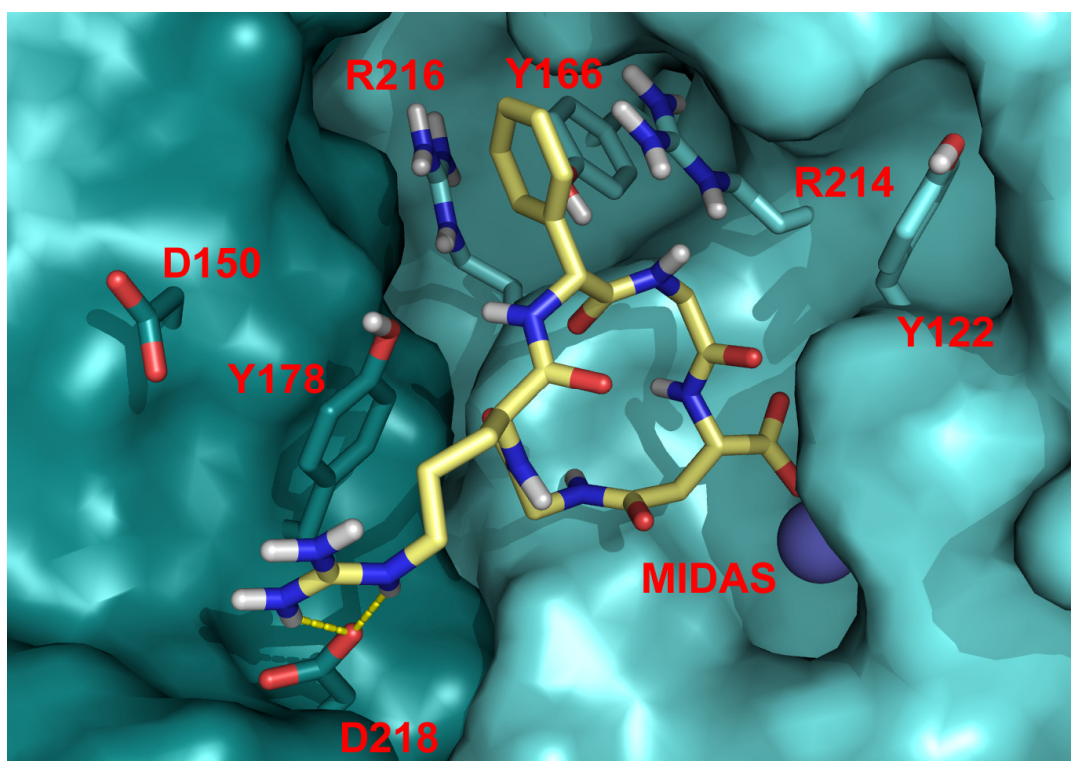
Figure III-6: Docked structure (alternative pose) of **76** (pale yellow) in the αvβ3 integrin binding pocket. The αv and β3 subunits are represented by the blue and cyan surface respectively. In both subunits amino acid side chains important for the ligand binding are highlighted as sticks. The metal ion in the MIDAS region is represented by a purple sphere.
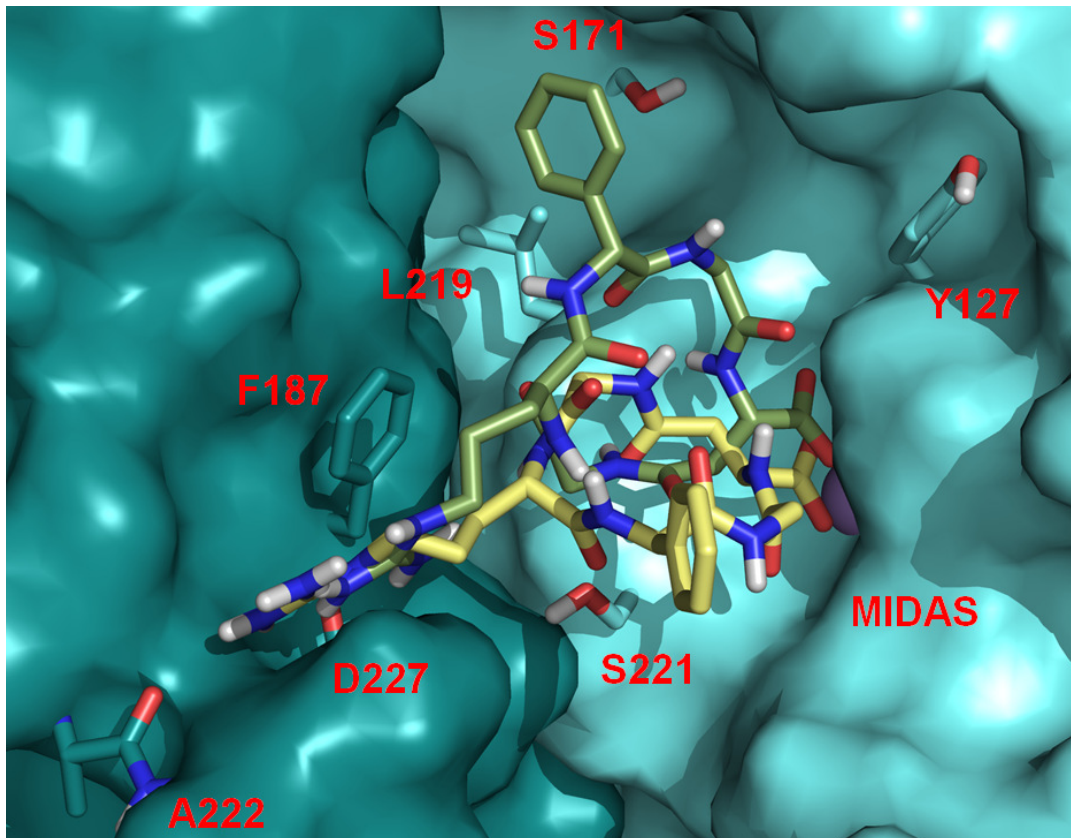
Figure III-7: The two main binding poses of **13** (yellow and green) in the α5β1 integrin binding pocket.

Integrin selective compounds may be used to target cells which express a specific integrin profile, as exemplified by the success of the αvβ3 and α5β1 selective drug Cilengitide. In order to test the binding capacity and specificity of compounds **27** and **76** also on living cells, mouse fibroblasts were pre-incubated expressing either only αvβ3 or only α5β1 with increasing concentrations of **27** and **76** before plating them on FN. The reduction of cell binding to FN via αvβ3 or α5β1 is relative to the binding constants of the cyclic peptides to the respective integrins (see Figure III-8 and Table III-9).
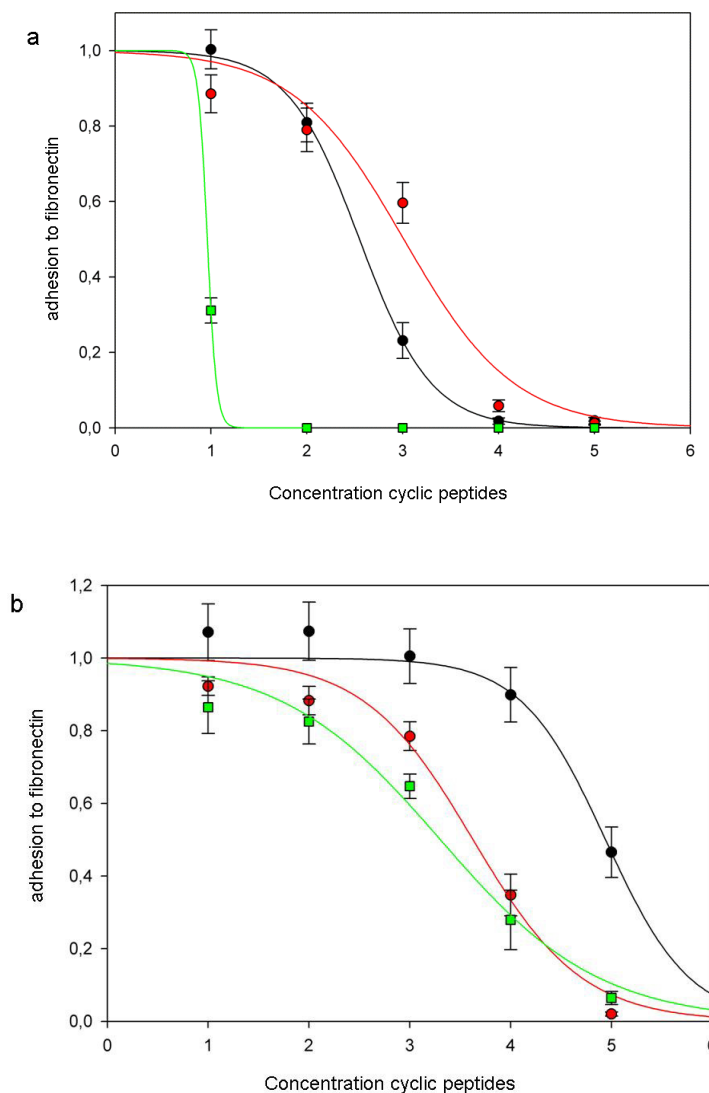
Figure III-8: *a)* Blocking assay of Cilengitide (green), **27** (red) and **76** (black) with αvβ3 expressing cells. *b)* Assay with α5β1 expressing cells; 1 = 10 nM, 2 = 100 nM, 3 = 1000 nM, 4 = 10000 nM, 5 = 100000 nM

Note that due to the different expression levels of integrins on the different cell lines (left and right column), only relative binding activities can be compared (see Table III-9). However, the data correlate nicely with the competitive solid-phase binding ELISA assay (see Tab. V-20).

For **27** the IC_{50} concentration for blocking α5β1 was approximately 20 fold lower than for **76**, but similar to the reference Cilengitide. On the other hand, the IC_{50} concentration for blocking αvβ3 was approximately 3 fold lower for **76** than for **27**.

Table III-9: Binding activities of head-to-tail cyclized *iso*DGR pentapeptides to mouse fibroblasts with selective expression of either α5β1 or αvβ3 integrin heterodimers.

Code	Sequence	IC_{50} (α5β1) [nM]	IC_{50} (αvβ3) [nM]
27	cyclo(-**phg**-*iso*DGR-**G**-)	4.2	1.0
76	cyclo(-**G**-*iso*DGR-**phg**-)	87	0.35
	Cilengitide	2.0	0.009

In summary, it was demonstrated that in agreement with binding constants measured with purified soluble receptors, the compounds **27** and **76** target α5β1 and αvβ3 selectively on cells. To the best of our knowledge, **27** is the first reported cyclic peptide based on a retro RGD sequence with nanomolar activity and selectivity for α5β1 reported. There are just some peptides found in cellular assays showing a similar activity, e.g., c(CRRETAWAC)[167] and in cyclic RGD peptides with β-amino acids.[168, 169] Such a biological profile could help to clarify the molecular basis of the cancer inhibitory effect of Cilengitide. Indeed, it is not fully understood whether the antitumor activity of Cilengitide is due to its αvβ3 or α5β1 inhibition.

Peptides containing the NGR and *iso*DGR motif are being used to target and visualize tumor neo-vasculature,[148] which may be an important future tool for drug delivery and tumor therapy.[156] It was observed that a free α-amino group next to the *iso*DGR lowers affinity whereas acetylation of this group increased the affinity but caused loss of specificity.[153] Head-to-tail cyclic *iso*DGR peptides are without a free α-amino groups, therefore a direct comparison of the stereochemistry and chemistry of the flanking residues is possible. The relative rigidity of the small cyclic peptides gives evidence that the aromatic substituent in the flanking amino acids is important for selectivity of these peptides for αvβ3 or α5β1 integrins, respectively. Furthermore,

the orientation of the crucial residues has been investigated and evidence for stereochemical control of activity is given. Hence, the findings are of interest for a rational design of *iso*DGR drug conjugates as well as for fusion proteins. Furthermore, these results are essential for a design of proteins using the NGR-*iso*DGR rearrangement as a controlled switch of binding affinities for different integrin subtypes in *in vivo* studies.

III.1.6. Design of Linear Peptides

Cyclization of peptides is a commonly used method to fix the biological conformation, and enhance their metabolic stability.[20] But fixation of the bioactive structure also leads to compounds which are not able to fit into a binding pocket. In contrast, linear peptides are more flexible, and therefore have more options to fit into a binding pocket. Hence, a small library of linear peptides was synthesized, based on the most active compounds **27** and **76** (see Table III-10).

Table III-10: *Receptor assays of linear peptides* **77-82**.

Code	Sequence	IC_{50} (α5β1) [nM]		IC_{50} (αvβ3) [nM]	
77	Ac-**phg**-*iso*DGR-G-OH	147	(± 55)	>10000	
78	Ac-*iso*DGR-G-**phg**-OH	1359	(± 704)	255	(± 110)
79	Ac-G-**phg**-*iso*DGR-OH	342	(± 144)	>10000	
80	Ac-G-*iso*DGR-**phg**-OH	454	(± 322)	600	(± 74)
81	Ac-**phg**-G-*iso*DGR-OH	297	(± 145)	>10000	
82	Ac-*iso*DGR-**phg**-G-OH	361	(± 139)	5677	(± 1905)

The peptides showed moderate to no affinity towards the integrins αvβ3 and α5β1. Even though the linear peptides have more conformational flexibility, they have lost activity and selectivity for both integrins. Hence, it could be shown that cyclization of *iso*DGR peptides is necessary to achieve integrin binding affinity. Additionally, the linear peptide NH_2-G*iso*DGRGGRVY-OH, analyzed by *Curnis et al.,*[153] also showed less affinity compared to its cyclic analogue. Therefore, further investigation of linear peptides containing the *iso*DGR sequence was not pursued.

III.1.7. Impact of Different Amino Acids on Distinct Position

The aromatic moiety of Phe in the *cyclo*(-RGDfV-) peptide is essential for the αvβ3 integrin binding, while Val can be replaced by other amino acids without affecting receptor affinity.[121] In the case of cyclic *iso*DGR peptides, an aromatic group also appears to be important for an integrin interaction. Moreover, the relative position of the aromatic moiety determines the affinity of the pentapeptides to either αvβ3 or α5β1. Nevertheless, to determine the influence of other amino acids on the binding ability to integrins, two libraries were synthesized. In one case, different amino acids were inserted next to isoAsp while Gly next to Arg was maintained (Table III-11). In the other case, the amino acid next to Arg was exchanged keeping Gly next to isoAsp (Table III-12).

Table III-11: *Receptor assays of tested compounds **83-94** with diverse amino acids next to isoAsp.*

Code	Sequence	IC_{50} (α5β1) [nM]		IC_{50} (αvβ3) [nM]	
84	*cyclo*(-**a**-*iso*DGR-G-)	227	(± 22)	11	(± 2)
86	*cyclo*(-**v**-*iso*DGR-G-)	84	(± 21)	53	(± 3)
87	*cyclo*(-P-*iso*DGR-G-)	862	(± 348)	145	(± 25)
88	*cyclo*(-**p**-*iso*DGR-G-)	3365	(± 211)	437	(± 81)
94	*cyclo*(-**w**-*iso*DGR-G-)	23	(± 1)	29	(± 2)

Interestingly, compounds **84**, **96**, and **98** showed nanomolar activity for αvβ3 though with moderate selectivity, while **94** is biselective with good affinity for both αvβ3 and α5β1 integrins.

Within the **83-94** series, the compounds tested show higher affinities towards αvβ3 than to α5β1, suggesting that Phg next to *iso*Asp is important for α5β1 integrin interaction. The biselective peptide **94** with tryptophan also shows that an aromatic moiety in this position is needed to gain α5β1 activity.

From the peptides **95-104**, those which are already tested are highly active for αvβ3. For this reason, D-Phg or an aromatic residue next to Arg seems to be essential for αvβ3 integrin binding. However, for better insight in the influence of the amino acids on the integrin affinity the complete biological data would be needed.

Table III-12: *Receptor assays of compounds **94-104** with diverse amino acids next to Arg.*

Code	Sequence	IC_{50} (α5β1) [nM]	IC_{50} (αvβ3) [nM]
96	*cyclo*(-G-*iso*DGR-**a**-)	315 (± 136)	4.4 (± 1.1)
98	*cyclo*(-G-*iso*DGR-**v**-)	34 (± 13)	1.6 (± 0.1)
100	*cyclo*(-G-*iso*DGR-**p**-)	60 (± 1)	13 (± 2)

III.1.8. Optimization via Combination of Different Approaches

The first results of the previous libraries raise the question if sequence combination of the most active compounds would lead to higher affinity. As **83**, **96**, and **98** have the highest activity for αvβ3, one peptide with two D-Ala flanking the *iso*DGR sequence (Table III-13, peptide **105**) and one peptide with a D-Ala next to *iso*Asp and a D-Val next to Arg (Table III-13, peptide **106**) were synthesized.

In the case of α5β1, D-Phg next to *iso*Asp seemed to be important. Hence, one peptide with D-Val (Table III-13, peptide **107**) and D-Pro (Table III-13, peptide **108**) next to Arg were synthesized, as **98** and **100** have good affinity for the α5β1 integrin.

Table III-13: *Receptor assays of compounds **105-108** combining different amino acids.*

Code	Sequence	IC_{50} (α5β1) [nM]	IC_{50} (αvβ3) [nM]
105	*cyclo*(-**a**-*iso*DGR-**a**-)	>10000	1238 (± 125)
106	*cyclo*(-**a**-*iso*DGR-**v**-)	167 (± 64)	721 (± 160)
107	*cyclo*(-**phg**-*iso*DGR-**v**-)	7.3 (± 0.8)	>10000
108	*cyclo*(-**phg**-*iso*DGR-**p**-)	7.0 (± 0.1)	>10000

Unfortunately, compounds **105** and **106** showed no improvement. They even lost affinity for both integrins. Here, one cause for this might be the slight differences in the αvβ3 testing system of our group and that of the Jerini AG. For this reason, direct comparison of results was not possible in the majority of cases with *iso*DGR peptides. Note that for RGD peptides and mimetics, the results are similar.

In contrast, compounds **107** and **108** exhibit a nearly 3 fold higher α5β1 activity than compound **26** but with higher selectivity. To our knowledge, these peptides are

among the most active and selective cyclic peptide ligands for α5β1 integrin reported so far.

Based on these promising results for α5β1, the next step was to test whether the change from a D-amino acid to an L-amino acid in compounds **107** and **108** would have an effect on the binding ability (Table III-14, peptides **109, 110**). Additionally, this D-amino acid was replaced by other amino acids, which could later be functionalized (Table III-14, peptides **111-118**). Functionalized peptides might be useful for coating of biomaterials or to can be radiolabeled and used for tumor imaging.

Table III-14: *Receptor assays of compounds **109-118** with **phg** and different amino acids next to R.*

Code	Sequence	IC_{50} (α5β1) [nM]		IC_{50} (αvβ3) [nM]	
109	*cyclo*(-**phg**-*iso*DGR-V-)	115	(± 15)	576	(± 49)
110	*cyclo*(-**phg**-*iso*DGR-P-)	111	(± 9)	675	(± 104)
111	*cyclo*(-**phg**-*iso*DGR-K-)	94	(± 4)	516	(± 41)
112	*cyclo*(-**phg**-*iso*DGR-**k**-)	8.7	(± 0.7)	>10000	
113	*cyclo*(-**phg**-*iso*DGR-E-)	92	(± 10)	3871	(± 435)
114	*cyclo*(-**phg**-*iso*DGR-**e**-)	11	(± 2)	>10000	
115	*cyclo*(-**phg**-*iso*DGR-Y-)	39	(± 3)	>10000	
116	*cyclo*(-**phg**-*iso*DGR-**y**-)	8.7	(± 1.6)	>10000	
117	*cyclo*(-**phg**-*iso*DGR-W-)	72	(± 10)	>10000	
118	*cyclo*(-**phg**-*iso*DGR-**w**-)	5.5	(± 1.2)	>10000	

Remarkably, peptide **118** with tryptophan exhibits a higher activity and selectivity for α5β1 integrin compared to **107** and **108**. Consequently, this compound is so far the most active and selective cyclic peptide ligand for α5β1 integrin. It is even in the range of the best α5β1 mimetics found in our group.[113] This demonstrates that a switch from peptides to mimetics to gain improvement on the binding ability is not always necessary. In contrast, the good water solubility of peptides makes them even more attractive for drug development.

All peptides with L-amino acids showed lower affinity and selectivity for α5β1 than their D-amino acid analogues. Gly is known to act almost as a D-amino acid and an exchange with D-amino acids has no substantial effect on the backbone configuration

of the peptide.[46] Therefore, it is not surprising that the replacement of Gly with D-amino acids leads to higher affinity compared to L-amino acids where the configuration might change.

Therefore, **112** *cyclo*(-phg-*iso*DGR-k-), was chosen for structure determination and docking investigations, because of its ability to add further functionalities via a linker. These investigations are still in progress. Additionally, **111** *cyclo*(-phg-*iso*DGR-K-) was selected for further research to determine the influence of the D- and L-residues. The docking experiments and cellular experiments will give more insight into the binding ability of these peptides.

As a next step, an N-methyl scan of **112** might, similarly to cilengitide, lead to further improvements in activity, selectivity and in oral bioavailability.

III.1.9. Design of Cyclic Hexapeptides

The results of the cyclic pentapeptides cause interest for the frequently used hexapeptides to determine if they also would lead to high affinity for αvβ3 and α5β1 integrins. Again, the FN-I$_5$ GNGRG loop was used as starting sequence, and one amino acid was added (see Table III-15).

So far, the compounds tested showed moderate to high affinity and selectivity for αvβ3. Only **121** is biselective with moderate activity for both αvβ3 and α5β1 integrins. However, for better prediction and potential optimization the complete biological data would be required.

Table III-15: *Receptor assays of cyclic hexapeptides **119-134**.*

Code	Sequence	IC_{50} (α5β1) [nM]		IC_{50} (αvβ3) [nM]	
119	*cyclo*(-G-*iso*DGR-G-A-)	590	(± 260)	7	(± 1)
120	*cyclo*(-G-*iso*DGR-G-**a**-)	356	(± 149)	4	(± 1)
121	*cyclo*(-G-*iso*DGR-G-V-)	55	(± 19)	51	(± 32)
122	*cyclo*(-G-*iso*DGR-G-**v**-)	106	(± 191)	86	(± 35)
123	*cyclo*(-G-*iso*DGR-G-P-)	893	(± 214)	20	(± 1)
124	*cyclo*(-G-*iso*DGR-G-**p**-)	1156	(± 441)	21	(± 22)

III.2.   Design of αvβ6 Selective Integrin Ligands

The integrin αvβ6 is expressed exclusively in epithelial cells. It binds via the RGD recognition sequence to its ligands, including the matrix proteins FN[170], tenascin[171], and vitronectin,[172] but also to the latency-associated peptide of transforming growth factor-β (TFG-β).[173] αvβ6 is generally not detectable on normal adult epithelial cells but is rapidly up-regulated during tissue remodeling, including inflammatory events[174], wound healing,[175] and tumor proliferation[176, 177] Based on this behavior and its presence in many carcinomas it should be considered as a potential therapeutic target[177]. To identify the precise role of integrins in diseases, highly active, specific, and well-defined inhibitors are required.

To enable the design of αvβ6 integrin ligands, a quick structure comparison of αvβ3 and αvβ6 was performed by *Luciana Marinelli* from the Università di Napoli "Federico II, Napoli".
The main difference between the SDL of αvβ3 and αvβ6 seems to be the larger binding pocket of αvβ6. This is due to the substitution of Tyr^{122} in αvβ6 by Ala. This Tyr is important for a π-π interaction between the D-Phe of Cilengitide with αvβ3 and therefore the substitution of Phe with a bulkier group or with D-Pro should be tolerated in αvβ6 but not in αvβ3. On the other hand, two Arg in αvβ3 are substituted with Ala and Ile, similarly to α5β1, hence the binding pocket of αvβ6 is larger than the binding pocket of αvβ3.

Due to the larger binding pocket of αvβ6, cyclo(-RGD**x**V-) peptides including a natural amino acid with bulkier side chains instead of Phe were synthesized (see Table III-16). The project was done in cooperation with Merck KGaA, Berlin, which performed the biological testing.

Table III-16: *Receptor assays of model peptides **135-138, 27 & 76**.*

Code	Sequence	IC_{50} (αvβ6) [nM]
Cilengitide	*cyclo*(-RGD-**f**-NMeV-)	~25000
135	*cyclo*(-RGD-**p**-V-)	>17000
136	*cyclo*(-RGD-**I**-V-)	~11000
137	*cyclo*(-RGD-**i**-V-)	>17000
138	*cyclo*(-RGD-**nle**-V)	~ 6500
27	*cyclo*(-**phg**-*iso*DGR-G-)	~11000
76	*cyclo*(-G-*iso*DGR-**phg**-)	>17000

Unfortunately, the tested compounds are inactive towards the αvβ6 integrin. Hence, the side chains of the natural amino acids might not be bulky enough. To verify this assumption, for example, a cyclic peptide containing an adamantan connected to the side chain might be a interesting approach. This however, is left for future research.

Nevertheless, the inactivity of **27** and **76** confirms their selectivity for α5β1 and αvβ3, respectively.

IV. Summary

In this thesis the rational design and the synthesis of head-to-tail-cyclized peptide libraries containing the new binding motive *iso*DGR is described. Moreover, insight and basic theories about the reasons for the observed difference in selectivity and activity of the created libraries were discussed.

The first approach imitated the sequence of the highly active *cyclo*(-RGDfV-) and the second mimicked the Gly-flanked NGR loop. However, the synthesized peptides showed only moderate activity or were completely inactive. In addition, it could be shown that the retro-inverso approach also leads to inactivity.

However, with the introduction of different aromatic residues (X) next to *iso*Asp in the cyclic pentapeptides *cyclo*(-X-*iso*DGR-G-), a potent candidate was found: compound **27** *cyclo*(-phg-*iso*DGR-G-) is both a highly active and a highly selective α5β1 ligand (see Table IV-1). In contrast, if the aromatic residue is located next to Arg, affinity for αvβ3 is gained, especially with compound **76** *cyclo*(-G-*iso*DGR-phg-) (see Table IV-1).

Table IV-1. Unequal influence of phenylglycine on integrin binding affinity.

Code	Sequence	IC_{50} (α5β1) [nM]	IC_{50} (αvβ3) [nM]
27	*cyclo*(-**phg**-*iso*DGR-**G**-)	19 (± 4)	>1000
76	*cyclo*(-**G**-*iso*DGR-**phg**-)	406 (± 191)	89 (± 19)

Head-to-tail-cyclized *iso*DGR peptides have no free α-amino groups, therefore a direct comparison of the stereochemistry and the influence of the flanking residues is possible. Here, the constrained small cyclic peptides influence the selectivity for αvβ3 or α5β1 integrins, depending on the flanking aromatic substituents. Furthermore, the orientation of the crucial residues has been investigated and their stereochemical control related to the activity could be shown. Moreover, the binding capacity and specificity of compounds **27** and **76** in living cells correlates nicely with the *in vitro* results.

Next, the influence of different amino acids was investigated revealing that Phg or an aromatic residue next to *iso*Asp is important in order to achieve interactions with α5β1. Otherwise, the compounds show good αvβ3 activity.

In order to improve the integrin affinity, the flanking amino acids of the most active compounds were combined, which in the case of α5β1 was successful with compounds **107** *cyclo*(-phg-*iso*DGR-v-) and **108** *cyclo*(-phg-*iso*DGR-p-). Their activity increased about three fold compared to compound **27**. Interestingly, the use of two *iso*DGR flanking D-amino acids leads to improved activity and higher selectivity. Furthermore, the change of the Arg neighboring group seems to have marginal effects on the α5β1 interaction. Compound **118** *cyclo*(-**phg**-*iso*DGR-**w**-) was revealed to be the most active and selective peptidic α5β1 ligand reported in the literature so far. Its activity and selectivity are even in the affinity range found for highly active mimetics.

Further, linear peptides were synthesized to determine their biological activity. Although the linear peptides are more flexible and therefore might fit easier in the binding pocket, they loose activity compared to their cyclic analogues. In contrast, the synthesized cyclic hexapeptides exhibit good αvβ3 affinity.

Recently, the αvβ6 integrin has been found to be present in many carcinomas making it an interesting potential therapeutical target. Based on the sequence cyclo(-RGD**x**V-), peptides with bulkier side chains were synthesized, as the binding pocket of αvβ6 is larger than that of αvβ3. Unfortunately, these compounds were completely inactive. Nevertheless, for compounds **27** and **76,** their selectivity could be shown for α5β1 and αvβ3, respectively. Despite the inactivity, the finding of potential αvβ6 inhibitors is still of great interest.

In summary, the discovery of highly active and selective compounds is of interest for the rational design of *iso*DGR drug conjugates as well as for fusion proteins. Furthermore, these results are essential for the design of proteins using the NGR-*iso*DGR rearrangement as a controlled switch of binding affinities for different integrin subtypes in *in vivo*.

V. Experimental Section

V.1. Materials and Methods

Mass spectra were obtained by *electrospray ionization* (ESI).

HPLC-ESI-MS spectra were recorded on a *Finnigan LCQ* combined with an HPLC system *Hewlett Packard HP1100* (column material: YMC-ODS-A C_{18}, 125 mm x 2 mm, 3 µm, flow rate: 0.2 mL / min).

HPLC-purifications was determined on the following system:
Pharmacia Basic 10 F, pump unit P-900, Detector UV-900, autosampler A 900, Software: Unicorn, Version 3.00; column material: YMC-ODS-A 120 5-C_{18} (8 µm, 250 x 4.6 mm), analytical.
HPLC-purifications were performed on the following system:
Pharmacia Basic 100 F, pump unit P-900, Detector UV-900, Software: Unicorn, Version 3.00; column material: YMC-ODS-A 120 10-C_{18} (10 µm, 250 x 20 mm) semipreparative; Different gradients of water and acetonitrile (+0.1% TFA) were used for HPLC separations.

Solid phase peptide synthesis and other reactions on solid phase with less than 1 g resin were performed in syringes (*Becton-Dickinson*) equipped with a polypropylene frit (*Vetter Labortechnik*). The loaded syringes were stuck into a rubber stopper connected to the rotor of a rotary evaporator and mixed by gentle rotation.

^{1}H-NMR and **^{13}C-NMR** spectra were recorded on Bruker DMX500 spectrometers. Chemical shifts (δ) are given in *parts per million* (ppm) relative to trimethylsilane (TMS). The following solvent peaks were used as internal standards: DMSO-d_6: 2.50 ppm (^{1}H-NMR) and 39.46 ppm (^{13}C-NMR). The assignment of protons and carbons was performed using 2D spectra (TOCSY, ROESY, E.COSY, HMBC).

V.2. General Procedures

V.2.1. GP1 (Loading of TCP-Resin)[178]

Chloro-TCP-resin (theoretical loading 0.94 mmol/g) was filled into a suitable syringe (20 mL for 1 g resin) equipped with a PP-frit and a canula. Fmoc-Arg(Pbf)-OH (1.2 eq, referring to theoretical loading) was dissolved in dry DCM (8 mL/g resin), treated with DIEA (2.5 eq., referring to amino acid), and sucked directly into the syringe with the resin and mixed by gentle rotation for 1 h. The remaining trityl chloride groups were capped by adding 0.2 mL methanol (per gram resin) and 0.2 eq. DIEA was added to the reaction mixture and was shaking the mixture for 15 min. The resin was washed thoroughly with DCM (3×), DMF (3×), NMP / methanol 1 : 1 (1x), and pure methanol (5×). After drying under vacuum, the resin was weighted and the real loading calculated with following equation:

$$c[mol/g] = \frac{m_{total} - m_{re\sin}}{(MW - 36.461) \times m_{total}}$$

Equation V-1: Calculation of resin loading. m_{total} = mass of loaded resin. m_{resin} = mass of unloaded resin. MW = molecular weight of immobilized amino acid.

To improve the reaction time, the loading was not calculated, hence an average loading of 0.5 mmol / g was assumed.

V.2.2. GP2 (Solid Phase Fmoc Deprotection)[52]

For Fmoc deprotection, the washed and swollen resin was treated twice with a solution of piperidine (20%) in NMP (v/v), 5 min and 15 min, respectively and washed 5 times with NMP.

V.2.3. GP3 (Solid Phase Peptide Coupling with HOBt / TBTU)[58]

The amino acid (2.5 eq., referring to resin loading) was dissolved for the coupling reaction in a 0.2 M solution of HOBt and TBTU in NMP (2.5 eq.). After addition of DIEA (6.5 eq.), the solution was mixed with the resin and shaken for 1 h at room temperature. The mixture was discarded and the resin washed 5 times with NMP.

V.2.4. GP4 (Cleavage of Side-Chain-Protected Peptides from TCP-Resin)

To cleave the peptide, the resin was swollen in DCM and then treated with a solution of 20% HFIP in DCM. After shaking for 20 min, the procedure was repeated twice and finally the resin was washed once with DCM. The collected solutions were concentrated *in vacuo*.

V.2.5. GP5 (Cleavage and Full Deprotection of Peptides from TCP-Resin)

The resin was swollen in DCM and then treated 3 times with a mixture of DCM, TFA, water and triisopropylsilane (47.5%, 47.5%, 2.5%, 2.5%, v/v/v/v) for 30 min. The combined solutions were monitored by ESI-MS until full deprotection was observed. The solvents were evaporated under reduced pressure and the crude product directly subjected to HPLC-purification on *reverse-phase* silica gel.

V.2.6. GP6 (Backbone Cyclization of Peptides Using DPPA)[17]

The linear, side-chain protected peptide was diluted with DMF to 10^{-3} - 10^{-4} M. After addition of DPPA (3 eq.) and $NaHCO_3$ (5 eq.), the mixture was stirred until all starting material was consumed (HPLC / LC-MS monitoring), usually 12 h. The solution was concentrated under reduced pressure and the cyclic peptide precipitated by addition of water. In case of an improper precipitation, water was substituted with brine. The peptide was spun down in a centrifuge, washed twice with water and dried under vacuum.

V.2.7. GP7 (Backbone Cyclization of Peptides Using HATU/HOBt)[44]

The linear, side-chain protected peptide was diluted with DMF to 10^{-3} - 10^{-4} M. After addition of HATU (3 eq.), HOBt (3 eq.), and Collidin (3 eq.), the mixture was stirred until all starting material was consumed (HPLC / LC-MS monitoring), usually 12 h. The solution was evaporated under reduced pressure and the cyclic peptide precipitated by addition of ethyl acetate. The solution was washed twice with a saturated solution of sodium hydrogen carbonate and once with brine. Finally the organic phase was dried under vacuum.

V.2.8. GP8 (Full Deprotection of Cyclic Peptides)

The cyclic peptide was treated with a mixture of TFA, water, triisopropylsilane (95%, 2.5%, 2.5%, v/v/v) for 3 h. The deprotected peptide was precipitated by adding diethyl ether and spun down in a centrifuge. Then washed twice with ether and dried under vacuum. The deprotection was monitored by ESI-MS.

The pure compound was obtained by *reversed-phase* high-performance liquid chromatography (RP-HPLC) purification. The peptides were characterized by ESI mass spectroscopy.

V.3. Preparation of Cyclic Peptides and Analytical Data for $\alpha v \beta 3$ and $\alpha 5 \beta 1$ Integrins
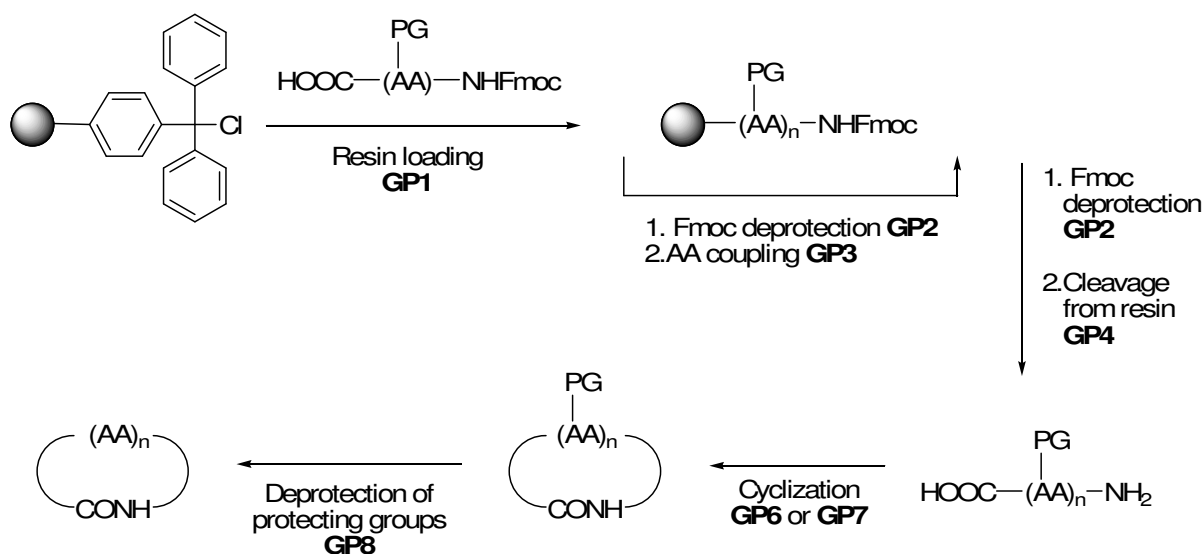
Scheme V-1: *Synthesis of cyclic peptides.*

The linear peptides were synthesized on TCP-resin (200 mg) according to the general procedures **GP1** (Loading), **GP2** (Fmoc-deprotection), **GP3** (Coupling), and **GP4** (Cleavage). In every case, Fmoc-L-Arg(Pbf)-OH or Fmoc-D-Arg(Pbf)-OH was coupled as first amino acid. The linear, side-chain protected peptides were cyclized and deprotected according to **GP6** and **GP8**. The crude peptides were purified by preparative *reverse phase* HPLC.

V.3.1. First *Iso*DGR Libraries Based on Cyclo(-RGDfV-)

Table V-1: *Amino acid building blocks used for solid phase synthesis*

Code	Amino acid	MW
R	Fmoc-Arg(Pbf)-OH	648.77
G	Fmoc-Gly-OH	297.31
*iso*D	Fmoc-Asp-O^{t}Bu	411.45
F	Fmoc-Phe-OH	387.43
A	Fmoc-Ala-OH	311.33
P	Fmoc-Pro-OH	337.37

Analytical data of the prepared peptides are presented in Table V-2.

Table V-2: *Analytical data of the compounds based on the highly active peptide cyclo(-RGDfV).*

Code	Sequence	ESI-MS m/z = [M+H]$^+$	HPLC (10-100%, 30 min) t_R [min]	Molecular formula
1	*cyclo*(-**f**-*iso*DGR-V-)	575.4	11.10	C$_{26}$H$_{38}$N$_8$O$_7$ MW = 574.63
2	*cyclo*(-F-**isod**GR-V-)	575.4	11.26	C$_{26}$H$_{38}$N$_8$O$_7$ MW = 574.63
3	*cyclo*(-F-*iso*D**G**R-V-)	575.4	11.27	C$_{26}$H$_{38}$N$_8$O$_7$ MW = 574.63
4	*cyclo*-(-F-*iso*DG**r**-V-)	575.4	11.22	C$_{26}$H$_{38}$N$_8$O$_7$ MW = 574.63
5	*cyclo*(-F-*iso*DGR-**v**-)	575.4	11.55	C$_{26}$H$_{38}$N$_8$O$_7$ MW = 574.63
6	*cyclo*(-**f**-*iso*DGR-VA-)	646.4	10.41	C$_{29}$H$_{43}$N$_9$O$_8$ MW = 645.71
7	*cyclo*(-F-**isod**GR-VA-)	646.4	10.33	C$_{29}$H$_{43}$N$_9$O$_8$ MW = 645.71
8	*cyclo*(-F-*iso*D**G**R-VA-)	646.4	8.00	C$_{29}$H$_{43}$N$_9$O$_8$ MW = 645.71
9	*cyclo*(-F-*iso*DG**r**-VA-)	646.4	10.11	C$_{29}$H$_{43}$N$_9$O$_8$ MW = 645.71
10	*cyclo*(-F-*iso*DGR-**v**A-)	646.4	10.56	C$_{29}$H$_{43}$N$_9$O$_8$ MW = 645.71
11	*cyclo*(-F-*iso*DGR-V**a**-)	646.4	10.16	C$_{29}$H$_{43}$N$_9$O$_8$ MW = 645.71
12	*cyclo*(-F-*iso*DGR-**p**V-)	672.5	11.46	C$_{31}$H$_{45}$N$_9$O$_8$ MW = 671.74
13	*cyclo*(-F-*iso*DGR-V**p**-)	672.4	11.07	C$_{31}$H$_{45}$N$_9$O$_8$ MW = 671.74
14	*cyclo*(-**p**-*iso*DGR-VF-)	672.5	11.11	C$_{31}$H$_{45}$N$_9$O$_8$ MW = 671.74

V.3.2. FN Loop as a New Pattern for *Iso*DGR Peptides

The series of compounds **15**-**22**, in which the structure mimics the GNGRG loop in FN were synthesized according to the general procedure **GP1**, **GP2**, **GP3**, **GP4**, **GP7,** and **GP8** (Scheme V-1) and purified by *reversed phase* HPLC. The analytical data of the prepared peptides is shown in Table V-3.

Table V-3: *Analytical data of the compounds mimicking the GNGRG loop in FN.*

Code	Sequence	ESI-MS m/z = [M+H]$^+$	HPLC (0-100%, 30 min) t_R [min]	Molecular formula
15	*cyclo*(-G-*iso*DGR-G-)	443.3	7.01	$C_{16}H_{26}N_8O_7$ MW = 442.43
16	*cyclo*(-G-**isod**GR-G-)	443.3	7.10	$C_{16}H_{26}N_8O_7$ MW = 442.43
17	*cyclo*(-G-*iso*DG**r**-G-)	443.3	7.17	$C_{16}H_{26}N_8O_7$ MW = 442.43

V.3.3. Investigation of the Importance of an Aromatic Moiety

In the series of compounds **23**-**34**, the Gly next to the *iso*Asp was replaced by one aromatic amino acid. They were synthesized according to the general procedure **GP1**, **GP2**, **GP3**, **GP4**, **GP7,** and **GP8** (Scheme V-1) using following building blocks (Table V-4). All compounds were purified by *reversed phase* HPLC.

Table V-4: *Unnatural amino acid building blocks.*

Code	Name	Building block structure	MW
Phg	Phenylglycine	FmocHN⟍ ⟋COOH	373.40
Hphe	Homophenylalanine	FmocHN⟍ ⟋COOH	401.45

The analytical data of the prepared peptides is shown in Table V-5.

Table V-5: *Analytical data of the compounds with one aromatic amino acid next to isoAsp.*

Code	Sequence	ESI-MS m/z = [M+H]$^+$	HPLC (0-100%, 30 min) t$_R$ [min]	Molecular formula
18	*cyclo*(-F-*iso*DGR-G-)	533.4	8.59	C$_{23}$H$_{32}$N$_8$O$_7$ MW = 532.24
19	*cyclo*(-**f**-*iso*DGR-G-)	533.6	8.02	C$_{23}$H$_{32}$N$_8$O$_7$ MW = 532.24
20	*cyclo*(-F-***iso*d**GR-G-)	533.4	8.67	C$_{23}$H$_{32}$N$_8$O$_7$ MW = 532.24
21	*cyclo*(-F-*iso*DG**r**-G-)	533.4	8.74	C$_{23}$H$_{32}$N$_8$O$_7$ MW = 532.24
22	*cyclo*(-Hphe-*iso*DGR-G-)	547.4	9.83	C$_{24}$H$_{34}$N$_8$O$_7$ MW = 546.58
23	*cyclo*(-**hphe**-*iso*DGR-G-)	547.4	9.54	C$_{24}$H$_{34}$N$_8$O$_7$ MW = 546.58
24	*cyclo*(-Hphe-***iso*d**GR-G-)	547.4	10.15	C$_{24}$H$_{34}$N$_8$O$_7$ MW = 546.58
25	*cyclo*(-Hphe-*iso*DG**r**-G-)	547.4	10.29	C$_{24}$H$_{34}$N$_8$O$_7$ MW = 546.58
26	*cyclo*(-Phg-*iso*DGR-G-)	519.3	6.83	C$_{22}$H$_{30}$N$_8$O$_7$ MW = 518.52
27	*cyclo*(-**phg**-*iso*DGR-G-)	519.2	6.95	C$_{22}$H$_{30}$N$_8$O$_7$ MW = 518.52
28	*cyclo*(-Phg-***iso*d**GR-G-)	519.3	7.18	C$_{22}$H$_{30}$N$_8$O$_7$ MW = 518.52
29	*cyclo*(-Phg-*iso*DG**r**-G-)	519.3	7.06	C$_{22}$H$_{30}$N$_8$O$_7$ MW = 518.52

V.3.4. The Retro-Inverso Approach

The inverso compounds **35**-**46** based on the *cyclo*(-X-*iso*DGR-G-) sequence, in which X represents the different aromatic amino acids, were synthesized according to the general procedure **GP1**, **GP2**, **GP3**, **GP4**, **GP7,** and **GP8** (Scheme V-1). All compounds were purified by *reversed phase* HPLC. The analytical data of the prepared peptides are shown in Table V-6.

Table V-6: *Analytical data of the inverso compounds of cyclo(-X-isoDGR-G-).*

Code	Sequence	ESI-MS $m/z =$ $[M+H]^+$	HPLC (0-100%, 30 min) t_R [min]	Molecular formula
30	*cyclo*(-G-**isod**G**r**-G-)	443.3	7.44	$C_{16}H_{26}N_8O_7$ MW = 442.43
31	*cyclo*(-**f**-**isod**GR-G-)	533.4	8.83	$C_{23}H_{32}N_8O_7$ MW = 532.24
32	*cyclo*(-**f**-*iso*DG**r**-G-)	533.3	8.63	$C_{23}H_{32}N_8O_7$ MW = 532.24
33	*cyclo*(-F-**isod**G**r**-G-)	533.3	8.16	$C_{23}H_{32}N_8O_7$ MW = 532.24
34	*cyclo*(-**f**-**isod**G**r**-G-)	533.4	8.75	$C_{23}H_{32}N_8O_7$ MW = 532.24
35	*cyclo*(-**hphe**-**isod**GR-G-)	547.4	10.09	$C_{24}H_{34}N_8O_7$ MW = 546.58
36	*cyclo*(-**hphe**-*iso*DG**r**-G-)	547.4	9.97	$C_{24}H_{34}N_8O_7$ MW = 546.58
37	*cyclo*(-Hphe-**isod**G**r**-G-)	574.4	9.72	$C_{24}H_{34}N_8O_7$ MW = 546.58
38	*cyclo*(-**hphe**-**isod**G**r**-G-)	547.4	9.97	$C_{24}H_{34}N_8O_7$ MW = 546.58
39	*cyclo*(-**phg**-**isod**GR-G-)	519.3	7.23	$C_{22}H_{30}N_8O_7$ MW = 518.52
40	*cyclo*(-**phg**-*iso*DG**r**-G-)	519.3	6.71	$C_{22}H_{30}N_8O_7$ MW = 518.52
41	*cyclo*(-Phg-**isod**G**r**-G-)	519.3	7.16	$C_{22}H_{30}N_8O_7$ MW = 518.52
42	*cyclo*(-**phg**-**isod**G**r**-G-)	519.3	7.36	$C_{22}H_{30}N_8O_7$ MW = 518.52

The retro compounds **47**-**58** based on the *cyclo*(-X-*iso*DGR-G-) sequence, in which X represents the different aromatic amino acids, were synthesized according to the general procedure **GP1**, **GP2**, **GP3**, **GP4**, **GP7,** and **GP8** (Scheme V-1). All compounds were purified by *reversed phase* HPLC. The analytical data of the prepared peptides is shown in Table V-7.
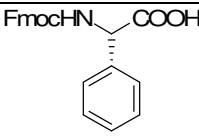
Table V-7: *Analytical data of the retro compounds of cyclo(-X-isoDGR-G-).*

Code	Sequence	ESI-MS m/z = [M+H]$^+$	HPLC (0-100%, 30 min) t_R [min]	Molecular formula
43	*cyclo*(-G-RG*isoD*-G-)	443.3	7.79	$C_{16}H_{26}N_8O_7$ MW = 442.43
44	*cyclo*(-G-**r**G*isoD*-G-)	443.3	7.49	$C_{16}H_{26}N_8O_7$ MW = 442.43
45	*cyclo*(-G-RG***isod***-G-)	443.3	7.45	$C_{16}H_{26}N_8O_7$ MW = 442.43
46	*cyclo*(-G-RG*isoD*-F-)	533.4	9.29	$C_{23}H_{32}N_8O_7$ MW = 532.24
47	*cyclo*(-G-**r**G*isoD*-F-)	533.4	9.19	$C_{23}H_{32}N_8O_7$ MW = 532.24
48	*cyclo*(-G-RG***isod***-F-)	533.4	9.31	$C_{23}H_{32}N_8O_7$ MW = 532.24
49	*cyclo*(-G-RG*isoD*-**f**-)	533.4	9.18	$C_{23}H_{32}N_8O_7$ MW = 532.24
50	*cyclo*(-G-RG*isoD*-Hphe-)	547.4	10.64	$C_{24}H_{34}N_8O_7$ MW = 546.58
51	*cyclo*(-G-**r**G*isoD*-Hphe-)	547.4	10.36	$C_{24}H_{34}N_8O_7$ MW = 546.58
52	*cyclo*(-G-RG***isod***-Hphe-)	547.4	10.61	$C_{24}H_{34}N_8O_7$ MW = 546.58
53	*cyclo*(-G-RG*isoD*-**hphe**-)	547.4	10.76	$C_{24}H_{34}N_8O_7$ MW = 546.58
54	*cyclo*(-G-RG*isoD*-Phg-)	519.3	8.18	$C_{22}H_{30}N_8O_7$ MW = 518.52
55	*cyclo*(-G-**r**G*isoD*-Phg-)	519.4	7.98	$C_{22}H_{30}N_8O_7$ MW = 518.52
56	*cyclo*(-G-RG***isod***-Phg-)	519.4	7.91	$C_{22}H_{30}N_8O_7$ MW = 518.52
57	*cyclo*(-G-RG*isoD*-**phg**-)	519.4	8.02	$C_{22}H_{30}N_8O_7$ MW = 518.52

The retro-inverso compounds **59**-**70** based on the *cyclo*(-X-*iso*DGR-G-) sequence, in which X represents the different aromatic amino acids, were synthesized according to the general procedure **GP1**, **GP2**, **GP3**, **GP4**, **GP7,** and **GP8** (Scheme V-1). All compounds were purified by *reversed phase* HPLC. The analytical data of the prepared peptides is shown in Table V-8.
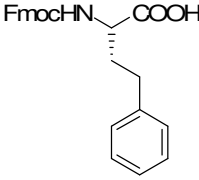
Table V-8: *Analytical data of the retro-inverso compounds of cyclo(-X-isoDGR-G-).*

Code	Sequence	ESI-MS m/z = $[M+H]^+$	HPLC (0-100%, 30 min) t_R [min]	Molecular formula
58	*cyclo*(-G-**rG***isod*-G-)	443.3	7.52	$C_{16}H_{26}N_8O_7$ MW = 442.43
59	*cyclo*(-G-**rG***isod*-F-)	533.3	9.34	$C_{23}H_{32}N_8O_7$ MW = 532.24
60	*cyclo*(-G-**rG***iso*D-**f**-)	533.3	9.00	$C_{23}H_{32}N_8O_7$ MW = 532.24
61	*cyclo*(-G-RG***isod*-f**-)	533.3	9.31	$C_{23}H_{32}N_8O_7$ MW = 532.24
62	*cyclo*(-G-**rG***isod*-**f**-)	533.3	9.46	$C_{23}H_{32}N_8O_7$ MW = 532.24
63	*cyclo*(-G-**rG***isod*-Hphe-)	547.4	10.66	$C_{24}H_{34}N_8O_7$ MW = 546.58
64	*cyclo*(-G-**rG***iso*D-**hphe**-)	547.4	10.47	$C_{24}H_{34}N_8O_7$ MW = 546.58
65	*cyclo*(-G-RG***isod*-hphe**-)	547.3	10.44	$C_{24}H_{34}N_8O_7$ MW = 546.58
66	*cyclo*(-G-**rG***isod*-**hphe**-)	547.3	10.47	$C_{24}H_{34}N_8O_7$ MW = 546.58
67	*cyclo*(-G-**rG***isod*-Phg-)	519.4	8.06	$C_{22}H_{30}N_8O_7$ MW = 518.52
68	*cyclo*(-G-**rG***iso*D-**phg**-)	519.4	7.90	$C_{22}H_{30}N_8O_7$ MW = 518.52
69	*cyclo*(-G-RG***isod*-phg**-)	519.4	8.00	$C_{22}H_{30}N_8O_7$ MW = 518.52
70	*cyclo*(-G-**rG***isod*-**phg**-)	519.3	8.20	$C_{22}H_{30}N_8O_7$ MW = 518.52

V.3.5. Influence of the Distinct Position of the Aromatic Moiety

In the series of compounds **71**-**77**, the Gly next to the Arg was replaced by one aromatic amino acid. They were synthesized according to the general procedure **GP1**, **GP2**, **GP3**, **GP4**, **GP7,** and **GP8** (Scheme V-1) and purified by *reversed phase* HPLC. The analytical data of the prepared peptides is shown in Table V-9.

Table V-9: *Analytical data of the compounds with one aromatic amino acid next to R.*

Code	Sequence	ESI-MS m/z = [M+H]$^+$	HPLC (0-100%, 30 min) t_R [min]	Molecular formula
71	*cyclo*(-G-*iso*DGR-F-)	533.4	8.20	$C_{23}H_{32}N_8O_7$ MW = 532.24
72	*cyclo*(-G-*iso*DGR-**f**-)	533.3	8.02	$C_{23}H_{32}N_8O_7$ MW = 532.24
73	*cyclo*(-G-*iso*DGR-Hphe-)	547.3	9.38	$C_{24}H_{34}N_8O_7$ MW = 546.58
74	*cyclo*(-G-*iso*DGR-**hphe**-)	547.4	9.53	$C_{24}H_{34}N_8O_7$ MW = 546.58
75	*cyclo*(-G-*iso*DGR-Phg-)	519.3	6.99	$C_{22}H_{30}N_8O_7$ MW = 518.52
76	*cyclo*(-G-*iso*DGR-**phg**-)	519.3	7.00	$C_{22}H_{30}N_8O_7$ MW = 518.52

V.3.6. Design of Linear Peptides

The series of compounds **83**-**88** are linear peptides based on the two active peptides containing D-Phg. They were synthesized according to the general procedure **GP1**, **GP2**, **GP3**, **GP4,** and **GP5** (Scheme V-1) and were purified by *reversed phase* HPLC. The analytical data of the prepared peptides is shown in Table V-10.

Table V-10: *Analytical data of linear peptides.*

Code	Sequence	ESI-MS m/z = [M+H]$^+$	HPLC (0-100%, 30 min) t_R [min]	Molecular formula
77	Ac-**phg**-*iso*DGR-G-OH	579.5	7.86	$C_{24}H_{34}N_8O_9$ MW = 578.57
78	Ac-*iso*DGR-G-**phg**-OH	579.5	7.90	$C_{24}H_{34}N_8O_9$ MW = 578.57
79	Ac-G-**phg**-*iso*DGR-OH	579.5	6.53	$C_{24}H_{34}N_8O_9$ MW = 578.57
80	Ac-G-*iso*DGR-**phg**-OH	579.5	7.73	$C_{24}H_{34}N_8O_9$ MW = 578.57
81	Ac-**phg**-G-*iso*DGR-OH	579.5	7.36	$C_{24}H_{34}N_8O_9$ MW = 578.57
82	Ac-*iso*DGR-**phg**-G-OH	579.5	7.13	$C_{24}H_{34}N_8O_9$ MW = 578.57

V.3.7. Impact of Different Amino Acids on Distinct Positions

The series of compounds **83**-**94**, in which the Gly next to the *iso*Asp was replaced by different amino acids, were synthesized according to the general procedure **GP1**, **GP2**, **GP3**, **GP4**, **GP7,** and **GP8** (Scheme V-1) using the following building blocks (Table V-11). All compounds were purified by *reversed phase* HPLC.

Table V-11: *Amino acid building blocks used for solid phase synthesis*

Code	Amino acid	MW
R	Fmoc-Arg(Pbf)-OH	648.77
G	Fmoc-Gly-OH	297.31
*iso*D	Fmoc-Asp-O^{t}Bu	411.45
A	Fmoc-Ala-OH	311.33
V	Fmoc-Val-OH	339.39
P	Fmoc-Pro-OH	337.37
K	Fmoc-Lys(Boc)-OH	468.54
Y	Fmoc-Tyr(O^{t}Bu)-OH	459.53
W	Fmoc-Trp(Boc)-OH	526.58

The analytical data of the prepared peptides is shown in Table V-12.

Table V-12: *Analytical data of the compounds with different amino acids next to isoAsp.*

Code	Sequence	ESI-MS m/z = [M+H]$^+$	HPLC (0-100%, 30 min) t_R [min]	Molecular formula
83	*cyclo*(-A-*iso*DGR-G-)	457.4	7.92	$C_{17}H_{28}N_8O_7$ MW = 456.45
84	*cyclo*(-**a**-*iso*DGR-G-)	457.3	7.46	$C_{17}H_{28}N_8O_7$ MW = 456.45
85	*cyclo*(-V-*iso*DGR-G-)	485.3	9.32	$C_{19}H_{32}N_8O_7$ MW = 484.51
86	*cyclo*(-**v**-*iso*DGR-G-)	485.3	9.09	$C_{19}H_{32}N_8O_7$ MW = 484.51
87	*cyclo*(-P-*iso*DGR-G-)	483.3	8.91	$C_{19}H_{30}N_8O_7$ MW = 482.49
88	*cyclo*(-**p**-*iso*DGR-G-)	483.3	8.53	$C_{19}H_{30}N_8O_7$ MW = 482.49
89	*cyclo*(-K-*iso*DGR-G-)	514.3	8.34	$C_{20}H_{35}N_9O_7$ MW = 513.55
90	*cyclo*(-**k**-*iso*DGR-G-)	514.3	8.10	$C_{20}H_{35}N_9O_7$ MW = 513.55
91	*cyclo*(-Y-*iso*DGR-G-)	549.4	9.87	$C_{23}H_{32}N_8O_8$ MW = 548.55
92	*cyclo*(-**y**-*iso*DGR-G-)	549.3	9.34	$C_{23}H_{32}N_8O_8$ MW = 548.55
93	*cyclo*(-W-*iso*DGR-G-)	572.3	11.52	$C_{25}H_{33}N_9O_7$ MW = 571.59
94	*cyclo*(-**w**-*iso*DGR-G-)	572.3	12.07	$C_{25}H_{33}N_9O_7$ MW = 571.59

The series of compounds **95**-**104**, in which the Gly next to the Arg was replaced by different amino acid were synthesized according to the general procedure **GP1**, **GP2**, **GP3**, **GP4**, **GP7,** and **GP8** (Scheme V-1). All compounds were purified by *reversed phase* HPLC. The analytical data of the prepared peptides is shown in Table V-13.

Table V-13: *Analytical data of the compounds with different amino acids next to R.*

Code	Sequence	ESI-MS m/z = [M+H]$^+$	HPLC (0-100%, 30 min) t_R [min]	Molecular formula
95	*cyclo*(-G-*iso*DGR-A-)	457.3	7.91	$C_{17}H_{28}N_8O_7$ MW = 456.45
96	*cyclo*(-G-*iso*DGR-**a**-)	457.3	7.21	$C_{17}H_{28}N_8O_7$ MW = 456.45
97	*cyclo*(-G-*iso*DGR-V-)	485.3	9.38	$C_{19}H_{32}N_8O_7$ MW = 484.51
98	*cyclo*(-G-*iso*DGR-**v**-)	485.3	9.07	$C_{19}H_{32}N_8O_7$ MW = 484.51
99	*cyclo*(-G-*iso*DGR-P-)	483.3	8.76	$C_{19}H_{30}N_8O_7$ MW = 482.49
100	*cyclo*(-G-*iso*DGR-**p**-)	483.3	8.50	$C_{19}H_{30}N_8O_7$ MW = 482.49
101	*cyclo*(-G-*iso*DGR-K-)	514.3	8.00	$C_{20}H_{35}N_9O_7$ MW = 513.55
102	*cyclo*(-G-*iso*DGR-**k**-)	514.3	7.91	$C_{20}H_{35}N_9O_7$ MW = 513.55
103	*cyclo*(-G-*iso*DGR-Y-)	549.3	9.41	$C_{23}H_{32}N_8O_8$ MW = 548.55
104	*cyclo*(-G-*iso*DGR-**y**-)	549.3	9.49	$C_{23}H_{32}N_8O_8$ MW = 548.55

V.3.8. Optimization via Combination of Different Approaches

The compounds **105**-**106** combine the pharmacophoric groups of the most active peptides for αvβ3 integrin. They were synthesized according to the general procedure **GP1**, **GP2**, **GP3**, **GP4**, **GP7,** and **GP8** (Scheme V-1). All compounds were purified by *reversed phase* HPLC. The analytical data of the prepared peptides is shown in Table V-14a.

Table V-14a: *Analytical data of the compounds combining different amino acids.*

Code	Sequence	ESI-MS m/z = [M+H]$^+$	HPLC (0-100%, 30 min) t_R [min]	Molecular formula
105	*cyclo*(-**a**-*iso*DGR-**a**-)	471.3	6.32	$C_{18}H_{30}N_8O_7$ MW = 470.48
106	*cyclo*(-**a**-*iso*DGR-**v**-)	499.3	9.32	$C_{20}H_{34}N_8O_7$ MW = 498.53

The compounds **107**-**108** combine the pharmacophoric groups of the most active peptides for α5β1 integrin. They were synthesized according to the general procedure **GP1**, **GP2**, **GP3**, **GP4**, **GP7,** and **GP8** (Scheme V-1). All compounds were purified by *reversed phase* HPLC. The analytical data of the prepared peptides is shown in Table V-14b.

Table V-14b: *Analytical data of the compounds combining different amino acids.*

Code	Sequence	ESI-MS m/z = [M+H]$^+$	HPLC (0-100%, 30 min) t_R [min]	Molecular formula
107	*cyclo*(-**phg**-*iso*DGR-**v**-)	561.4	9.01	$C_{25}H_{36}N_8O_7$ MW = 560.60
108	*cyclo*(-**phg**-*iso*DGR-**p**-)	559.3	9.29	$C_{25}H_{34}N_8O_7$ MW = 558.59

The compounds **109**-**118** are based on the α5β1 active lead structure *cyclo*(-**phg**-*iso*DGR-X-), in which X represent the different amino acids. They were synthesized according to the general procedure **GP1**, **GP2**, **GP3**, **GP4**, **GP7,** and **GP8** (Scheme V-1). All compounds were purified by *reversed phase* HPLC. The analytical data of the prepared peptides is shown in Table V-15.

Table V-15: *Analytical data of the compounds with **phg** and different amino acids next to R.*

Code	Sequence	ESI-MS m/z = [M+H]$^+$	HPLC (0-100%, 30 min) t$_R$ [min]	Molecular formula
109	*cyclo*(-**phg**-*iso*DGR-V-)	561.4	8.33	$C_{25}H_{36}N_8O_7$ MW = 560.60
110	*cyclo*(-**phg**-*iso*DGR-P-)	599.4	8.44	$C_{25}H_{34}N_8O_7$ MW = 558.59
111	*cyclo*(-**phg**-*iso*DGR-K-)	590.4	6.43	$C_{26}H_{39}N_9O_7$ MW = 589.64
112	*cyclo*(-**phg**-*iso*DGR-**k**-)	590.4	5.99	$C_{26}H_{39}N_9O_7$ MW = 589.64
113	*cyclo*(-**phg**-*iso*DGR-E-)	591.4	7.53	$C_{25}H_{34}N_8O_9$ MW = 590.59
114	*cyclo*(-**phg**-*iso*DGR-**e**-)	591.4	7.18	$C_{25}H_{34}N_8O_9$ MW = 590.59
115	*cyclo*(-**phg**-*iso*DGR-Y-)	625.4	9.10	$C_{29}H_{36}N_8O_8$ MW = 624.64
116	*cyclo*(-**phg**-*iso*DGR-**y**-)	625.4	9.42	$C_{29}H_{36}N_8O_8$ MW = 624.64
117	*cyclo*(-**phg**-*iso*DGR-W-)	648.4	11.14	$C_{31}H_{37}N_9O_7$ MW = 647.68
118	*cyclo*(-**phg**-*iso*DGR-**w**-)	648.4	11.28	$C_{31}H_{37}N_9O_7$ MW = 647.68

V.3.9. Design of Cyclic Hexapeptides

The series of compounds **119**-**134** are cyclic hexapeptides based on the FN loop and with different amino acids in addition. They were synthesized according to the general procedure **GP1**, **GP2**, **GP3**, **GP4**, **GP7,** and **GP8** (Scheme V-1). All compounds were purified by *reversed phase* HPLC. The analytical data of the prepared peptides is shown in Table V-16.

Table V-16: *Analytical data of cyclic hexapeptides.*

Code	Sequence	ESI-MS m/z = [M+H]$^+$	HPLC (0-100%, 30 min) t_R [min]	Molecular formula
119	*cyclo*(-G-*iso*DGR-G-**A**-)	514.3	8.76	$C_{19}H_{31}N_9O_8$ MW = 513.50
120	*cyclo*(-G-*iso*DGR-G-**a**-)	514.3	8.36	$C_{19}H_{31}N_9O_8$ MW = 513.50
121	*cyclo*(-G-*iso*DGR-G-**V**-)	452.4	9.58	$C_{21}H_{25}N_9O_8$ MW = 541.56
122	*cyclo*(-G-*iso*DGR-G-**v**-)	452.4	9.26	$C_{21}H_{25}N_9O_8$ MW = 541.5
123	*cyclo*(-G-*iso*DGR-G-**P**-)	540.5	8.60	$C_{21}H_{33}N_9O_8$ MW = 539.54
124	*cyclo*(-G-*iso*DGR-G-**p**-)	540.4	8.76	$C_{21}H_{33}N_9O_8$ MW = 539.54
125	*cyclo*(-G-*iso*DGR-G-**K**-)	571.3	9.20	$C_{22}H_{38}N_{10}O_8$ MW = 570.60
126	*cyclo*(-G-*iso*DGR-G-**k**-)	571.3	8.89	$C_{22}H_{38}N_{10}O_8$ MW = 570.60
127	*cyclo*(-G-*iso*DGR-G-**Y**-)	606.3	10.55	$C_{25}H_{35}N_9O_9$ MW = 605.60
128	*cyclo*(-G-*iso*DGR-G-**y**-)	606.4	10.41	$C_{25}H_{35}N_9O_9$ MW = 605.60
129	*cyclo*(-G-*iso*DGR-G-**F**-)	590.4	8.03	$C_{25}H_{35}N_9O_8$ MW = 589.60
130	*cyclo*(-G-*iso*DGR-G-**f**-)	590.4	8.59	$C_{25}H_{35}N_9O_8$ MW = 589.60
131	*cyclo*(-G-*iso*DGR-G-**Hphe**-)	604.4	8.40	$C_{26}H_{27}N_9O_8$ MW = 603.63
132	*cyclo*(-G-*iso*DGR-G-**hphe**-)	604.4	8.57	$C_{26}H_{27}N_9O_8$ MW = 603.63
133	*cyclo*(-G-*iso*DGR-G-**Phg**-)	576.3	7.12	$C_{24}H_{33}N_9O_8$ MW = 575.57
134	*cyclo*(-G-*iso*DGR-G-**phg**-)	576.3	7.34	$C_{24}H_{33}N_9O_8$ MW = 575.57
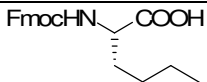
V.4. Preparation and Analytical Data of Cyclic Peptides for αvβ6 Integrin

The series of compounds **135**-**138** which should bind to αvβ6 were synthesized according to the general procedure **GP1**, **GP2**, **GP3**, **GP4**, **GP7,** and **GP8** (Scheme V-1) using the following building blocks (Table V-18 and Table V-19). All compounds were purified by *reversed phase* HPLC.

Table V-17: *Amino acid building blocks used for solid phase synthesis*

Code	Amino acid	MW
R	Fmoc-Arg(Pbf)-OH	648.77
G	Fmoc-Gly-OH	297.31
D	Fmoc-Asp(O^{t}Bu)-OH	411.45
V	Fmoc-Phe-OH	387.43
P	Fmoc-Pro-OH	337.37
L	Fmoc-Leu-OH	353.41
I	Fmoc-Ile-OH	353.41

Table V-18: *Unnatural amino acid building blocks.*

Code	Name	Building block structure	MW
NLe	Norleucine	FmocHN␣␣COOH	353.41

The analytical data of the prepared peptides is shown in Table V-20.

Table V-19: *Analytical data of compounds synthesized for the αvβ6 integrin approach.*

Code	Sequence	ESI-MS m/z = [M+H]$^+$	HPLC (0-100%, 30 min) t_R [min]	Molecular formula
135	*cyclo*(-RGD-**p**-V-)	525.4	7.94	C$_{22}$H$_{36}$N$_8$O$_7$ MW = 524.42
136	*cyclo*(-RGD-**I**-V-)	541.4	10.94	C$_{23}$H$_{40}$N$_8$O$_7$ MW = 540.61
137	*cyclo*(-RGD-**i**-V-)	541.5	10.55	C$_{23}$H$_{40}$N$_8$O$_7$ MW = 540.61
138	*cyclo*(-RGD-**nle**-V)	541.4	1107	C$_{23}$H$_{40}$N$_8$O$_7$ MW = 540.61

V.5.   Biological Assays

V.5.1. Solid Phase Binding Assay

The biological testings were performed primarly by *Dr. Dörte Vossmeyer, Dr. Grit Zahn* and *Dr. Roland Stragies* at Jerini AG (Berlin) but then resumed from *Dr. Carlos Mas-Moruno* and Dipl. Chem. *Alexander Bochen* in our group. Several results are already published in *Angew. Chem. Int. Ed.* **2010**, *49*, 9278-9281.

The inhibiting activity and integrin selectivity of the integrin inhibitors were determined in a solid phase binding assay using soluble integrins and coated extracellular matrix proteins. Binding of integrins was then detected by specific antibodies in an enzyme-linked immunosorbent assay. FN and vitronectin were purchased from Sigma (St. Louis, MO), the integrin $\alpha5\beta1$ was purchased from R&D Systems (Minneapolis, MN), and the integrin $\alpha v\beta3$ from Chemicon (Chemicon Europe, Germany). The integrin antibodies were purchased from Pharmingen, BD Bioscience Europe (mouse anti-human CD51 / CD61, and mouse anti-human CD49e) and Sigma (anti-mouse-HRP conjugate). The detection of HRP was performed using HRP substrate solution 3.3.5.5'-tetramethylethylenediamine (TMB, Seramun, Germany) and 2 M H_2SO_4 for stopping the reaction. The developed color was measured at 450 nm with a POLARstar Galaxy plate reader (BMG Labtechnologies). Every concentration was analyzed twice. To evaluate the resulting inhibition curves OriginPro 7.5G software was used. The turning point describes the IC_{50} value.

For the $\alpha5\beta1$ assay, BRAND flat-bottom 96-well ELISA plates were coated over night at 4 °C with FN (0.50 µg/mL) in 15 mM Na_2CO_3, 35 mM $NaHCO_3$, pH 9.6. Plates were subsequently washed three times with PBST buffer (137 mM NaCl, 2.7 mM KCl, 10 mM Na_2HPO_4, 2 mM KH_2PO_4, 0.01% Tween 20, pH 7.4) and blocked for one hour at room temperature with 150 µL/well of TSB-buffer (20 mM Tris-HCl, 150 mM NaCl, 1 mM $CaCl_2$, 1 mM $MgCl_2$, 1 mM $MnCl_2$, pH 7.5, 1% BSA). Soluble integrin $\alpha5\beta1$ (1.0 µg/mL) and a serial dilution of integrin inhibitor in TSB were incubated in the coated wells for 1 h at room temperature. The plate was then washed three times with PBST buffer and 100 L/well of primary antibody (CD49e) were incubated at 1.0 µg/mL in TSB (1:500 dilution) for 1 h at room temperature. After washing three times with PBST, 100 µL/well of the secondary anti-body (anti-mouse-HRP conjugate) were applied at 2.0 µg/mL in TSB (1:385 dilution) for 1 h at room

temperature. After this treatment the plate was washed three times and the binding visualized as described above.

For the αvβ3 assay, plates were coated with vitronectin (1.0 µg/mL) and blocked as described for α5β1. Soluble αvβ3 (1.0 µg/mL) was incubated with a serial dilution of integrin inhibitor for 1 h at room temperature. Primary (CD51 / CD61, 2.0 µg/mL, 1:250 dilution) and secondary antibody (anti-mouse-HRP conjugate, 1.0 µg/mL, 1:770 dilution) were applied each for 1 h at room temperature and the binding visualized as described above.

The peptides **1-17**, **20**, **21**, **24**, **25**, **28**, **29**, **30-42**, **84**, **86-88**, **94**, **96**, **98**, and **100** were tested by Jerini AG (Berlin) with a slightly different method.[135]

V.5.2. Cellular Assay

The assays were performed by *Dr. Herbert Schiller* in the group of *Prof. Dr. Reinhard Fässler*, Max Planck Institute of Biochemistry (Martinsried), as published in *Angew. Chem. Int. Ed.* **2010**, *49*, 9278-9281.

Mouse fibroblast cell lines expressing either αvβ3 or α5β1 were generated from fibroblasts derived from the kidney of $\alpha_v^{flox/flox}$, $\beta_1^{flox/flox}$, $\beta_2^{-/-}$, $\beta_7^{-/-}$ mice. Cells were immortalized by retroviral transduction of the SV40 large T and cloned. Subsequently the cells were retrovirally transduced with mouse αv or β1 integrin expression constructs. Endogenous β1 and αv integrin loci were deleted by adenoviral cre-recombinase transduction. Selective expression of αvβ3 or α5β1 was verified by flow cytometry and immunoblotting.

To evaluate cell adhesion 96 well plates were coated for 2 h at room temperature with 5 µg/mL FN in PBS and then blocked with 1% bovine serum albumin. Fibroblasts expressing αvβ3 or α5β1 were incubated with increasing concentrations (10 - 100000 nM) of the cyclic peptides for 20 min on ice. Then 40000 cells/well were seeded onto the FN coated plates in presence of the cyclic peptides and incubated for 40 min at 37 °C. After washing off non-adherent cells the adherent cells were fixed, stained with crystal violet and the relative percentage of adherent cells was

determined as previously described.[179] The percentage of adherent cells treated with increasing cyclic peptide concentrations relative to untreated cells was calculated from 3 independent experiments. To calculate IC_{50} values dose response curves were fitted onto the data using the SigmaPlot software.

Table V-20: Relative binding activities.

IC_{50} ratios	α5β1 cell line	αvβ3 cell line
Cellular adhesion blocking assay:		
Ratio IC_{50} 27/76	0.05	2.8
Ratio IC_{50} Cil/27	0.47	0.009
Ratio IC_{50} Cil/76	0.09	0.02
Competitive solid phase ELISA:		
Ratio IC_{50} 27/76	0.05	11.23
Ratio IC_{50} cil/27	0.78	0.00054
Ratio IC_{50} cil/76	0.04	0.006

V.6. NMR Structure Calculation

The structures were calculated by *Dr. Andreas Frank* in our group, as published in *Angew. Chem. Int. Ed.* **2010**, *49*, 9278-9281.

5 mg of each of the peptides **27** and **76** were dissolved in 500 µL d_6-DMSO; the solvent was also used for the lock-signal. All spectra were recorded on a Bruker DMX500 spectrometer equipped with a 5 mm TXI RT probe head and referenced to the B_0 magnetic field. Purity and conformational equilibria of the compounds were checked via [1]H-1D spectra. For both peptides, only one signal set was found. Atom and atom group assignment was done via E.COSY[180] and TOCSY[181] spectra; sequential assignment was accomplished by through-bond connectivities from heteronuclear multiple bond correlation (^{1}H,^{13}C-HMBC)[182] spectra. Connectivities were proved by interresidual scalar couplings, e.g., between carbonyl carbons and adjacent amide protons. ROESY[183] spectra were recorded to extract information about pair-wise proton-proton distances. Homonuclear J-couplings were extracted from E.COSY spectra. For TOCSY, ROESY, and E.COSY spectra, 16 k data points were recorded in the direct dimensions and 512 data points in the indirect dimensions

(2 k data points for E.COSY). QSINE window functions and zero filling to twice the number of recorded points were used for processing. HMBC spectra were recorded with 4 k data points in the F2 and 256 data points in the F1 dimensions; for processing, SINE and QSINE functions as well as zero filling to twice the number of recorded points were used. TOCSY spectra were recorded with a mixing time of 80 ms, ROESY spectra with a mixing time of 150 ms, thus avoiding unwanted effects caused by spin diffusion. The temperature of all measurements was 300 K. The software tools TOPSPIN and SPARKY were utilized to process spectra, to assign resonances, and for ROE peak volume integration. Proton distances were calculated according to the isolated two-spin approximation.[184] No ROE offset correction was performed since biasing offset effects at the field strength used in this case are rather small. The integrated volumes of ROE cross peaks were converted to proton–proton distances by the help of calibration to distances between methylene protons (1.78 Å). Upper and lower distance restraints were obtained by adding and subtracting 10 % to / from the calculated experimental values, thus accounting for experimental errors and simulation uncertainties.

Calculation of the most representative conformations of **27** and **76** was done by distance geometry (DG) and molecular dynamics (MD) simulations. Metric matrix DG calculations were carried out with a distance geometry algorithm utilizing random metrization.[185] Experimental distance restraints which are more restrictive than the geometric distance bounds (holonomic restraints) were used to create the final distance matrix. All structure templates were first embedded in four dimensions and then partially minimized using conjugate gradient minimization followed by distance-driven dynamics (DDD) wherein only distance constraints were used.[186] The DDD simulation was carried out at 1000 K for 50 ps with a gradual reduction in temperature over the next 30 ps. The DDD procedure utilized holonomic and experimental distance constraints plus a chiral penalty function for the generation of violation energies and forces. A distance matrix was calculated from each structure, and the EMBED algorithm was used to compute Cartesian coordinates in three dimensions.[185] 50 structures were calculated for each peptide, and > 95 % of the structure bundles of both peptides did not show any significant violations (> 0.12 Å). MD calculations were carried out with the program Gromacs version 3.3.3.[187] The Gromos G53a6 force field as implemented in Gromacs was used for parametrization

of the peptide and DMSO solvent molecules.[166] The most representative DG structures of the peptides were first energy minimized by the conjugate-gradient[188] algorithm and then placed in truncated octahedral simulation boxes with the box walls being at least 1.6 nm away from the solutes. The boxes were each filled with more than 600 DMSO solvent molecules and subsequently energy minimized with the steepest descent algorithm whereas all atoms of the solutes were positionally restrained to their original positions (F = 2.5 E+005 kJ / mol). Afterwards, both boxes were heated up to 360 K (higher simulation temperatures compared to experimental ones in order to overcome higher energy barriers) in six steps and the position restraints were stepwise lowered until the positional forces reach 0 kJ / mol (each equilibrium run was simulated for 50 ps). The average temperature was maintained via the Berendsen[189] algorithm as implemented in Gromacs 3.3.3. Then, Berendsen pressure coupling[189] was turned on for 500 ps. Finally, the production runs for both peptides were started with simulation durations of 250 ns. Intermolecular interactions were treated with a twin-range cutoff of 0.8 nm and 1.4 nm. The pair-lists were updated each after five integration steps. Behind the long-range cutoff, a reaction-field (epsilon_rf = 38) was used to calculate long-range Coulombic interactions. A leap-frog algorithm was utilized to integrate Newton's equation of motion with a integration time step of 2 fs.[190] All bonds were constrained applying the SHAKE[191] algorithm. In addition, periodic boundary conditions were utilized and the center-of-mass motion was removed every 500 integration steps. The two peptides were simulated both as fully neutral (ARG and isoASP uncharged) and as zwitter ionic (ARG and isoASP charged) species in separated runs. Evaluation of ROE based distance restraints and of J-couplings was performed via tools as implemented in the Gromos2005 MD software package.[192] Pseudo-atom and multiplicity corrections for distance restraints were applied as described by *Koning et al.*[193]

V.6.1. NMR and MD Data of 27

V.6.1.1. Assignment (given in ppm)

1DPHG			2IASP			3GLY			4ARG			5GLY		
NH	---	8.60	NH	---	7.84	NH	---	8.42	NH	---	8.42	NH	---	8.03
HA	---	5.50	HA	---	4.47	HA1	pro-R	3.61	HA	---	4.06	HA1	pro-R	3.70
HD*	---	7.46	HB1	pro-R	2.57	HA2	pro-S	3.89	HB1	pro-R	1.61	HA2	pro-S	3.88
HE*	---	7.35	HB2	pro-S	2.82				HB2	pro-S	1.79			
HZ	---	7.33							HG*	---	1.51			
									HD*	---	3.12			
									HE	---	7.66			

V.6.1.2. ROE Distance Restraints

	Assignment				Experimental (Å)		Zwitter (Å)		Uncharged (Å)		Combined (Å)	
No	AS-1	At-1	AS-2	At-2	Upper	Lower	Calc	Viol	Calc	Viol	Calc	Viol
01	1DPHG	NH	1DPHG	HA	3.20	2.62	2.68		2.72		2.70	
02	2IASP	NH	1DPHG	HA	3.54	2.90	3.13		2.87	- 0.03	3.00	
03	2IASP	NH	2IASP	HA	2.84	2.32	2.69		2.73		2.71	
04	3GLY	NH	2IASP	HA	4.21	3.45	4.02		3.81		3.92	
05	2IASP	NH	2IASP	HB1	3.75	3.07	3.35		3.18		3.27	
06	3GLY	NH	2IASP	HB1	3.00	2.46	2.60		3.35	+ 0.35	2.85	
07	2IASP	NH	2IASP	HB2	3.56	2.92	2.63	- 0.29	3.78	+ 0.22	2.97	
08	3GLY	NH	2IASP	HB2	2.64	2.16	2.39		2.28		2.33	
09	1DPHG	NH	2IASP	NH	2.77	2.27	2.49		2.64		2.55	
10	4ARG	NH	4ARG	HA	3.14	2.56	2.76		2.13	- 0.43	2.39	- 0.17
11	5GLY	NH	4ARG	HA	2.76	2.26	2.82	+ 0.06	2.19	- 0.07	2.46	
12	4ARG	HA	4ARG	HB2	2.87	2.35	2.57		2.49		2.54	
13	4ARG	HE	4ARG	HB2	3.71	3.03	3.48		3.78	+ 0.07	3.60	
14	4ARG	NH	4ARG	HB2	3.37	2.75	3.11		3.66	+ 0.29	3.32	
15	1DPHG	NH	5GLY	HA2	3.01	2.47	2.34	- 0.13	2.41	- 0.06	2.37	- 0.10
16	1DPHG	NH	5GLY	HA1	3.35	2.75	3.18		3.29		3.23	
17	1DPHG	NH	5GLY	NH	3.09	2.53	3.17	+ 0.08	2.83		3.00	
18	4ARG	NH	5GLY	NH	3.16	2.58	2.60		3.07		2.78	
19	2IASP	HA	2IASP	HB1	2.68	2.20	2.40		2.34		2.37	
20	3GLY	NH	2IASP	NH	3.69	3.01	3.90	+ 0.21	3.82	+ 0.13	3.86	+ 0.17
21	5GLY	NH	2IASP	NH	3.95	3.23	3.99	+ 0.04	2.86	- 0.37	3.29	
22	5GLY	NH	5GLY	HA1	2.93	2.39	2.65		2.73		2.69	
23	5GLY	NH	5GLY	HA2	2.93	2.39	2.57		2.50		2.54	
24	1DPHG	NH	4ARG	NH	5.39	4.41	5.16		5.18		5.17	
25	3GLY	NH	3GLY	HA1	2.73	2.23	2.29		2.28		2.28	

	Assignment			Experimental (Å)		Zwitter (Å)		Uncharged (Å)		Combined (Å)	
26	3GLY	NH	3GLY	HA2	2.52	2.06	2.66	+ 0.14	2.73	+ 0.21	2.69	+ 0.17
27	2IASP	HA	2IASP	HB2	2.95	2.41	2.70		2.34	- 0.07	2.51	
28	1DPHG	HE*	1DPHG	HA	5.74	2.98	4.71		4.71		4.71	
29	1DPHG	NH	1DPHG	HE*	6.22	3.38	4.96		4.80		4.88	
30	2IASP	NH	1DPHG	HE*	6.80	3.84	5.37		6.03		5.63	
31	1DPHG	NH	1DPHG	HD*	5.30	2.62	2.70		2.61	- 0.01	2.66	
32	2IASP	NH	1DPHG	HD*	5.95	3.15	3.19		3.57		3.35	
33	4ARG	HD*	4ARG	HB2	4.00	2.54	2.83		2.93		2.87	
34	4ARG	HA	4ARG	HD*	4.20	2.70	3.64		3.11		3.35	

V.6.1.3.   J-Couplings

Assignment				Zwitter (Hz)			Uncharged (Hz)			Combined (Hz)		
AS	At-1	At-2	Chiral	Exp	Calc	Viol	Exp	Calc	Viol	Exp	Calc	Viol
1DPHG	NH	HA	---	8.5	8.0	0.5	8.5	8.0	0.5	8.5	8.0	0.5
2IASP	NH	HA	---	7.9	7.5	0.4	7.9	6.9	1.0	7.9	7.3	0.6
2IASP	HA	HB1	pro-R	4.1	3.3	0.8	4.1	3.2	0.9	4.1	3.3	0.8
2IASP	HA	HB2	pro-S	7.0	9.4	2.4	7.0	3.8	3.2	7.0	6.9	0.1
3GLY	NH	HA1	pro-R	5.4	5.3	0.1	5.4	6.0	0.6	5.4	5.7	0.3
3GLY	NH	HA2	pro-S	6.6	5.8	0.8	6.6	5.5	1.1	6.6	5.7	0.9
4ARG	NH	HA	---	6.2	8.0	1.8	6.2	6.7	0.5	6.2	7.4	1.2
4ARG	HA	HB1	pro-R	9.0	8.7	0.3	9.0	11.1	2.1	9.0	9.8	0.8
4ARG	HA	HB2	pro-S	5.6	5.2	0.4	5.6	3.8	1.8	5.6	4.5	1.1
5GLY	NH	HA1	pro-R	5.0	5.4	0.4	5.0	4.2	0.8	5.0	4.9	0.1
5GLY	NH	HA2	pro-S	6.9	5.1	1.8	6.9	7.2	0.3	6.9	6.1	0.8

V.6.2. NMR and MD Data of 76

V.6.2.1.   Assignment (given in ppm)

1DPHG			2GLY			3IASP			4GLY			5ARG		
NH	---	8.61	NH	---	8.65	NH	---	7.77	NH	---	8.47	NH	---	8.02
HA	---	5.27	HA1	pro-R	3.66	HA	---	4.48	HA1	pro-R	3.56	HA	---	4.32
HD*	---	7.39	HA2	pro-S	3.78	HB1	pro-R	2.63	HA2	pro-S	3.79	HB1	pro-R	1.51
HE*	---	7.35				HB2	pro-S	2.78				HB2	pro-S	1.73
HZ	---	7.37										HG*	---	1.41
												HD*	---	3.09
												HE	---	7.57

V.6.2.2. ROE Distance Restraints

No	AS-1	At-1	AS-2	At-2	Experimental (Å)		Zwitter (Å)		Uncharged (Å)		Combined (Å)	
					Upper	Lower	Calc	Viol	Calc	Viol	Calc	Viol
01	1DPHG	HA	1DPHG	NH	3.45	2.82	2.77	- 0.05	2.80	- 0.02	2.79	- 0.03
02	1DPHG	HA	2GLY	NH	2.81	2.30	2.39		2.37		2.38	
03	2GLY	NH	2GLY	HA2	3.06	2.50	2.63		2.67		2.65	
04	2GLY	NH	2GLY	HA1	3.07	2.51	2.46	- 0.05	2.39	- 0.12	2.43	- 0.08
05	3IASP	NH	2GLY	HA1	3.43	2.81	3.19		3.23		3.21	
06	2GLY	NH	3IASP	NH	3.24	2.65	3.65	+ 0.42	3.05		3.30	+ 0.07
07	3IASP	NH	3IASP	HA	2.97	2.43	2.76		2.72		2.74	
08	4GLY	NH	3IASP	HA	4.06	3.32	3.59		3.64		3.62	
09	3IASP	NH	3IASP	HB1	4.38	3.58	3.51	- 0.07	3.34	- 0.24	3.42	- 0.16
10	4GLY	NH	3IASP	HB1	3.20	2.62	2.84		3.42	+ 0.22	3.08	
11	3IASP	NH	3IASP	HB2	3.86	3.16	2.49	- 0.67	3.81		2.89	- 0.27
12	4GLY	NH	3IASP	HB2	2.90	2.38	2.33	- 0.05	2.52		2.41	
13	5ARG	NH	4GLY	HA2	3.54	2.90	3.07		3.16		3.11	
14	5ARG	NH	4GLY	HA1	3.15	2.58	2.25	- 0.33	2.46	- 0.12	2.35	- 0.23
15	1DPHG	NH	5ARG	NH	3.80	3.11	3.98	+ 0.17	3.52		3.72	
16	4GLY	NH	5ARG	NH	3.56	2.91	4.06	+ 0.51	2.98		3.36	
17	1DPHG	NH	5ARG	HA	2.61	2.14	2.19		2.17		2.18	
18	5ARG	NH	5ARG	HA	3.38	2.76	2.74	- 0.02	2.46	- 0.30	2.58	- 0.18
19	5ARG	NH	5ARG	HB2	3.16	2.59	2.41	- 0.18	2.65		2.52	- 0.07
20	5ARG	HA	5ARG	HB2	2.95	2.41	2.70		2.74		2.72	
21	5ARG	HE	5ARG	HB2	3.64	2.98	3.55		3.66	+ 0.02	3.61	
22	5ARG	NH	5ARG	HB1	3.81	3.12	3.07	- 0.05	3.33		3.19	
23	5ARG	HA	5ARG	HB1	3.09	2.53	2.57		2.52	- 0.01	2.55	
24	1DPHG	NH	1DPHG	HD*	4.23	2.72	2.66	- 0.06	2.78		2.72	
25	1DPHG	HD*	2GLY	NH	5.16	3.48	3.56		3.46	- 0.02	3.51	
26	5ARG	HD*	5ARG	HB2	3.62	2.22	2.87		2.99		2.93	
27	5ARG	HD*	5ARG	HB1	4.19	2.69	2.84		2.85		2.85	
28	5ARG	HA	5ARG	HD*	4.59	3.02	3.57		3.33		3.44	
29	5ARG	HG*	5ARG	NH	4.87	3.24	3.28		3.44		3.36	
30	5ARG	HA	5ARG	HG*	4.30	2.78	2.68	- 0.10	2.74	- 0.04	2.71	- 0.07
31	5ARG	HB1	5ARG	HG*	3.88	2.44	2.47		2.47		2.47	
32	1DPHG	NH	1DPHG	HE*	5.36	3.65	4.89		5.09		4.99	
33	1DPHG	HA	1DPHG	HE*	4.81	3.20	4.70		4.69		4.69	

V.6.2.3. J-Couplings

Assignment				Zwitter (Hz)			Uncharged (Hz)			Combined (Hz)		
AS	At-1	At-2	Chiral	Exp	Calc	Viol	Exp	Calc	Viol	Exp	Calc	Viol
1DPHG	NH	HA	---	7.3	8.6	1.3	7.3	7.7	0.4	7.3	8.1	0.8
2GLY	NH	HA1	pro-R	6.4	6.7	0.3	6.4	5.7	0.7	6.4	6.2	0.2
2GLY	NH	HA2	pro-S	5.9	5.5	0.4	5.9	5.9	0.0	5.9	5.7	0.2
3IASP	NH	HA	---	8.2	7.0	1.2	8.2	8.2	0.0	8.2	7.6	0.6
3IASP	HA	HB1	pro-R	3.5	3.6	0.1	3.5	2.8	0.7	3.5	3.2	0.3
3IASP	HA	HB2	pro-S	7.5	3.5	4.0	7.5	11.2	3.7	7.5	7.4	0.1
4GLY	NH	HA1	pro-R	5.4	5.7	0.3	5.4	4.7	0.7	5.4	5.2	0.2
4GLY	NH	HA2	pro-S	6.5	6.4	0.1	6.5	7.0	0.5	6.5	6.7	0.2
5ARG	NH	HA	---	7.3	7.3	0.0	7.3	6.7	0.6	7.3	7.0	0.3
5ARG	HA	HB1	pro-R	8.5	9.8	1.3	8.5	8.7	0.2	8.5	9.2	0.7
5ARG	HA	HB2	pro-S	5.4	4.7	0.7	5.4	5.5	0.1	5.4	5.1	0.3

V.7. Molecular Docking

The docking simulations were performed by *Dr. Luciana Marinelli* and *Dr. Sandro Cosconati* in the group of of *Prof. Dr. Ettore Novellino* at the Università di Napoli "Federico II, Napoli" (Italy), as published in *Angew. Chem. Int. Ed.* **2010**, *49*, 9278-9281.

V.7.1. Docking Simulation

Molecular docking of **27** and **76** in the X-ray three-dimensional structure of αvβ3 (PDB code: 1L5G)[74] and in the α5β1 homology model,[135] was carried out using the AutoDock 4.0 software package as implemented through the graphical user interface AutoDockTools (ADT 1.5.2).[194]

V.7.2. Ligand and Protein Setup

For peptides **27** and **76**, the conformations in solution as experimentally determined by NMR, distance geometry, and subsequent molecular dynamics (restrained MD), were used as starting conformation. During the docking process the backbone conformation was held fix, while the side chain dihedral angles were free to rotate. Partial atomic charges were assigned by using the Gasteiger-Marsili formalism.

V.7.3. Docking Setup

The docking area has been defined by a box, centered on the coordinate of the metal in the MIDAS region. Grid points of 70×70×70 with 0.375 Å spacing were calculated around the docking area for all the ligand atom types using AutoGrid4. For each ligand, 100 separate docking calculations were performed. Each docking calculation consisted of 10 million energy evaluations using the Lamarckian genetic algorithm local search (GALS) method. A low-frequency local search according to the method of Solis and Wets was applied to docking trials to ensure that the final solution represents a local minimum. Each docking run was performed with a population size of 150, and 300 rounds of Solis and Wets local search were applied with a probability of 0.06. A mutation rate of 0.02 and a crossover rate of 0.8 were used to generate new docking trials for subsequent generations. The GALS method evaluates a population of possible docking solutions and propagates the most successful individuals from each generation into the next one. The docking results from each of the 100 calculations were clustered on the basis of root-mean square deviation (rmsd = 1.5 Å) between the Cartesian coordinates of the ligand atoms and were ranked on the basis of the free energy of binding. However, for each ligand, the free energy of binding as well as the consonance with experimental data, such as receptor-mutagenesis and ligands SARs, were taken into account for the choice of the published binding modes.

VI.   References

[1]   B. A. Kohler; E. Ward; B. J. McCarthy; M. J. Schymura; L. A. G. Ries; C. Eheman; A. Jemal; R. N. Anderson; U. A. Ajani; B. K. Edwards: *'Annual Report to the Nation on the Status of Cancer, 1975-2007, Featuring Tumors of the Brain and Other Nervous System'* in *J. Nat. Cancer Inst.* **2011**.

[2]   *'Krebs in Deutschland 2005/2006 Häufigkeit und Trends', Vol. 7. Auflage*, Robert Koch-Institu und Gesellschaft der epidemiologischen Krebsregister in Deutschland e. V., Westkreuz-Druckerei, Berlin, **2010**.

[3]   J. M. Bishop: *'Molecular themes in oncogenesis'* in *Cell* **1991**, *64*, 235-248.

[4]   J. S. Kerr; A. M. Slee; S. A. Mousa: *'The αv integrin antagonists as novel anti-cancer agents: an update'* in *Exp. Opin. Invest. Drugs* **2002**, *11*, 1765-1774.

[5]   S. Kim; K. Bell; S. A. Mousa; J. A. Varner: *'Regulation of angiogenesis in vivo by ligation of integrin $\alpha 5 \beta 1$ with the central cell binding domain of fibronectin.'* in *Am. J. Path.* **2000**, *156*, 1345-1362.

[6]   E. F. Plow; T. A. Haas; L. Zhang; J. Loftus; J. W. Smith: *'Ligand Binding to Integrins'* in *J. Biol. Chem.* **2000**, *275*, 21785-21788.

[7]   M. A. Dechantsreiter; E. Planker; B. Mathä; E. Lohof; G. Hölzemann; A. Jonczyk; S. L. Goodman: *'N-methylated cyclic peptides as highly active and selective $\alpha v \beta 3$ integrin antagonists'* in *J. Med. Chem.* **1999**, *42*, 3033-3040.

[8]   C. Mas-Moruno; F. Rechenmacher; H. Kessler: *'Cilengitide: The First Anti-Angiogenic Small Molecule Drug Candidate. Design, Synthesis and Clinical Evaluation'* in *Anti-Cancer Agents Med. Chem.* **2010**, *10*, 753-768.

[9]   F. Curnis; R. Longhi; L. Crippa; A. Cattaneo; E. Dondossola; A. Bachi; A. Corti: *'Spontaneous formation of L-isoaspartate and gain of function in fibronectin'* in *J. Biol. Chem.* **2006**, *281*, 36466-36476.

[10]   T. Geiger; S. Clarke: *'Deamidation, isomerization, and racemization at asparaginyl and aspartyl residues in peptides. Succinimide-linked reactions that contribute to protein degradation.'* in *J. Biol. Chem.* **1987**, *262*, 785-794.

[11]   T. R. Gadek; J. B. Nicholas: *'Small molecule antagonists of proteins'* in *Biochem. Pharmacol.* **2003**, *65*, 1-8.

[12]   P. L. Toogood: *'Inhibition of protein-protein interactions by small molecules: Approaches and progress'* in *J. Med. Chem.* **2002**, *45*, 1543-1558.

[13]   M. R. Arkin; J. A. Wells: *'Small molecule inhibitors of protein-protein interactions: Progressing towards a dream'* in *Nat. Rev. Drug Discov.* **2004**, *3*, 301-317.

[14]   D. T. Krieger: *'Brain peptides: what, where and why'* in *Science* **1983**, *222*, 975-985.

[15]   G. Schmidt: *'Recent developements in the field of biologically active peptides'* in *Top. Curr. Chem.* **1986**, *136*, 109-159.

[16]   A. Giannis: *'Peptidomimetics for Receptor Ligands-Discovery, Developement and Medcal Perspectives'* in *Angew. Chem. Int. Ed.* **1993**, *32*, 1244-1267.

[17]   J. Gante; H. Kessler; C. Gibson: *'Synthesis of Peptides and Peptidomimetics'* in: *'Houben-Weyl: Methods of Organic Chemistry', Vol. E 22c* (Ed.: A. F. M. Goodmann, L. Moroder, C. Toniolo), Thieme Verlag, Stuttgart, New York, **2003**, pp. 311-323.

[18]   V. J. Hruby; F. al-Obeidi; W. Kazmierski: *'Emerging approaches in the molecular design of receptor-selective peptide ligands: conformational, topographical and dynamic considerations.'* in *Biochem. J.* **1990**, *268*, 249-262.

[19]   J. Rizo; L. M. Gierasch: *'Constrained Peptides: Models of Bioactive Peptides and Protein Substructures'* in *Annu. Rev. Biochem.* **1992**, *61*, 387-416.

[20]   H. Kessler: *'Conformation and biological activity of cyclic peptides'* in *Angew. Chem. Int. Ed.* **1982**, *21*, 512-523.

[21]   J. Chatterjee; C. Gilon; A. Hoffman; H. Kessler: *'N-Methylation: A New Perspective in Peptide Medicinal Chemistry'* in *Acc. Chem. Res.* **2008**, *41*, 1331-1342.

[22]   J. Gante: *'Peptidomimetics: Taylored Enzyme Inhibitors'* in *Angew. Chem. Int. Ed.* **1994**, *33*, 1699-1720.

[23]   H. J. Böhm: *'De novo design of protein ligands'* in *Nachr. Chem. Tech. Lab.* **1993**, *41*, 711-712.

[24]   A. Hillisch; L. F. Pineda; R. Hilgenfeld: *'Utility of homology models in the drug discovery process'* in *Drug Discov. Today* **2004**, *9*, 659-669.

[25]   C. Hansch; P. P. Maloney; T. Fujita: *'Correlation of Biological Activity of Phenoxyacetic Acids with Hammett Substituent Constants and Partition Coefficients'* in *Nature* **1962**, *194*, 178-180.

[26] C. A. Lipinski; F. Lombardo; B. W. Dominy; P. J. Feeney: *'Experimental and computational approaches to estimate solubility and permeability in drug discovery and development settings'* in *Adv. Drug Deliv. Rev.* **1997**, *23*, 3-25.

[27] C. A. Lipinski; F. Lombardo; B. W. Dominy; P. J. Feeney: *'Experimental and computational approaches to estimate solubility and permeability in drug discovery and development settings'* in *Adv. Drug Deliv. Rev.* **2001**, *46*, 3-26.

[28] D. F. Veber; S. R. Johnson; H. Y. Cheng; B. R. Smith; K. W. Ward; K. D. Kopple: *'Molecular properties that influence the oral bioavailability of drug candidates'* in *J. Med. Chem.* **2002**, *45*, 2615-2623.

[29] E. Fischer: *'Einfluss der Configuration auf die Wirkung der Enzyme'* in *Chem. Ber.* **1894**, *27*, 2985-2993.

[30] C. Gilon; D. Halle; M. Chorev; Z. Selinger; G. Byk: *'Backbone cyclization: A new method for conferring conformational constraint on peptides'* in *Biopolymers* **1991**, *31*, 745-750.

[31] E. Fischer: *'Faraday lecture. Synthetical chemistry in its relation to biology'* in *J. Chem. Soc.* **1907**, *91*, 1749-1765.

[32] C. M. Deber; V. Madison; E. R. Blout: *'Why cyclic peptides? Complementary approaches to conformations'* in *Acc. Chem. Res.* **1976**, *9*, 106-113.

[33] D. E. Koshland, Jr.: *'Correlation of Structure and Function in Enzyme Action'* in *Science* **1963**, *142*, 1533-1541.

[34] D. E. Koshland: *'Application of a Theory of Enzyme Specificity to Protein Synthesis'* in *Proc. Nat. Acad. Sci. U.S.A.* **1958**, *44*, 98-104.

[35] B. Charpentier; A. Dor; P. Roy; P. England; H. Pham; C. Durieux; B. P. Roques: *'Synthesis and binding affinities of cyclic and related linear analogues of CCK8 selective for central receptors'* in *J. Med. Chem.* **1989**, *32*, 1184-1190.

[36] F. Al-Obeidi; A. M. Castrucci; M. E. Hadley; V. J. Hruby: *'Potent and prolonged acting cyclic lactam analogues of alpha-melanotropin: design based on molecular dynamics'* in *J. Med. Chem.* **1989**, *32*, 2555-2561.

[37] D. F. Veber; F. W. Holly; R. F. Nutt; S. J. Bergstrand; S. F. Brady; R. Hirschmann; M. S. Glitzer; R. Saperstein: *'Highly active cyclic and bicyclic somatostatin analogues of reduced ring size'* in *Nature* **1979**, *280*, 512-514.

[38] H. Kessler in *Vorlesung "Industrielle Wirkstoffforschung"*, **2005**.

[39] R. Kishore; S. Raghothama; P. Balaram: *'Cystine peptides: the intramolecular antiparallel beta-sheet conformation of a 20-membered cyclic peptide disulfide'* in *Biopolymers* **1987**, *26*, 873-891.

[40] C. Toniolo: *'Structure of conformationally constrained peptides: from model compounds to bioactive peptides'* in *Biopolymers* **1989**, *28*, 247-257.

[41] C. Gilon; C. Mang; E. Lohof; A. Friedler; H. Kessler: *'Synthesis of Cyclic Peptides'* in: *'Methods of Organic Chemistry (Houben-Weyl)', Vol. E 22* (Eds.: K. H. Büchel, J. Falbe, H. Hagemann, M. Hanack, D. Klamann, R. Kreher, H. Kropf, M. Regitz, E. Schaumann), Georg Thieme Verlag, Stuttgart, **2003**, pp. 461-542.

[42] J. S. Richardson: *'The anatomy and taxonomy of protein structure'* in *Adv. Protein Chem.* **1981**, *34*, 167-339.

[43] C. M. Venkatachalam: *'Stereochemical criteria for polypeptides and proteins. V. Conformation of a system of three linked peptide units'* in *Biopolymers* **1968**, *6*, 1425-1436.

[44] B. Laufer: Doktorarbeit *'Synthesis of highly active and selective peptides and peptidomimetics'*, Technische Universität München (München), **2009**.

[45] A. Cornish-Bowden: *'Nomenclature and Symbolism for Amino Acids and Peptides'* in *Eur. J. Biochem.* **1984**, *138*, 9-37.

[46] M. Kurz: *'Cyclische Modellpeptide als Template für ein konformationell orientiertes Peptiddesign'*, Technische Universität München (München), **1991**.

[47] R. Schwyzer; J. P. Carrión; B. Gorup; H. Nolting; A. Tun-Kyi: *'Verdoppelungserscheinungen beim Ringschlus von Peptiden; Relative Bedeutung der sterischen Hinderung und der Assoziation über Wasserstoff-Brücken bei Tripeptiden. Spektroskopische Versuche zur Konformationsbestimmung'* in *Hel. Chim. Acta.* **1964**, *47*, 441-464.

[48] R. B. Merrifield: *'Solid Phase Peptide Synthesis. I. The Synthesis of a Tetrapeptide'* in *J. Am. Chem. Soc.* **1963**, *85*, 2149-2154.

[49] B. Merrifield: *'Solid Phase Synthesis (Nobel lecture)'* in *Angew. Chem. Int. Ed. Engl.* **1985**, *24*, 799-810.

[50] E. Fischer: *' Derivatives of glycine, alanine, and leucine'* in *Chem. Ber.* **1902**, *35*, 1095-1106.

[51] M. Bergmann; L. Zervas: *'A general process for the synthesis of peptides'* in *Dtsch. Chem. Ges.* **1932**, *65*, 1192-1201.

[52]   L. A. Carpino; G. Y. Han: *'9-Fluorenylmethoxycarbonyl Amino-Protecting Group'* in *J. Org. Chem.* **1972**, *37*, 3404-3409.

[53]   L. A. Carpino; B. J. Cohen; K. E. Stephens; S. Y. Sadataalaee; J. H. Tien; D. C. Langridge: *'((9-Fluorenylmethyl)Oxy)Carbonyl (Fmoc) Amino-Acid Chlorides - Synthesis, Characterization, and Application to the Rapid Synthesis of Short Peptide Segments'* in *J. Org. Chem.* **1986**, *51*, 3732-3734.

[54]   G. B. Fields; R. L. Noble: *'Solid phase peptide synthesis utilizing 9-fluorenylmethoxycarbonyl amino acids'* in *Int. J. Pept. Protein Res.* **1990**, *35*, 161-214.

[55]   J. Barbara; P. Flanagan: *'Blood transfusion risk: protecting against the unknown'* in *Bmj* **1998**, *316*, 717-718.

[56]   C. Chan; D. White: *'Fmoc solid phase peptide synthesis: a practical approach'* in *Oxford University Press* **2000**.

[57]   F. Manzenrieder: Doktorarbeit *'New Approaches to Discover Protease Inhibitros: By de novo Rational Structure Based (BACE1) and by Development and Use of ^{31}P NMR as Veratile Tool to Screen Compounds Libraries'*, Technische Universität München (München), **2008**.

[58]   R. Knorr; A. Trzeciak; W. Bannwarth; D. Gillessen: *'New Coupling Reagents in Peptide Chemistry'* in *Tetrahedron Lett.* **1989**, *30*, 1927-1930.

[59]   G. C. Alghisi; C. Rüegg: *'Vascular Integrins in Tumor Angiogenesis: Mediators and Therapeutic Targets'* in *Endothelium* **2006**, *13*, 113-135.

[60]   R. Burke: *'Intervebrate Integrins: Structure, Function and Evolution'* in *Int. Rev. Cytology* **1999**, *191*, 257-284.

[61]   M. D. Pierschbacher; E. Ruoslahti: *'Cell attachment activity of fibronectin can be duplicated by small synthetic fragments of the molecule'* in *Nature* **1984**, *309*, 30-33.

[62]   R. Pytela; M. D. Pierschbacher; E. Ruoslahti: *'Identification and isolation of a 140 kd cell surface glycoprotein with properties expected of a fibronectin receptor'* in *Cell* **1985**, *40*, 191-198.

[63]   R. Pytela; M. D. Pierschbacher; E. Ruoslahti: *'A 125/115-kDa cell surface receptor specific for vitronectin interacts with the arginine-glycine-aspartic acid adhesion sequence derived from fibronectin'* in *Proc. Natl. Acad. Sci. USA* **1985**, *82*, 5766-5770.

[64]   C. M. Isacke; M. A. Horton: *'The Adhesion Molecule Facts Book'*, Academic Press, London, **2000**.

[65]   S. Suzuki; W. S. Agraves; R. Pytela; H. Arai; T. Krusius; M. D. Pierschbacher; E. Ruoslahti: *'cDNA and amino acid sequences of the cell adhesion protein receptor recognizing vitronectin reveal a transmembrane domain and homologies with other adhesion protein receptors.'* in *Proc. Natl. Acad. Sci. USA* **1986**, *83*, 8614-8618.

[66]   J. W. Tamkun; D. W. DeSimone; D. Fonda; R. S. Patel; C. Buck; A. F. Horwitz; R. O. Hynes: *'Structure of integrin, a glycoprotein involved in the transmembrane linkage between fibronectin and actin'* in *Cell* **1986**, *46*, 271-282.

[67]   H. Jin; J. Varner: *'Integrins: Roles in cancer developement and as treatment agents'* in *Brit. J. Cancer* **2004**, *90*, 561-565.

[68]   H. Yusuf-Makagiansar; M. E. Anderson; T. V. Yakovleva; J. S. Murray; T. J. Siahaan: *'Inhibition of LFA-1/ICAM-1 and VLA-4/VCAM-1 as a therapeutic approach to inflammation and autoimmune diseases'* in *Med. Res. Rev.* **2002**, *22*, 146-167.

[69]   A. I. Rojas; H. Ahmed: *'Adhesion receptors in health and disease'* in *Criti. Rev. Oral Biol. M.* **1999**, *10*, 337-358.

[70]   K. J. Clemetson; J. M. Clemetson: *'Integrins and cardiovascular disease'* in *Cell. Mol. Life Sci.* **1998**, *54*, 502-513.

[71]   M. J. Humphries: *'Integrin Structure'* in *Biochem. Soc. Trans.* **2000**, *28*, 311-339.

[72]   M. V. Nermut; N. M. Green; P. Eason; S. S. Yamada; K. M. Yamada: *'Electron microscopy and structural model of human fibronectin receptor'* in *EMBO J.* **1988**, *7*, 4093-4099.

[73]   J. P. Xiong; T. Stehle; B. Diefenbach; R. Zhang; R. Dunker; D. Scott; A. Joachimiak; S. L. Goodman; M. A. Arnaout: *'Crystal Structure of the Extracellular Segment of Integrin $\alpha v \beta 3$'* in *Science* **2001**, *294*, 339-345.

[74]   J. P. Xiong; T. Stehle; R. Zhang; A. Joachimiak; M. Frech; S. L. Goodman; M. A. Arnaout: *'Crystal Structure of the Extracellular Segment of Integrin $\alpha v \beta 3$ in Complex with an Arg-Gly-Asp Ligand'* in *Science* **2002**, *296*, 151-155.

[75]   M. Schottelius; B. Laufer; H. Kessler; H. J. Wester: *'Ligands for mapping $\alpha v \beta 3$-integrin expression in vivo'* in *Acc. Chem. Res.* **2009**, *42*, 969-980.

[76]   P. Bork; T. Doerks; T. A. Springer; B. Snel: *'Domains in plexins: links to integrins and transcription factors'* in *Trends Biochem. Sci.* **1999**, *24*, 261-263.

[77]   M. Rocco; C. Rosano; J. W. Weisel; D. A. Horita; R. R. Hantgan: *'Integrin conformational regulation: uncoupling extension/tail separation from changes in the head region by a multiresolution approach'* in *Structure* **2008**, *16*, 954-964.

[78]   J. O. Lee; P. Rieu; M. A. Arnaout; R. Liddington: *'Crystal structure of the A domain from the alpha subunit of integrin CR3 (CD11b/CD18)'* in *Cell* **1995**, *80*, 631-638.

[79]   D. F. Legler; G. Wiedle; F. P. Ross; B. A. Imhof: *'Superactivation of integrin avb3 by low antagonist concentration'* in *J. Cell Sci.* **2001**, *114*, 1545-1553.

[80]   T. Xiao; J. Takagi; B. S. Coller; J. H. Wang; T. A. Springer: *'Structural basis for allostery in integrins and binding to fibrinogen-mimetic therapeutics'* in *Nature* **2004**, *432*, 59-67.

[81]   M. A. Arnaout; B. Mahalingam; J.-P. Xiong: *'Integrin Structure, Allostery, and Bidirectional Signaling'* in *Annu. Rev. Cell Dev. Biol.* **2005**, *21*, 381-410.

[82]   B. H. Luo; C. V. Carman; T. A. Springer: *'Structural basis of integrin regulation and signaling'* in *Annu. Rev. Immunol.* **2007**, *25*, 619-647.

[83]   T. L. Lau; C. Kim; M. H. Ginsberg; T. S. Ulmer: *'The structure of the integrin alphaIIbbeta3 transmembrane complex explains integrin transmembrane signalling'* in *EMBO J.* **2009**, *28*, 1351-1361.

[84]   M. Hoefling; H. Kessler; K.-E. Gottschalk: *'The Transmembrane Structure of Integrin aIIbb3 - Significance to Signal Transduction'* in *Angew. Chem. Int. Ed.* **2009**, *48*, 6590-6593.

[85]   H. Yin; J. S. Slusky; B. W. Berger; R. S. Walters; G. Vilaire; R. I. Litvinov; J. D. Lear; G. A. Caputo; J. S. Bennett; W. F. DeGrado: *'Computational Design of Peptides That Target Transmembrane Helices'* in *Science* **2007**, *315*, 1817-1822.

[86]   J. Zhu; C. V. Carman; M. Kim; M. Shimaoka; T. A. Springer; B.-H. Luo: *'Requirement of α nd β subunit transmembrane helix separation for integrin outside-in signaling'* in *Blood* **2007**, *110*, 2475-2483.

[87]   K. E. Gottschalk; P. D. Adams; A. T. Brunger; H. Kessler: *'Transmembrane signal transduction of the $\alpha v \beta 3$ integrin'* in *Protein Sci.* **2002**, *11*, 1800-1812.

[88]   M. Karin; Y. Cao; F. R. Greten; Z. W. Li: *'NF-kappaB in cancer: from innocent bystander to major culprit'* in *Nat. Rev. Cancer* **2002**, *2*, 301-310.

[89]   D. A. Cheresh; D. G. Stupack: *'Integrin-mediated death: An explaination of the integrin-knockout phenotype?'* in *Nat. Med.* **2002**, *8*, 193-194.

[90]   T. Arndt; U. Arndt; U. Reuning; H. Kessler: *'Integrins in Angiogenesis: Implications for tumor therapy'* in: *'Cancer Therapy. Molecular Targets in Tumor-Host Interactions.'* (Ed.: G. F. Weber), Horizon Bioscience, Norfolk, U.K., **2005**, pp. 93-141.

[91]   K. A. Reesquist; E. Ross; E. A. Koop; R. M. Wolthuis; F. J. Zwartkruis; Y. van Kooyk; M. Salmon; C. D. Buckley; J. L. Bos: *'The small GTPase, Rap1, mediates CD31-induced integrin adhesion'* in *J. Cell Biol.* **2000**, *148*, 1151-1158.

[92]   Z. Zhang; K. Vuori; H. Wang; J. C. Reed; E. Ruoslahti: *'Integrin activation by R-ras'* in *Cell* **1996**, *85*, 61-69.

[93]   F. Diaz-Gonzalez; J. Forsyth; B. Steiner; M. H. Ginsberg: *'Trans-dominant inhibition of integrin function'* in *Mol. Biol. Cell* **1996**, *7*, 1939-1951.

[94]   D. Heckmann: *'Design and Synthesis of Selektive Ligands for the $\alpha5\beta1$ Integrin Receptors and Cyclic Peptides as Affinity Ligands for Factor VIII Prification'*, Technische Universität München (München), **2007**.

[95]   G. Müller; M. Gurrath; H. Kessler: *'Pharmacophore refinement of gpIIb/IIIa antagonists based on comparative studies of antiadhesive cyclic and acyclic RGD peptides'* in *J. Comp.-Aid. Mol. Des.* **1994**, *8*, 709-730.

[96]   J. A. Eble; K. Kühn: *'Integrin-Ligand Interaction'*, Springer-Verlag, Heidelberg, **1997**.

[97]   R. Pankov; K. M. Yamada: *'Fibronectin at a glance'* in *J. Cell Sci.* **2002**, *115*, 3861-3863.

[98]   J. R. Potts; I. D. Campbell: *'Fibronectin structure and assembly'* in *Curr. Opin. Cell Biol.* **1994**, *6*, 648-655.

[99]   D. F. Mosher: *'Assembly of fibronectin into extracellular matrix'* in *Curr. Opin. Struc. Biol.* **1993**, *3*, 214-222.

[100] R. O. Hynes: *'A reevaluation of integrins as regulators of angiogenesis'* in *Nat. Med.* **2002**, *8*, 918-921.

[101] G. D. Hartman; M. S. Egbertson; W. Halczenko; W. L. Laswell; M. E. Duggan; R. L. Smith; A. M. Naylor; P. D. Manno; R. J. Lynch; G. Zhang; C. T.-C.

Chang; R. J. Gould: *'Non-peptide fibrinogen receptor antagonists. 1. Discovery and design of exosite inhibitors'* in *J. Med. Chem.* **1992**, *35*, 4640-4642.

[102] E. Mutschler; G. Geisslinger; K. H.K.; M. Schäfer-Korting: *'Arzneimittelwirkungen Lehrbuch der Pharmakologie und Toxikologie'*, Wissenschaftliche Verlagstgesellschaft mbH, Stuttgart, **2001**.

[103] D. A. Reardon; L. B. Nabors; R. Stupp; T. Mikkelsen: *'Cilengitide: an integrin-targeting arginine-glycine-aspartic acid peptide with promising activity for glioblastoma multiforme'* in *Exp. Opin. Invest. Drugs* **2008**, *17*, 1225-1235.

[104] J. M. Smallheer; C. A. Weigelt; F. J. Woerner; J. S. Wells; W. F. Daneker; S. A. Mousa; R. R. Wexler; P. K. Jadhav: *'Synthesis and biological evaluation of nonpeptide integrin antagonists containing spirocyclic scaffolds'* in *Bioorg. Med. Chem. Lett.* **2004**, *14*, 383-387.

[105] L. Marinelli; A. Meyer; D. Heckmann; A. Lavecchia; E. Novellino; H. Kessler: *'Ligand binding analysis for human $\alpha5\beta1$ integrin: Strategies for designing new $\alpha5\beta1$ integrin antagonists'* in *J. Med. Chem.* **2005**, *48*, 4204-4207.

[106] C. Gibson; G. A. G. Sulyok; D. Hahn; S. L. Goodman; G. Hölzemann; H. Kessler: *'Nonpeptidic $\alpha v\beta3$ integrin antagonist libaries: on-bead screening and mass spectometric identification without tagging'* in *Angew. Chem. Int. Ed.* **2001**, *40*, 165-169.

[107] S. L. Goodman; G. Holzemann; G. A. Sulyok; H. Kessler: *'Nanomolar small molecule inhibitors for $\alpha v\beta6$, $\alpha v\beta5$, and $\alpha v\beta3$ integrins'* in *J. Med. Chem.* **2002**, *45*, 1045-1051.

[108] J. H. Hutchinson; W. Halczenko; K. M. Brashear; M. J. Breslin; P. J. Coleman; T. Duong le; C. Fernandez-Metzler; M. A. Gentile; J. E. Fisher; G. D. Hartman; J. R. Huff; D. B. Kimmel; C. T. Leu; R. S. Meissner; K. Merkle; R. Nagy; B. Pennypacker; J. J. Perkins; T. Prueksaritanont; G. A. Rodan; S. L. Varga; G. A. Wesolowski; A. E. Zartman; S. B. Rodan; M. E. Duggan: *'Nonpeptide alphavbeta3 antagonists. 8. In vitro and in vivo evaluation of a potent alphavbeta3 antagonist for the prevention and treatment of osteoporosis'* in *J. Med. Chem.* **2003**, *46*, 4790-4798.

[109] J. J. Marugán; C. Manthey; B. Anaclerio; L. Lafrance; T. Lu; T. Markotan; K. A. Leonard; C. Crysler; E. Eisennagel; M. Dasgupta; B. Tomczuk: *'Design, Synthesis and Biological Evaluation of Novel Potent and Selective avb3/avb5*

Integrin Dual Inhibitors with Improved Bioavailability. Selection of the Molecular Core.' in *J. Med. Chem* **2005**, *48*, 926-934.

[110] A. Meyer: *'Strukturbasiertes Design selektiver Inhibitoren von Protein-Protein Wechselwirkungen und Enzymen'*, Technical University Munich (Munich), **2006**.

[111] J. Takagi; T. Kamata; J. Meredith; M. Puzon-McLaughlin; Y. Takada: *'Changing Ligand Specificities of avb1 and avb3 Integrins by Swapping a Short Diverse Sequence of the Subunit'* in *J. Biol. Chem.* **1997**, *272*, 19794-19800.

[112] L. Marinelli; K.-E. Gottschalk; A. Meyer; E. Novellino; H. Kessler: *'Human integrin αvβ5: Homology modeling and ligand binding'* in *J. Med. Chem.* **2004**, *47*, 4166-4177.

[113] D. Heckmann; A. Meyer; B. Laufer; G. Zahn; R. Stragies; H. Kessler: *'Rational design of highly active and selective ligands for the α5β1 integrin receptor'* in *ChemBioChem* **2008**, *9*, 1397-1407.

[114] J. Folkman: *'Angiogenesis in cancer, vascular, rheumatoid and other disease'* in *Nat. Med.* **1995**, *1*, 17-31.

[115] B. Eliceiri; D. A. Cheresh: *'The role of αv integrins during angiogenesis: insights into potential mechanisms of action and clinical development'* in *J. Clin. Invest.* **1999**, *103*, 1227-1230.

[116] J. Folkman: *'Tumor angiogenesis: therapeutic implications'* in *New Engl. J. Med.* **1971**, *285*, 1182-1186.

[117] J. Folkman: *'Role of Angiogenesis in tumor growth and metastasis'* in *Sem. Oncology* **2002**, *29*, 15-18.

[118] G. C. Tucker: *'αv integrin inhibitors and cancer therapy'* in *Curr. Opin. Invest. Drugs* **2003**, *4*, 722-731.

[119] D. A. Cheresh; R. C. Spiro: *'Biosynthetic and functional properties of an Arg-Gly-Asp-directed receptor involved in human melanoma cell attachment to vitronectin, fibrinogen, and von Willebrand factor'* in *J. Biol. Chem.* **1987**, *262*, 17703-17711.

[120] M. Aumailley; M. Gurrath; G. Müller; J. Calvete; R. Timpl; H. Kessler: *'Arg-Gly-Asp constrained within cyclic peptides: Strong and selective inhibitors of cell adhesion to vitronectin and laminin fragment P1'* in *FEBS Lett.* **1991**, *291*, 50-54.

[121] R. Haubner; R. Gratias; B. Diefenbach; S. L. Goodman; A. Jonczyk; H. Kessler: *'Structural and functional aspects of RGD-containing cyclic pentapeptides as highly potent and selective integrin $\alpha v\beta 3$ antagonists'* in *J. Am. Chem. Soc.* **1996**, *118*, 7461-7472.

[122] P. C. Brooks; A. M. Montgomery; M. Rosenfeld; R. A. Reisfeld; T. Hu; G. Klier; D. A. Cheresh: *'Integrin $\alpha v\beta 3$ antagonists promote tumor regression by inducing apoposis of angiogenic blood vessels'* in *Cell* **1994**, *79*, 1157-1164.

[123] B. Eliceiri; R. Klemke; S. Strömblad; D. A. Cheresh: *'Integrin $\alpha v\beta 3$ requirement for sustained mitogen-activated protein kinase activity during angiogenesis'* in *J. Cell Biol.* **1998**, *140*, 1255-1263.

[124] M. Scatena; M. Almeida; M. L. Chaisson; N. Fausto; R. F. Nicosia; C. M. Giachelli: *'NFkappaB mediates $\alpha v\beta 3$ integrin- induced cell survival'* in *J. Cell Biol.* **1998**, *141*, 1083-1093.

[125] S. Strömblad; J. C. Becker; M. Yebra; P. C. Brooks; D. A. Cheresh: *'Suppression of p53 activity and p21WAF1/CIP1 expression by vascular cell integrin avb3 during angiogenesis'* in *J. Clin. Invest.* **1996**, *98*, 426-433.

[126] D. G. Stupack; X. S. Puente; S. Boutsaboualoy; C. M. Storgard; D. A. Cheresh: *'Apoptosis of adherent cells by recruitment of caspase 8 to unligated integrins'* in *J. Cell Biol.* **2001**, *155*, 459-470.

[127] T. V. Byzova; C. K. Goldman; N. Pampori; K. A. Thomas; A. Bett; S. J. Shattil; E. F. Plow: *'A mechanism for modulation of cellular responses to VEGF: activation of the integrins'* in *Mol. Cell* **2000**, *6*, 851-860.

[128] B. L. Bader; H. Rayburn; D. Crowley; R. O. Hynes: *'Extensive vasculogenesis, angiogenesis and organogenesis preceed lethaly in mice lacking all αv integrins'* in *Cell* **1998**, *95*, 507-519.

[129] D. Taverna; H. Moher; D. Crowley; L. Borsig; A. Vaki; R. O. Hynes: *'Increased primary tumor growth in mice null for $\beta 3$ or $\beta 3/\beta 5$ or selectins'* in *Proc. Natl. Acad. Sci. USA* **2004**, *101*, 763-768.

[130] L. E. Reynolds; L. Wyder; J. C. Lively; D. Taverna; S. D. Robinson; X. Huang; D. Sheppard; R. O. Hynes; K. Hodivala-Dilke: *'Enhanced pathological angiogenesis in mice lacking $\beta 3$ integrin or $\beta 3$ and $\beta 5$ integrin'* in *Nat. Med.* **2002**, *8*, 27-34.

[131] K. O. Simon; E. M. Nutt; D. G. Abraham; G. A. Rodan; L. T. Duong: *'The αvβ3 integrin regulates α5β1-mediated cell migration towards fibronectin'* in *J. Biol. Chem.* **1997**, *272*, 29380-29389.

[132] S. Kim; M. Bakre; H. Yin; J. A. Varner: *'Inhibition of endothelial cell survival and angiogenesis by protein kinase A'* in *J. Clin. Invest.* **2002**, *110*, 933-941.

[133] S. Kim; M. Harris; J. A. Varner: *'Regulation of integrin αvβ3- mediated endothelial cell migration and angiogenesis by integrin α5β1 and protein kinase A'* in *J. Biol. Chem.* **2000**, *275*, 33920-33928.

[134] R. Stragies; F. Osterkamp; G. Zischinsky; D. Vossmeyer; H. Kalkhof; U. Reimer; G. Zahn: *'Design and synthesis of a new class of selective integrin α5β1 antagonists'* in *J. Med. Chem.* **2007**, *50*, 3786-3794.

[135] D. Heckmann; A. Meyer; L. Marinelli; G. Zahn; R. Stragies; H. Kessler: *'Probing integrin selectivity: rational design of highly active and selective ligands for the α5β1 and αvβ3 integrin receptor'* in *Angew. Chem. Int. Ed.* **2007**, *46*, 3571-3574.

[136] M. R. Morgan; A. Byron; M. J. Humphries; M. D. Bass: *'Giving off mixed signals - "Distinct functions of α5β1 and αvβ3 integrins in regulating cell behaviour'* in *IUBMB Life* **2009**, *61*, 731-738.

[137] S. Takahashi; M. Leiss; M. Moser; T. Ohashi; D. Heckmann; A. Pfeifer; J. Takagi; H. Kessler; H. P. Erickson; R. Fässler: *'The RGD motif in fibronectin is essential for mouse development but dispensable for fibronectin fibril assembly'* in *J. Biol. Chem.* **2007**, *178*, 167-178.

[138] M. Bodanzsky: *'Principles of Peptide Synthesis'*, Springer Laboratory, Berlin, **1993**.

[139] R. Tyler-Cross; V. Schirch: *'Effects of amino acid sequence, buffers, and ionic strength on the rate and mechanism of deamidation of asparagine residues in small peptides.'* in *J. Biol. Chem.* **1991**, *266*, 22549-22556.

[140] N. E. Robinson; A. B. Robinson: *'Molecular clocks'* in *Proc. Natl. Acad. Sci. USA* **2001**, *98*, 944-949.

[141] J. Lanthier; R. R. Desrosiers: *'Protein l-isoaspartyl methyltransferase repairs abnormal aspartyl residues accumulated in vivo in type-I collagen and restores cell migration'* in *Exp. Cell Res.* **2004**, *293*, 96-105.

[142] N. E. Robinson; A. B. Robinson: *'Amide molecular clocks in drosophila proteins: potential regulators of aging and other processes'* in *Mech. Ageing Dev.* **2004**, *125*, 259-267.

[143] K. J. Reissner; D. W. Aswad: *'Deamidation and isoaspartate formation in proteins: unwanted alterations or surreptitious signals?'* in *Cell. Mol. Life Sci.* **2003**, *60*, 1281-1295.

[144] J. Xu; L. M. Maurer; B. R. Hoffmann; D. S. Annis; D. F. Mosher: *'iso-DGR Sequences Do Not Mediate Binding of Fibronectin N-terminal Modules to Adherent Fibronectin-null Fibroblasts'* in *J. Biol. Chem.* **2010**, *285*, 8563-8571.

[145] E. Koivunen; D. A. Gay; E. Ruoslahti: *'Selection of Peptides Binding to the α5β1 Integrin from Phage Display Library'* in *J. Biol. Chem.* **1993**, *268*, 20205-20210.

[146] E. Koivunen; B. Wang; E. Ruoslahti: *'Isolation of a highly specific ligand for the α5β1 integrin from a phage display library'* in *J. Cell Biol.* **1994**, *124*, 373-380.

[147] W. Arap; R. Pasqualini; E. Ruoslahti: *'Cancer Treatment by Targeted Drug Delivery to Tumor Vasculature in a Mouse Model'* in *Science* **1998**, *279*, 377-380.

[148] A. Corti; F. Curnis; W. Arap; R. Pasqualini: *'The neovasculature homing motif NGR: more than meets the eye'* in *Blood* **2008**, *112*, 2628-2635.

[149] J. Yan; A. D. Kline; H. Mo; M. J. Shapiro; E. R. Zartler: *'A Novel Method for the Determination of Stereochemistry in Six-Membered Chairlike Rings Using Residual Dipolar Couplings'* in *J. Org. Chem.* **2003**, *68*, 1786-1795.

[150] E. Ruoslahti: *'RGD and other Recognition Sequences for Iintegrins'* in *Annu. Rev. Cell Dev. Biol.* **1996**, *12*, 697-715.

[151] A. Spitaleri; S. Mari; F. Curnis; C. Traversari; R. Longhi; C. Bordignon; A. Corti; G. P. Rizzardi; G. Musco: *'Structural basis for the interaction of isoDGR with the RGD-binding site of αvβ3 integrin'* in *J. Biol. Chem.* **2008**, *283*, 19757-19768.

[152] A. Corti; F. Curnis: *'Isoaspartate-dependent molecular switches for integrin-ligand recognition'* in *J. Cell Sci.* **2011**, *124*, 515-522.

[153] F. Curnis; A. Cattaneo; R. Longhi; A. Sacchi; A. M. Gasparri; F. Pastorino; P. Di Matteo; C. Traversari; A. Bachi; M. Ponzoni; G.-P. Rizzardi; A. Corti: *'Critical Role of Flanking Residues in NGR-to-isoDGR Transition and CD13/Integrin Receptor Switching'* in *J. Biol. Chem.* **2010**, *285*, 9114-9123.

[154] F. Curnis; A. Sacchi; A. Gasparri; R. Longhi; A. Bachi; C. Doglioni; C. Bordignon; C. Traversari; G. P. Rizzardi; A. Corti: *'Isoaspartate-glycine-arginine: A new tumor vasculature-targeting motif'* in *Cancer Res.* **2008**, *68*, 7073-7082.

[155] T. Weide; A. Modlinger; H. Kessler: *'Spatial Screening for the Identification of the Bioactive Conformation of Integrin Ligands'* in *Top. Curr. Chem.* **2007**, *272*, 1-50.

[156] A. Meyer; J. Auernheimer; A. Modlinger; H. Kessler: *'Targeting RGD recognizing integrins: drug development, biomaterial research, tumor imaging and targeting'* in *Curr. Pharm. Des.* **2006**, *12*, 2723-2747.

[157] H. Kessler; R. Gratias; G. Hessler; M. Gurrath; G. Müller: *'Conformation of cyclic peptides. Principle concepts and the design of selectivity and superactivity in bioactive sequences by 'spatial screening''* in *Pure Appl. Chem.* **1996**, *68*, 1201-1206.

[158] P. Di Matteo; F. Curnis; R. Longhi; G. Colombo; A. Sacchi; L. Crippa; M. P. Protti; M. Ponzoni; S. Toma; A. Corti: *'Immunogenic and structural properties of the Asn-Gly-Arg (NGR) tumor neovasculature-homing motif'* in *Mol. Immunol.* **2006**, *43*, 1509-1518.

[159] M. M. Shemyakin; Y. A. Ovchinnikov; V. T. Ivanov: *'Topochemical investigations of peptide systems'* in *Angew. Chem. Int. Ed.* **1969**, *8*, 492-499.

[160] J. Wermuth; S. L. Goodman; A. Jonczyk; H. Kessler: *'Stereoisomerism and biological activity of the selective and superactive $\alpha v\beta 3$ integrin inhibitor cyclo(-RGDfV-) and its retro-inverso peptide'* in *J. Am. Chem. Soc.* **1997**, *119*, 1328-1335.

[161] L. Gentilucci; G. Cardillo; S. Spampinato; A. Tolomelli; F. Squassabia; R. De Marco; A. Bedini; M. Baiula; L. Belvisi; M. Civera: *'Antiangiogenic Effect of Dual/Selective $\alpha 5\beta 1/\alpha v\beta 3$ Integrin Antagonists Designed on Partially Modified Retro-Inverso Cyclotetrapeptide Mimetics'* in *J. Med. Chem.* **2009**, *53*, 106-118.

[162] N. Greenspoon; R. Hershkoviz; R. Alon; D. Varon; B. Shenkman; G. Marx; S. Federman; G. Kapustina; O. Lider: *'Structural analysis of integrin recognition and the inhibition of integrin-mediated cell functions by novel nonpeptidic surrogates of the Arg-Gly-Asp sequence'* in *Biochemistry* **1993**, *32*, 1001-1008.

[163] M. Gurrath; G. Müller; H. Kessler; M. Aumailley; R. Timpl: *'Conformation/activity studies of rationally designed potent anti-adhesive RGD peptides'* in *Eur. J. Biochem.* **1992**, *210*, 911-921.

[164] M. Pfaff; K. Tangemann; B. Müller; M. Gurrath; G. Müller; H. Kessler; R. Timpl; J. Engel: *'Selective recognition of cyclic RGD peptides of NMR defined conformation by αIIbβ3, αvβ3, and α5β1 integrins'* in *J. Biol. Chem.* **1994**, *269*, 20233-20238.

[165] E. Lindahl; B. Hess; D. van der Spoel: *'GROMACS 3.0: a package for molecular simulation and trajectory analysis'* in *J. Mol. Model.* **2001**, *7*, 306-317.

[166] C. Oostenbrink; T. A. Soares; N. F. A. van der Vegt; W. F. van Gunsteren: *'Validation of the 53A6 GROMOS force field'* in *Eur. Biophys. J.* **2005**, *34*, 273-284.

[167] E. Koivunen; B. Wang; E. Ruoslahti: *'Isolation of a highly specific ligand for the alpha 5 beta 1 integrin from a phage display library'* in *J Cell Biol* **1994**, *124*, 373-380.

[168] D. Zimmermann; E. W. Guthöhrlein; M. Maleševic; K. Sewald; L. Wobbe; C. Heggemann; N. Sewald: *'Integrin α5β1 Ligands: Biological Evaluation and Conformational Analysis'* in *ChemBioChem* **2005**, *6*, 272-276.

[169] S. Urman; K. Gaus; Y. Yang; U. Strijowski; N. Sewald; S. De Pol; O. Reiser: *'The Constrained Amino Acid β-Acc Confers Potency and Selectivity to Integrin Ligands'* in *Angew. Chem. Int. Ed.* **2007**, *46*, 3976-3978.

[170] A. Weinacker; A. Chen; M. Agrez; R. I. Cone; S. Nishimura; E. Wayner; R. Pytela; D. Sheppard: *'Role of the integrin αvβ6 in cell attachment to fibronectin. Heterologous expression of intact and secreted forms of the receptor.'* in *J. Biol. Chem.* **1994**, *269*, 6940-6948.

[171] A. L. Prieto; G. M. Edelman; K. L. Crossin: *'Multiple integrins mediate cell attachment to cytotactin/tenascin '* in *Proceedings of the National Academy of Sciences of the United States of America* **1993** *90* 10154-10158

[172] X. Huang; J. Wu; S. Spong; D. Sheppard: *'The integrin αvβ6 is critical for keratinocyte migration on both its known ligand, fibronectin, and on vitronectin'* in *J. Cell Sci.* **1998**, *111*, 2189-2195.

[173] J. S. Munger; X. Huang; H. Kawakatsu; M. J. D. Griffiths; S. L. Dalton; J. Wu; J.-F. Pittet; N. Kaminski; C. Garat; M. A. Matthay; D. B. Rifkin; D. Sheppard: *'A*

Mechanism for Regulating Pulmonary Inflammation and Fibrosis: The Integrin αvβ6 Binds and Activates Latent TGF β1' in *Cell* **1999**, *96*, 319-328.

[174] X. Z. Huang; J. F. Wu; D. Cass; D. J. Erle; D. Corry; S. G. Young; R. V. Farese; D. Sheppard: *'Inactivation of the integrin β6 subunit gene reveals a role of epithelial integrins in regulating inflammation in the lung and skin.'* in *J. Cell Biol.* **1996**, *133*, 921-928.

[175] K. Haapasalmi; K. Zhang; M. Tonnesen; J. Olerud; D. Sheppard; T. Salo; R. Kramer; R. A. F. Clark; V. J. Uitto; H. Larjava: *'Keratinocytes in human wounds express alpha v beta 6 integrin'* in *J. Invest. Dermatol.* **1996**, *106*, 42-48.

[176] J. Breuss; J. Gallo; H. DeLisser; I. Klimanskaya; H. Folkesson; J. Pittet; S. Nishimura; K. Aldape; D. Landers; W. Carpenter; a. et: *'Expression of the β6 integrin subunit in development, neoplasia and tissue repair suggests a role in epithelial remodeling'* in *J. Cell Sci.* **1995**, *108*, 2241-2251.

[177] G. J. Thomas; M. L. Nyström; J. F. Marshall: *'αvβ6 integrin in wound healing and cancer of the oral cavity'* in *J. Oral Pathol. Med.* **2006**, *35*, 1-10.

[178] K. Barlos; D. Gatos; J. Kallitsis; G. Papaphotiu; P. Sotiriu; W. Q. Yao; W. Schäfer: *'Synthesis of Protected Peptide-Fragments Using Substituted Triphenylmethyl Resins'* in *Tetrahedron Lett.* **1989**, *30*, 3943-3946.

[179] H. B. Schiller; A. Szekeres; B. R. Binder; H. Stockinger; V. Leksa: *'Mannose 6-Phosphate/Insulin-like Growth Factor 2 Receptor Limits Cell Invasion by Controlling αvβ3 Integrin Expression and Proteolytic Processing of Urokinase-type Plasminogen Activator Receptor'* in *Mol. Biol. Cell* **2009**, *20*, 745-756.

[180] C. Griesinger; O. W. Sørensen; R. R. Ernst: *'Practical Aspects of the E-Cosy Technique - Measurement of Scalar Spin Spin Coupling-Constants in Peptides'* in *J. Magn. Reson.* **1987**, *75*, 474-492.

[181] J. Cavanagh; M. Rance: *'Sensitivity Improvement in Isotropic Mixing (TOCSY) Experiments'* in *J. Magn. Reson.* **1990**, *88*, 72-85.

[182] A. Bax; M. F. Summers: *'H-1 and C-13 Assignments from Sensitivity-Enhanced Detection of Heteronuclear Multiple-Bond Connectivity by 2D Multiple Quantum NMR'* in *J. Am. Chem. Soc.* **1986**, *108*, 2093-2094.

[183] C. Griesinger; R. R. Ernst: *'Frequency offset effects and their elimination in NMR rotating-frame cross-relaxation spectroscopy'* in *J. Magn. Res.* **1987**, *75*, 261-271.

[184] H. Kessler; C. Griesinger; R. Kerssebaum; K. Wagner; R. R. Ernst: *'Separation of Cross-Relaxation and J Cross-Peaks in 2D Rotating-Frame NMR Spectroscopy'* in *J. Am. Chem. Soc.* **1987**, *102*, 607-609.

[185] T. F. Havel: *'An evaluation of computational strategies for use in the determination of protein structure from distance constraints obtained by nuclear magnetic resonance'* in *Prog Biophys Mol Biol* **1991**, *56*, 43-78.

[186] D. F. Mierke; A. Geyer; H. Kessler: *'Coupling constants and hydrogen bonds as experimental restraints in a distance geometry refinement protocol'* in *Int. J. Pept. Protein Res.* **1994**, *44*, 325-331.

[187] H. J. C. Berendsen; D. van der Spoel; R. van Drunen: *'GROMACS: A message-passing parallel molecular dynamics implementation'* in *Comput. Phys. Commun.* **1995**, *91*, 43-56.

[188] K. Zimmermann: *'ORAL: All purpose molecular mechanics simulator and energy minimizer'* in *J. Comput. Chem.* **1991**, *12*, 310-319.

[189] H. J. C. Berendsen; J. P. M. Postma; W. F. van Gunsteren; A. DiNola; J. R. Haak: *'Molecular dynamics with coupling to an external bath'* in *J. Chem. Phys.* **1984**, *81*, 3684-3690.

[190] R. W. Hockney; S. P. Goel; J. W. Eastwood: *'Quiet high-resolution computer models of a plasma'* in *J. Comput. Phys.* **1974**, *14*, 148-158.

[191] J.-P. Ryckaert; G. Ciccotti; H. J. C. Berendsen: *'Numerical integration of the cartesian equations of motion of a system with constraints: molecular dynamics of n-alkanes'* in *J. Comput. Phys.* **1977**, *23*, 327-341.

[192] M. Christen; P. H. Hünenberger; D. Bakowies; R. Baron; R. Burgi; D. P. Geerke; T. N. Heinz; M. A. Kastenholz; V. Kräutler; C. Oostenbrink; C. Peter; D. Trzesniak; W. F. van Gunsteren: *'The GROMOS software for biomolecular simulation: GROMOS05'* in *J. Comput. Chem.* **2005**, *26*, 1719-1751.

[193] T. M. G. Koning; R. Boelens; R. Kaptein: *'Calculation of the nuclear overhauser effect and the determination of proton-proton distances in the presence of internal motions'* in *J. Magn. Reson.* **1990**, *90*, 111-123.

[194] R. Huey; G. M. Morris; A. J. Olson; D. S. Goodsell: *'A semiempirical free energy force field with charge-based desolvation'* in *J. Comput. Chem.* **2007**, *28*, 1145-1152.